1. Report No. FHWA/TX-91+1209-1	2. Government Accession No.	3. Recipient's Catalog No.

4. Title and Subtitle BONDING OF EXTERNAL TENDONS AT DEVIATORS	5. Report Date January 1991
	6. Performing Organization Code

7. Author's) B. J. Radloff, M. E. Kreger, and J. E. Breen	8. Performing Organization Report No. Research Report 1209-1

9. Performing Organization Name and Address Center for Transportation Research The University of Texas at Austin Austin, Texas 78712-1075	10. Work Unit No.
	11. Contract or Grant No. Research Study 3-5-89/0-1209
	13. Type of Report and Period Covered

12. Sponsoring Agency Name and Address Texas State Department of Highways and Public Transportation; Transportation Planning Division P. O. Box 5051 Austin, Texas 78763-5051	Final
	14. Sponsoring Agency Code

15. Supplementary Notes

Study conducted in cooperation with the U. S. Department of Transportation, Federal Highway Administration. Research Study Title: "Effect of Improved Bonding of External Tendons and the Use of Supplemental Continuous Bonded Tendons in External Post-Tensioned Bridges"

16. Abstract

This report is the first in a series outlining a major study of techniques for improving the ductility and strength of post-tensioned concrete box girder bridges through improved bonding of external tendons. It presents a detailed state-of-the-art report concerning bonding of tendons through cement grouting. More importantly, it presents the results of a series of realistic pullout tests for tendons grouted in curved deviator pipes typical of modern segmental technology. Six specimens were tested with varying deviation angles and ratio of prestressing tendon area to duct cross-sectional areas. Detailed measurements and observation of overall behavior led to a very good understanding of the bond-slip relationship for the tendons in the local region of the curved deviator.

In addition to the full-scale direct tension bond stress-slip tests of full-scale deviator specimens, two additional test series are reported. The first is a series of residual tension load tests in which the state of stress of tendons discretely bonded at multiple points was investigated by selective cutting between bonding points and measuring the residual load patterns. The second is a series of eighteen tests evaluating different materials and procedures for remedial bonding of tendons at pass through locations.

The tests reported herein provide the basis for formulations of a general bond stress-slip model for tendons grouted through steel deviator ducts which is useful for computer based calculations of the behavior of discretely bonded tendons in externally post-tensioned bridges. In addition, friction loss coefficients for curved ducts were verified and efficient techniques for remedial bonding of external tendons at diaphragm pass through locations were developed.

17. Key Words ductility, strength, bonding, post-tensioned concrete, box girder bridges, tendons, cement grouting, segmental, deviation angles, curved deviator	18. Distribution Statement No restrictions. This document is available to the public through the National Technical Information Service, Springfield, Virginia 22161.

19. Security Classif. (of this report) Unclassified	20. Security Classif. (of this page) Unclassified	21. No. of Pages 150	22. Price

Form DOT F 1700.7 (8-69)

BONDING OF EXTERNAL TENDONS

AT DEVIATORS

by

B.J. Radloff, M.E. Kreger and J.E. Breen

Research Report No. 1209-1
Research Project 3-5-89-1209

"Effect of Improved Bonding of External Tendons and the Use of
Supplemental Continuous Bonded Tendons in External Post-
Tensioned Bridge"

Conducted for

Texas
State Department of Highways and Public Transportation

in Cooperation with the

U.S. Department of Transportation

Federal Highway Administration

by

CENTER FOR TRANSPORTATION RESEARCH
BUREAU OF ENGINEERING RESEARCH
THE UNIVERSITY OF TEXAS AT AUSTIN

January 1991

The contents of this report reflect the views of the authors, who are responsible for the facts and the accuracy of the data presented herein. The contents do not necessarily reflect the official views or policies of the Federal Highway Administration. This report does not constitute a standard, specification, or regulation.

PREFACE

This report is the first report in a series which summarizes an investigation of the effect of improved bonding of external tendons on the behavior of precast segmental box girder bridges with external tendons. This report gives a state-of-the-art overview of the available tendon force transfer in external tendon bridges due to the method of attachment or bonding of the tendons to the box girders at intermediate points or deviators. This report presents the results of a series of detailed deviator tests in which full-size grouted tendons were pulled through typical curved deviators, and outlines design procedures and recommendations based on those tests.

The work is part of research project 3-5-89-1209 entitled "Effect of Improved bonding of External Tendons and the Use of Supplemental Continuous Bonded Tendons in External Post-Tensioned Bridges." The research was conducted by the Phil M. Ferguson Structural Engineering Laboratory as part of the overall research programs of the Center for Transportation Research of The University of Texas at Austin. The work was sponsored jointly by the Texas State Department of Highways and Public Transportation and the Federal Highway Administrations under an agreement with The University of Texas at Austin and the State Department of Highways and Public Transportation.

Liaison with the State Department of Highways and Public Transportation was maintained through the contact representative, Mr. Alan Matejowsky, who provided a great deal of insight and advice on segmental technology.

This portion of the overall study was co-directed by John E. Breen, who holds the Nasser I. Al-Rashid Chair in Civil Engineering, and Michael E. Kreger, Associate Professor of Civil Engineering. The development of the deviator pullout testing rig and the supervision of bonded deviator tests were the direct responsibility of Brock J. Radloff, Assistant Research Engineer. The studies on improved bonding techniques for the large model and on bonding characteristics of tendons done during demolition of the large model were the joint responsibility of Mr. Radloff and Azez Hindi, Assistant Research Engineer. Development of this report and the tendon bond-slip design recommendations were the direct responsibility of Mr. Radloff. This report is based on his M.S. thesis (Ref. 53).

SUMMARY

This report is the first in a series outlining a major study of techniques for improving the ductility and strength of post-tensioned concrete box girder bridges through improved bonding of external tendons. It presents a detailed state-of-the-art report concerning bonding of tendons through cement grouting. More importantly, it presents the results of a series of realistic pullout tests for tendons grouted in curved deviator pipes typical of modern segmental technology. Six specimens were tested with varying deviation angles and ratio of prestressing tendon area to duct cross-sectional areas. Detailed measurements and observation of overall behavior led to a very good understanding of the bond-slip relationship for the tendons in the local region of the curved deviator.

In addition to the full-scale direct tension bond stress-slip tests of full-scale deviator specimens, two additional test series are reported. The first is a series of residual tension load tests in which the state of stress of tendons discretely bonded at multiple points was investigated by selective cutting between bonding points and measuring the residual load patterns. The second is a series of eighteen tests evaluating different materials and procedures for remedial bonding of tendons at pass through locations.

The tests reported herein provide the basis for formulations of a general bond stress-slip model for tendons grouted through steel deviator ducts which is useful for computer based calculations of the behavior of discretely bonded tendons in externally post-tensioned bridges. In addition, friction loss coefficients for curved ducts were verified and efficient techniques for remedial bonding of external tendons at diaphragm pass through locations were developed.

IMPLEMENTATION

This report provides a detailed background and specific recommendations for considering friction losses and bond stress - slip relationships for external tendons in the curved deviator regions of segmentally constructed box girder bridges. It provides specific information and design constants for evaluating tendon stress and improving ductility useful in design and analysis of these key connection regions for the external post-tensioning systems for bridges. The primary use of this report will be to provide specific design information for bridge design level engineers in assessing the behavior of the local tendon connection and its effect on overall bridge behavior. The results of this study are given in forms of friction coefficients, ultimate bond stresses, and a suggested bond stress - slip relation for typical curved deviator section. These values can be used in determining actual effective tendon stresses and in evaluating the deformation and strength capacity of overloaded bridges. The values presented are applicable to straight or curved deviator ducts and would be conservative for tendons grouted in the center of straight ducts.

TABLE OF CONTENTS

LIST OF TABLES

LIST OF FIGURES

CHAPTER 1

Introduction

1.1 Background

Post-tensioned concrete box-girders are used extensively in the U.S. for the construction of medium to moderately long-span highway bridges. These structures are constructed rapidly and economically using the balanced cantilever or span-by-span erection methods with prefabricated or cast-in- place box-girder segments. The economic advantages of segmental box-girder construction are reflected by the number of these structures that have been built in the U.S. since the technology was developed in the 1970's [1]. An important development in U.S. box-girder construction, within the last decade, is the use of external post-tensioning tendons (tendons external to the concrete cross-section), as compared to traditional internal tendons which are located in ducts within the webs or flanges. For segmental precast box-girder construction, the internal tendon ducts caused severe congestion within the concrete cross-section and misalignment problems at segment joints [2]. Furthermore, the possibility of corroded tendons caused great concern, especially since the tendons which were cast into the concrete could not be inspected or replaced. External tendons were seen as a way of reducing the congestion, speeding and simplifying the construction process for the precasting and erection of the segments, and providing a means to inspect and replace the tendons in cases of unforseen corrosion or damage. Several impressive externally post-tensioned concrete box-girder bridges have been built in the U.S. since the first structure, the Long Key Bridge, was completed in 1980. The Texas State Department of Highways and Public Transportation is currently constructing several miles of elevated highway in San Antonio using a segmental precast box-girder with external tendons (the low cost alternate bid by the contractor).

Internal post-tensioning refers to the placement of tendons in ducts which are embedded within the webs and flanges of the box-girder section. After the precast segments are assembled (or after the concrete is placed and cured) the tendons are pulled through the ducts and stressed. The tendons are cement grouted after post-tensioning. The grout bonds the tendon to the duct and concrete section along the full length of the tendon, and provides corrosion protection for the tendon.

External post-tensioning consists of tendons which are relocated from the webs and flanges of the concrete section and are placed within the void of the box-girder. In order to achieve the required tendon profile, tendons are passed through deviation devices (deviators) cast monolithically with the concrete box sections at discrete points along the span length. A common form of deviator is a small block or saddle located at the junction of the web and the flange of the box section. Tendons are typically anchored in thick, full-depth diaphragms over the piers and generally overlap at the same location for continuity. The concept of external post-tensioning is clearly illustrated in the cutaway view of Long
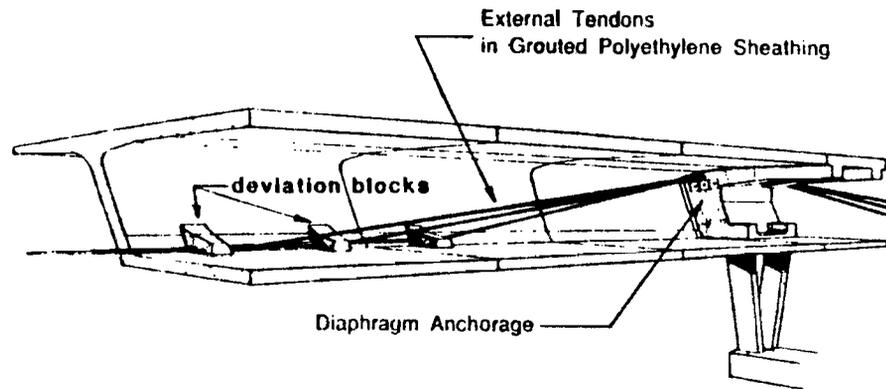
Figure 1.1 External post-tensioning in Long Key Bridge (from Ref. 3).
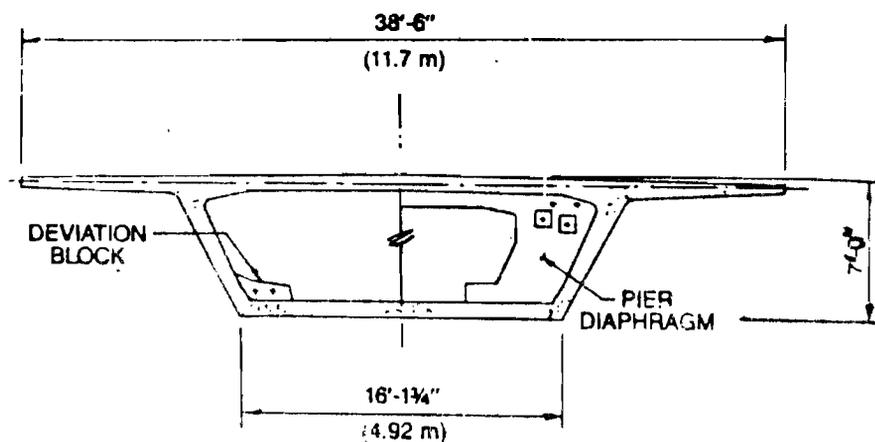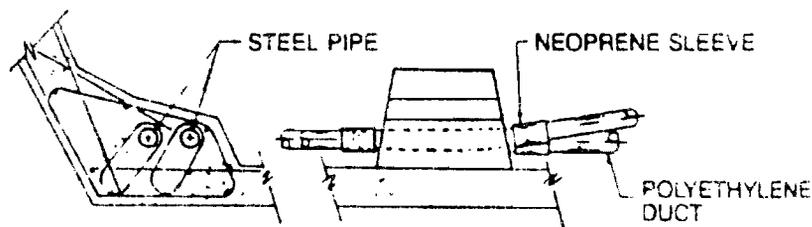
Figure 1.2 Typical segment and deviator detail (from Ref. 29).

Key Bridge in Fig. 1.1. For U.S. construction practice, the tendons are connected to the concrete box section at the anchorage and deviation locations only. Between these points of attachment, the tendons are enclosed in high density polyethylene (HDPE) sheathing. At the deviation locations, the tendons are passed through curved steel deviator pipes which are embedded in the deviation blocks and are connected to the HDPE tubing (Fig. 1.2). After stressing and anchoring, the tendon is cement grouted along its entire length. The grout bonds the tendon to the deviator pipe and concrete section at the deviation and

anchorage locations, and provides corrosion protection. The details outlined above apply to U.S. construction of non-replaceable tendons only. A review of replaceable tendons, as used in Europe, is provided later in this chapter. External tendons are considered unbonded since most of the tendon length is not attached to the concrete section and strains in the tendon are independent of strains in the adjacent concrete section.

1.2 Advantages and Disadvantages of External Post-Tensioning

Powell [2] presented a comprehensive review of the advantages and disadvantages of external prestressing. The following is a brief summary of Powell's observations.

<u>Advantages</u>

1) Concrete section is free of ducts:

   a) Thinner web sections can be used.

   b) The segment reinforcing cages can be assembled rapidly since placement and positioning of the ducts is no longer necessary and interference of the ducts with the reinforcement is eliminated. Segments can be standardized and fabricated more efficiently.

   c) Reduced congestion in the cross-section results in easier placement of concrete and better consolidation.

2) Access to the external tendon ducts is improved. This simplifies installation and grouting procedures and allows for tendon inspection and possible replacement. Furthermore, it is relatively simple to make provisions in the original design for adding supplementary tendons to counteract increased live loads or excessive stress losses in the original tendons.

3) Prestress losses due to friction are reduced. Losses from curvature friction are about the same as for internal tendons. However, wobble effects are effectively eliminated.

4) Conventional fatigue is significantly reduced since the unbonded tendon undergoes very little stress variation under service loads.

5) Corrosion protection for the continuous external tendon duct is more effective than for internal ducts which are discontinuous at segment joints. Furthermore, cracks in the superstructure do not have any consequences for the corrosion of the tendons.

6) Misalignment of internal tendon ducts at segment joints is eliminated.

4

7) Shorter-span segmental bridges can be constructed very rapidly using the span-by-span erection method.

Disadvantages

1) For a closed box-girder section, the external tendon eccentricities are limited to the inside surface of the top and bottom flanges. The limited eccentricity reduces the flexural efficiency of the box-girder section for both service and ultimate loads.

2) For an external tendon which is attached to the concrete section at the ends of the span only, the tendon strains at a given cross-section are not a function of the concrete strain at the level of the tendon. Consequently, tendon elongations must be determined from the deformation of the structure as a whole. Since strains in the unbonded tendon are distributed, theoretically, over the entire tendon length, stresses in the tendon at ultimate do not increase significantly over stressing levels. When the crushing strain is reached in the concrete at the critical section, the tendon stress is low, resulting in reduced flexural strength. Furthermore, for unbonded construction, flexural rotations which are concentrated at initial crack locations (or joint locations) result in premature crushing of the concrete and reduced ductility. These disadvantages are often theoretical, however, since tendon sizes are usually governed by service-level stress conditions, rather than ultimate conditions.

3) Tendon forces are transferred to the structure at deviation and anchorage locations only. Proper detailing for the diffusion of high local forces at these locations is critical since the failure of one of these elements could be catastrophic.

4) Misaligned deviation devices can lead to concentrated stress points on the external tendons and the possibility of fretting fatigue failure.

5) Unrestrained external tendons can vibrate under the passage of live load.

6) External tendons are vulnerable to the effects of fire and vehicle impact.

1.3 Flexural Behavior of External Tendon Girders

Externally post-tensioned girders have two ranges of behavior [3]. Up to the point of cracking of the cross section (or joint opening), the load deflection response of the structure is linear. After cracking, plastic hinges form at the critical joints and the structure behaves as a mechanism. The ultimate flexural strength is reached when the critical concrete hinge approaches its rotational capacity [4]. Since the ultimate state is reached by crushing of the concrete rather than by yielding of the reinforcement, the external tendon girder may fail in a non-ductile manner.

1.3.1 Before Cracking.   For an unbonded system, where the tendon is attached to the concrete at the end anchorages only, the tendon strain is not compatible with the strain in the adjacent concrete section. If friction between the tendon and duct is neglected, tendon strain is constant over the length between the anchorage points. The increase in tendon strain during loading can therefore be calculated from the total tendon elongation over the entire tendon length. This leads to relatively small increases in tendon stress under the application of service live loads.

1.3.2 After Cracking or Joint Opening.   In a segmental externally post-tensioned girder, a dry segment joint will begin to open when the initial precompression in the bottom flange is reduced to zero. At this point the girder begins to hinge at this critical section. If the segments are considered as rigid bodies, the tendon elongation can be calculated from the rotation or opening of the segments (or hinge) at the critical joint [4]. The increase in tendon stress can also be determined by considering the unbonded length of the tendon on either side of the hinge location. The ultimate flexural strength of the girder is then governed by the rotational capacity of the concrete at the hinge location. Bonding the tendons at discrete points along the span length (ie. at deviation locations) would reduce the unbonded length, and yield higher tendon stresses at critical sections and greater ultimate flexural strength for the girder.

1.3.3 Comparison between Bonded and Unbonded Systems.   Beams with external tendons exhibit lower ultimate strength and reduced ductility when compared to beams with fully bonded reinforcement. Figure 1.3 shows a theoretical moment deflection curve for a simple monolithic beam model with bonded internal tendons. It also shows test results for the same member with a combination of internal bonded tendons and external unbonded tendons, as well as results for unbonded tendons alone. This comparison illustrates the reduced strength and possible loss of ductility for the unbonded external tendon case. Other experimental studies have confirmed this trend [5,6,7].

As outlined above, flexural rotations in members with unbonded reinforcement are concentrated at a few large initial crack (or joint opening) locations and the ultimate strength is governed by the rotational capacity of the concrete at these locations. Early compressive failure at the top flange is typical (see Fig. 1.4). For segmental bridges, the absence of normal reinforcement across the open joints worsens the condition. Stresses in the unbonded tendons do not approach yield and consequently do not have a significant effect on the ultimate strength.

In a fully bonded system, before cracking or joint opening, the change in tendon strain is assumed to be the same as the change in the concrete section strain at the level of the tendon. After cracking, the tendon is fully bonded to the concrete on either side of the crack location and tendon stress increases result from the elongation related to the crack opening. This leads to large numbers of small, well distributed cracks, increased tendon stresses, higher ultimate strength, and improved ductility. The ultimate flexural strength

6

of the beam with bonded tendons is primarily controlled by the tendon properties and not by the concrete.
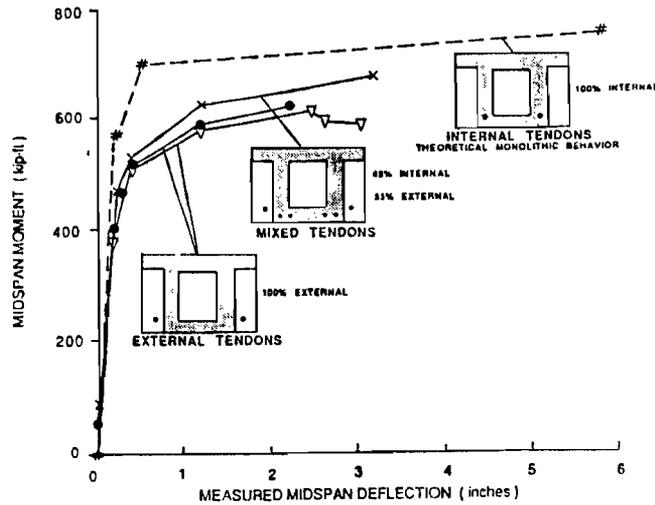
Notes:
Midspan Moment = dead load moment + applied load moment
Measured midspan deflection = deflection due to applied load only

— — # — Monolithic, bonded internal tendons (theoretical)
— • — Segmental, external tendons, dry joints, cement grouted ducts
— ▽ — Segmental, external tendons, dry joints, grease-injected ducts
— × — Segmental, mixed tendons, dry joints, cement grouted ducts

Figure 1.3   Reduced strength and ductility for external tendon case (from Ref. 2).

1.4 External Tendon - Deviator Details

1.4.1 Deviators.   The deviators are the critical element in an externally prestressed girder since, other than at anchorage locations, it is the only point of positive attachment of the external tendon to the concrete section (for U.S. practice). There are four primary types of deviators: (1) the diaphragm (see Fig. 1.5), (2) the stiffener or rib (see Fig. 1.6), (3) the saddle or block (see Fig. 1.7), and (4) prefabricated saddles (see Fig 1.8). The first three types are cast monolithically with the box-girder section and contain curved steel ducts which provide a pathway for the external tendon. The prefabricated saddles take various forms and are installed after the box section is cast. For cases where the external tendon geometry interferes with rib and diaphragm deviators, or intermediate diaphragms, blockouts are provided to permit the tendon to pass through freely (termed "pass-through" locations).

1.4.2 Bonded vs. Unbonded External Prestressing.   External prestressing tendon-duct systems that have been developed within the last ten years can be divided into two main classes:
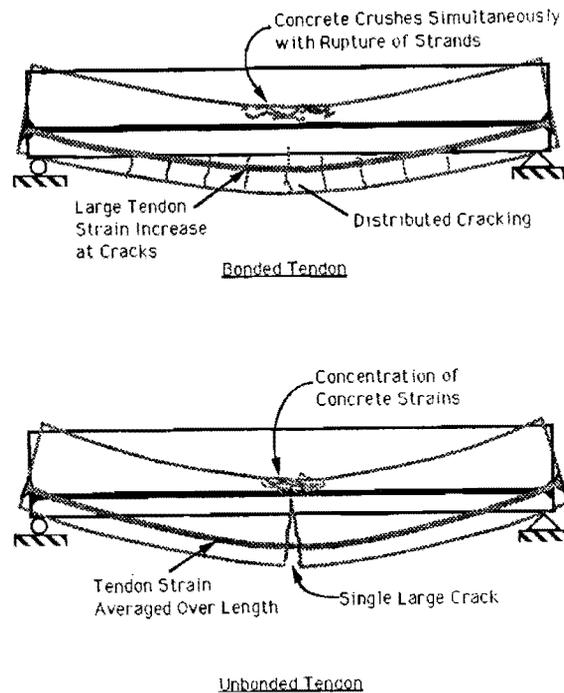
Figure 1.4   Reduced efficiency for unbonded tendons (adapted from Ref. 2).
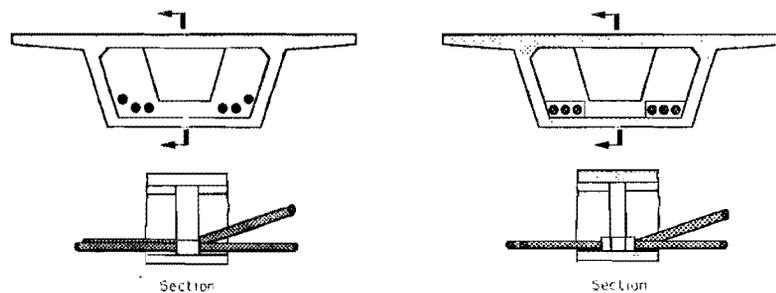
Figure 1.5   Typical shapes for diaphragm deviators (from Ref. 2).

- External prestressing bonded to the superstructure at a minimum number of points

- Unbonded external prestressing

Bonded external pre-stressing is used widely for bridges in the United States, while in Europe the majority of external tendon structures use unbonded external prestressing.

8

Mixed prestressing systems, which combine the use of bonded internal prestressing and external prestressing, are also widely used.

U.S. practice consists of bonding the external tendons at the end anchorages and at deviators within the span. Rigid steel ducts are embedded in the deviator blocks and are connected to HDPE (high density polyethylene) sheathing (see Fig. 1.9). The tendon is placed and grouted in the traditional manner and is bonded through the length of the deviator pipe by the cement grout.

In Europe, several methods of unbonded external prestressing have been used, all of which permit relatively simple replacement of the external tendons without demolition to the superstructure. Traditionally, non adhering tendon ducts were injected with grease or paraffin wax instead of cement grout. While this method is still used, the most common current French practice, as outlined by Jartoux and Lacroix [8], consists of continuous HDPE sheathing which is cement grouted. At the deviation and anchorage locations, the tendon is passed through the steel deviation pipes in a double duct arrangement (see Figs. 1.10 and 1.11). A new form of external tendon system has recently been developed from unbonded monostrand systems which are frequently used in building construction [8]. The tendon consists of wax coated mono-strands in individual HDPE sheaths, also placed within a larger HDPE duct (see Fig. 1.12). The duct is cement grouted prior to stressing the strands. The grout fills the voids and ensures proper spacing between the individual strand sheaths. This prevents potentially damaging contact stresses between the mono-strands at the deviation locations. The mono-strands are stressed individually and are replaceable. This system has the following advantages: (1) large tendons can be stressed with single strand jacks, (2) reduced friction at deviation points, and (3) better environmental protection [8].

1.4.3 Bond and Slip of Tendons at Deviators.
The ultimate flexural strength and ductility of an
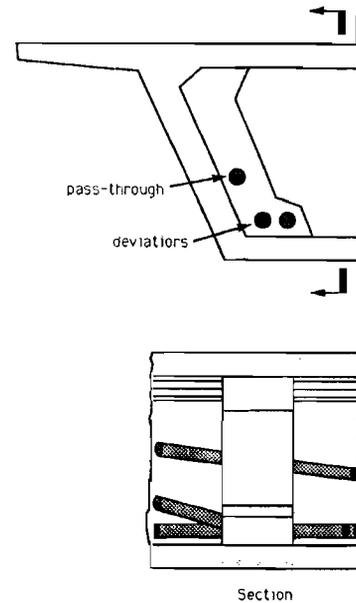
Figure 1.6   Typical shape for rib deviator (adapted from REf. 2).
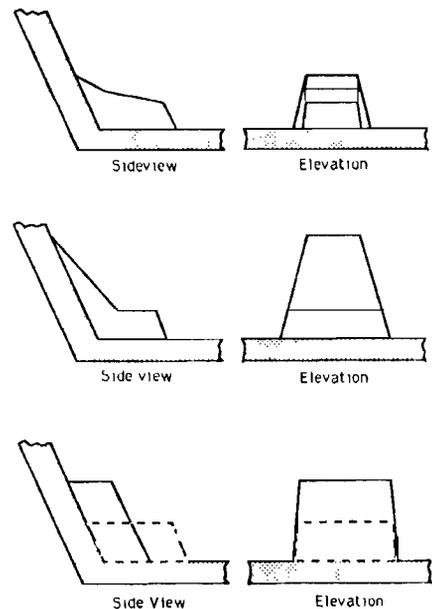
Figure 1.7   Typical shapes for deviator blocks (from Ref. 2).
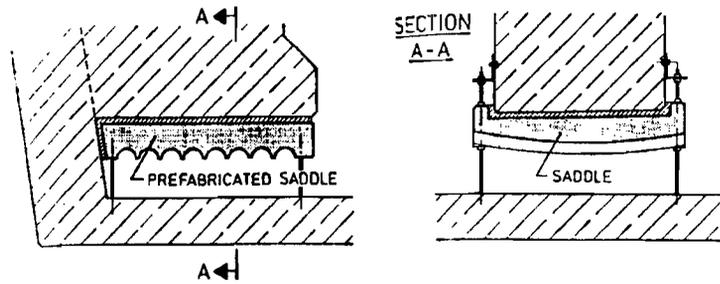
Figure 1.8   Prefabricated saddle block (from Ref. 8).
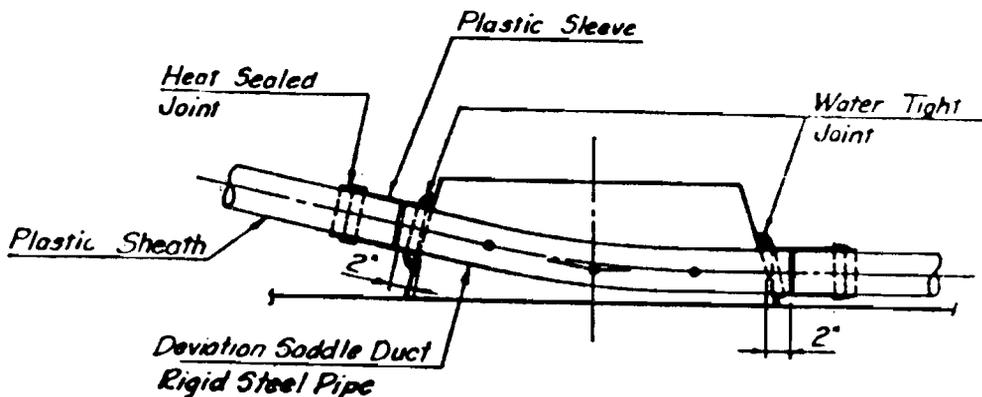
Figure 1.9   Duct-sheathing attachment (from Ref. 2).

external tendon girder can be improved by bonding the tendon to the concrete section at a number of discrete points along the span length (ie. partially bonded external prestressing). Bonding the tendon at deviator locations will reduce the unbonded length of the tendon and yield higher tendon stresses at critical moment sections, thereby increasing the flexural strength of the girder. Bonding at discrete points along the span will also distribute flexural deformations and improve ductility. However, in order for stresses in the external tendon to increase as anticipated, the tendon must remain bonded through the deviator during ultimate load conditions. For bonded external prestressing (US practice), this means that the stress differential in the tendon (difference in tendon stress on each side of the deviator) must be resisted by the bond of the cement grout through the deviator. This bond mechanism will be investigated in this report for curved and straight deviator pipes, using tendons which are stressed prior to grouting.

The slip of the tendon through the deviator duct is another important factor which affects the overall flexural behavior of an external tendon girder. The stresses developed in the external tendons depend not only upon the girder deformation between successive deviators, but also upon the slip of the tendons at these locations (see Fig. 1.13). Two basic assumptions can be used to obtain bounds for the solution. First, it can be assumed that the tendons slip freely at all deviators. This will yield the longest free length for the tendon,
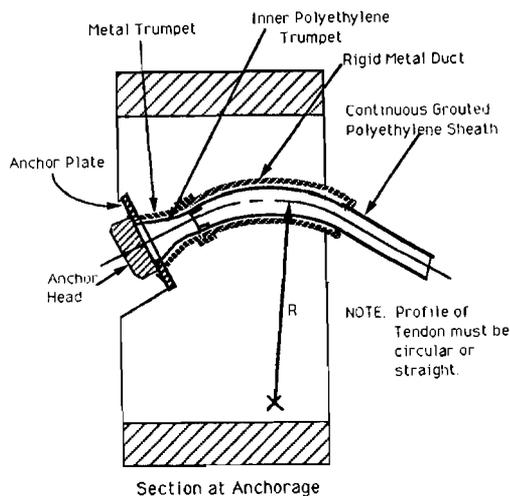
Figure 1.10   "Double duct" for replace-able tendons (from Ref. 2).

small tendon stress increases, and a lower bound estimate for the ultimate strength. The second assumption that can be made is that the tendons do not slip relative to the deviator. In this case an upper bound to the ultimate strength will be obtained. The actual behavior of a girder with discretely bonded external prestressing, however, lies between these two extremes and can only be determined by considering the bond-slip relationship of the grouted tendons. This report will investigate this relationship for cement grouted tendons. For unbonded external prestressing, such as the French double duct system, the effect of friction and slip between the tendon duct and steel deviation pipe must be considered.

1.4.4   Remedial Bonding of External Tendons.   This report is part of a larger study which included an investigation of the effects of improved bonding of external tendons for externally post-tensioned bridges. The research was conducted at Ferguson Structural Engineering Laboratory under the sponsorship of the Texas State Department of Highways and Public Transportation and the Federal Highway Administration. The scope of this investigation included the testing of a quarter-scale model of a three-span externally post-tensioned precast segmental box-girder bridge. The tendons in this structure were bonded at all diaphragm locations where the tendons were deviated (ie. by cement grouting). At all other diaphragm locations, the tendons were simply passed through the diaphragms. This setup was intended to model the tendon pass-through locations which occur in existing structures as outlined previously. Part of the

Figure 1.11   "Double duct" configuration at deviators (from Ref. 2).

investigation described herein consists of a preliminary satellite study to evaluate methods for bonding the external tendons at these diaphragm pass-through locations.

1.5   Objectives of Research

The primary objectives of this study are:

1) To determine the level of effective bond stress that can be developed through curved and straight deviators using current U.S. grouting procedures for bonded external tendons.

2) To establish a bond-slip relationship for grouted multi-strand tendons which can be used in a finite element program for the modelling of external tendon bridges.

3) To recommend limits for the effective bond stresses that can be developed through a deviator, and to recommend methods for remedial bonding of external tendons at diaphragm pass-through locations.

A secondary objective is to determine the coefficient of angular friction associated with galvanized steel deviator pipes.

1.6 Scope

PE pipe

Bundle of individually greased and plastic-sheathed strands

Cement grout

To fulfill the goals outlined above, three series of tests were performed. The first series consisted of direct tension bond-slip tests of six full scale tendon-deviator specimens. The principal variables investigated were the

Figure 1.12 Tendon consisting of HDPE sheathed monostrands, grouted before stressing (from Ref. 8).

deviation angles of the curved ducts and the ratio of prestressing tendon area to duct cross-sectional area. The second series involved the testing of a dismantled span of the box-girder bridge model outlined above. The tests consisted of successively cutting the external tendons and monitoring the stress differences across the diaphragm locations where the tendons were bonded. These tests are outlined in Chapter 3, Section 3.2. The final series consisted of testing various epoxy resin materials for the bonding of tendons at pass-through locations.

This report is organized as follows: Chapter 2 contains a review of pertinent literature on the general bond characteristics of prestressed strand, and more specifically, the bond-slip relationship of cement-grouted multi-strand tendons in steel ducts. Chapter 3 covers the experimental program and also includes test results. Test results are evaluated

12

and discussed in Chapter 4. Conclusions and general recommendations are summarized in Chapter 5. This report is based on the thesis of the senior author (53).
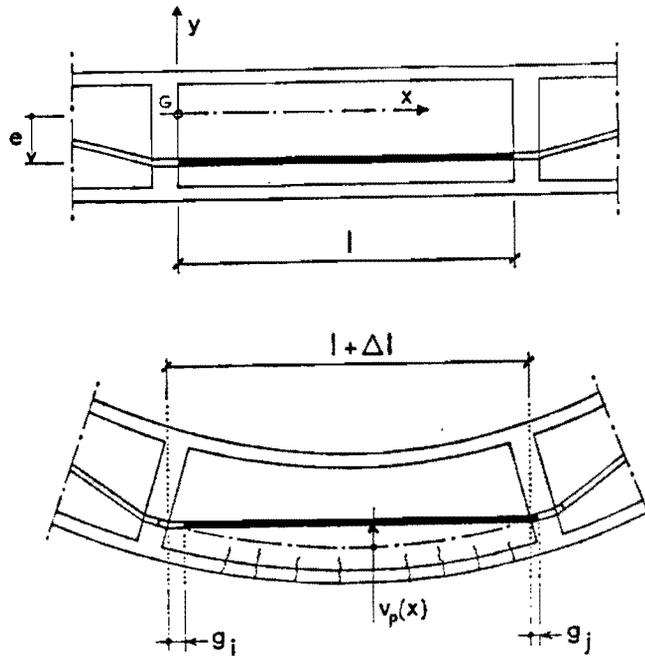
$$\Delta\sigma = E(\Delta l - gi - gj)/l$$

where $\Delta\sigma$ = Change in Tendon Stress
   E = Tangent Modulus of Tendon
   Δl = Elongation of Concrete Section at the Level
      of the Tendon
   gi, gj = Tendon Slip on Two Succesive Deviators
      l = Original Tendon Length Between Deviators

Figure 1.13   Deformation of external tendon (from Ref. 42).

CHAPTER 2

Literature Review and Background Information

2.1 Introduction

The ability of reinforced concrete to support load depends primarily upon the intimate linkage between the concrete and reinforcing steel. Effective transfer of force between the two materials is achieved by shear stresses (bond stresses) which act at the interface between the bar and the concrete and by bearing of the concrete on the lugs of the bar. Given its fundamental importance to many aspects of reinforced concrete behavior, a great deal of research effort has been expended investigating this bond mechanism for normal reinforcing steel and concrete. With the introduction of prestressed concrete, and particularly pretensioned concrete which depends totally on bond for strand anchorage, considerable research emphasis has also been placed upon the bond characteristics of various types of prestressing steels. Recent developments in partial prestressing have also made the bond performance of grouted post-tensioning tendons an important consideration. This chapter provides background information on the bond characteristics of seven-wire prestressing strand. It specifically focuses on experimental results related to strand pullout tests and the bond-slip relationship of cement grouted multi-strand tendons in steel ducts.

2.2 Bond Characteristics of Prestressing Strand

2.2.1 General. In a pretensioned member, two aspects of bond between the prestressing steel and the concrete must be considered. The first relates to the transfer of the prestressing force from the strand to the concrete over a certain distance from the ends of the member. The mechanism which accomplishes this function is known as transfer bond, and the length over which the strand force is transferred is defined as the prestress transfer length. In a pretensioned flexural member, the prestressing steel also serves a second function similar to that of ordinary reinforcement in concrete. That is, it develops bond stresses as a result of loads applied externally to the member. For a fully prestressed concrete member in an uncracked condition, these stresses are negligible. However, if flexural cracking occurs, the strand stress increases above the effective prestress level, and high flexural bond forces develop between the strand and concrete in the vicinity of the cracks (for a bonded strand).

A similar situation exists for a segmental post-tensioned bridge with discretely bonded external tendons. For a segmental structure with dry joints between segments, flexural bond stresses are developed between the external tendon and the grout throughout the length of a deviator pipe after the initial precompression in the extreme segment fibers is reduced to zero (decompression load) and the dry segment joints begin to open. Similarly, for a segmental structure with epoxied joints, these bond stresses develop after the cracking

13

tensile stress is exceeded and the cracks begin to open. For loads less than the decompression or cracking loads, the tendon stress increases are negligible (see Section 2.2.3) [3,6]. Beyond these load levels, however, the tendon stresses increase as shown in Fig. 2.1. Initially, the increased loads and moments are resisted primarily by an increase in the internal lever arm between the tensile force in the tendon and the compressive force in the concrete section. When the concrete compressive stresses are concentrated in the top flange of the concrete section, additional moments at the section must be resisted by increased tendon forces (see point C in Fig. 2.1) [3]. If the segments are considered as rigid bodies, the tendon elongations can be determined from the rotation of the segments at the joint. The tendon stress increases can also be calculated by considering the unbonded length of the tendon on either side of the joint location and the increase in moment at a particular section. At ultimate load, tendon stress differences developed across the deviators are resisted by flexural bond stresses between the strand and grout at deviator locations (for U.S. practice).

There are three main factors which contribute to bond between prestressing strand and concrete: adhesion, friction, and mechanical resistance. The first component, adhesion, can only be present if no slip has taken place between the steel and concrete. For example, in the prestress transfer zone of a pretensioned girder, the reduction in steel strain does not equal the compressive strain in the concrete at the same section [9]. Since there is relative movement, or slip, between the steel and concrete, adhesion is destroyed and cannot contribute to prestress transfer bond. Transfer bond is primarily due to a mechanical interlock (Hoyer effect) and friction. The Hoyer effect occurs as stress in the pretensioned strand is released. At the now unstressed end of the tendon, the diameter of the strand increases due to the Poisson effect, and a high radial pressure is exerted on the surrounding concrete. This produces a "wedging" action and high frictional resistance in the transfer zone. In addition, some degree of mechanical resistance is developed as the strand slips in the transfer zone and the pitch of the strand changes with respect to the surrounding helical impression in the concrete [10].

Flexural bond stresses develop away from the transfer zone for beams which have been loaded to cracking, as outlined above. High local bond stresses in the vicinity of cracks cause slip to occur over a small portion of the strand length adjacent to the crack (see Fig. 2.2). This slip destroys adhesion between the strand and concrete and reduces the maximum available bond stress [9]. As slip progresses from the center of the beam to the end, adhesion is eliminated and the remaining bond is provided by friction and mechanical resistance [10].

Flexural bond stresses occur in a pretensioned member when the prestressing steel and the concrete are loaded in tension. For a strand loaded in tension, it would be expected that the radial contraction associated with elongation would reduce the frictional resistance developed between the strand and concrete. The strand elongation, however, changes the pitch of the helical wires with respect to the impression in the concrete and causes increased normal and frictional forces which tend to compensate for the effect of the

a. TENDON STRESS RESPONSE

b. KEY POINTS FOR TENDON STRESSES
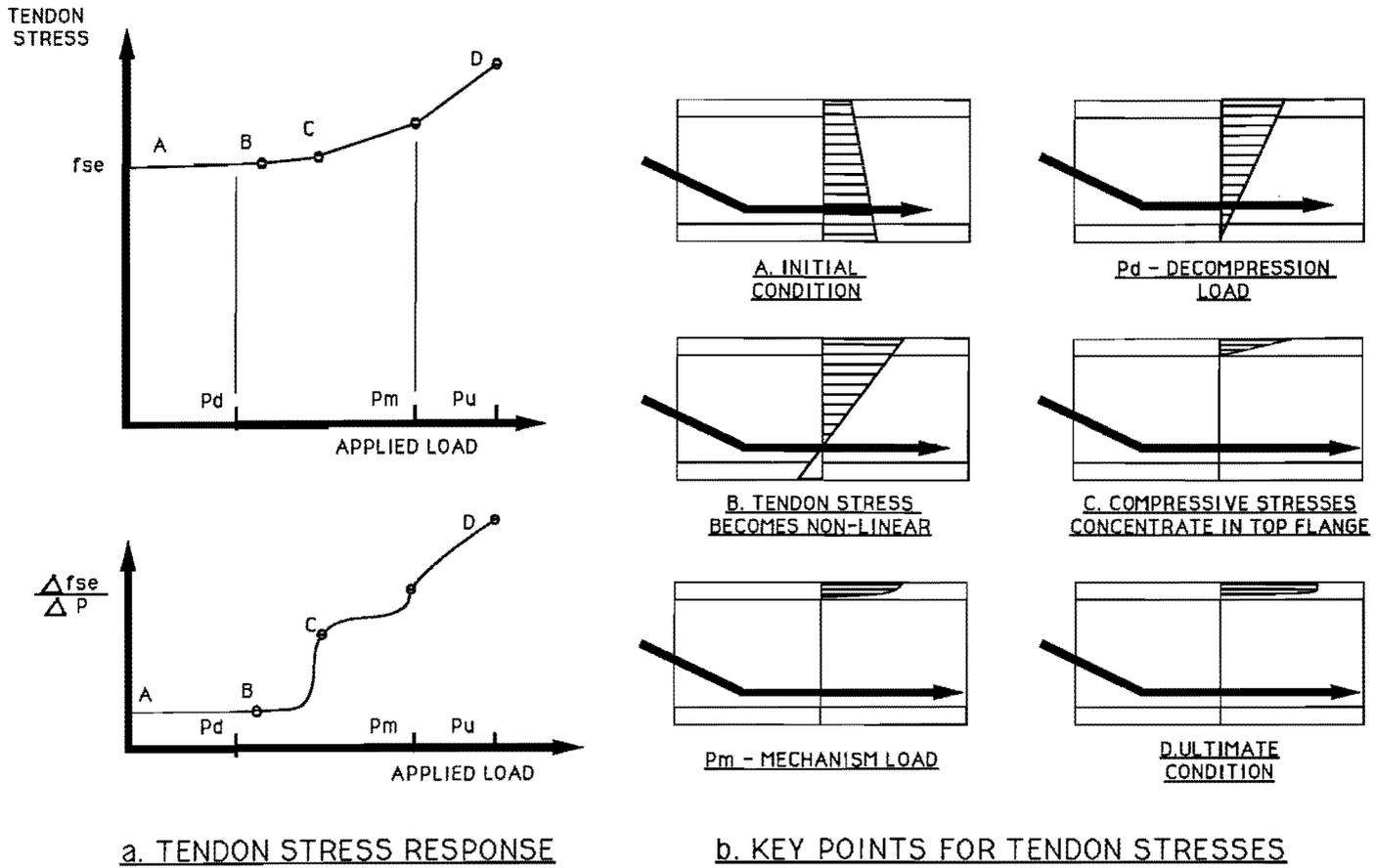
Figure 2.1   Tendon Stress Response to Applied Load (From Ref. 3)

16

contraction [11]. The center wire of the seven wire strand is held in position by lateral pressure exerted by the exterior wires which tend to straighten under tension. As the strand pitch changes, it also provides a means of mechanical interlock which prevents the strand from unscrewing as it slips through the concrete. However, in comparison to deformed reinforcing bars, which have ribs or lugs, the helical wire pattern of the strand does not provide positive mechanical resistance.

2.2.2 Physical Characteristics of the Bond Mechanism. The results of many experimental investigations have shown that the bond mechanism between prestressing strand and concrete (or grout) is extremely complex and influenced by a number of variables. Among the most fundamental, the following can be cited:

Figure 2.2   Distribution of stress and local slip along cracked element.

1)   Concrete (or grout) consolidation around the strand surface. Stocker and Sozen studied the effect of concrete consistency on bond performance of seven-wire strand [12]. A constant concrete strength was used and slump was varied by changing the fine and coarse aggregate ratios. The high slump concrete achieved the greatest bond strength. It was concluded that the favorable bond characteristics developed by the high slump concrete could be attributed to higher compressive shrinkage stresses which caused increased contact stresses on the strands. The effect of concrete settlement and bleeding on bond strength was also studied. Specimens were cast with concrete depth below the strands varying from -30 inches. Using the two-inch depth as a reference, the average bond stress was reduced by approximately 35% for concrete depths greater than ten inches. Anderson and Anderson also concluded that the primary cause of poor bond performance was inadequate concrete consolidation and bleeding [13].

2)   Surface condition of the strand. Test results indicate that flexural and transfer bond performance of rusted strand is up to 30% better than that of strand with a clean bright surface [9,10]. Strands coated with oil do not exhibit any significant reduction in transfer or flexural bond performance [13].

3)   Concrete (or grout) strength. Among the available body of research data, conclusions about the effect of concrete strength on bond are inconsistent. The most comprehensive study was carried out by Karr et al. [14]. It was concluded that

concrete strength had practically no influence on transfer length for strand sizes up to 1/2 inch diameter (with concrete strengths varying from 1660 to 5000 psi). These results were confirmed by other studies of beam flexural bond and pullout tests [9,11]. On the other hand, the strand pullout test results of Stocker and Sozen [12] demonstrated a 10% increase in bond strength for each 1000 psi increase in concrete strength (for strengths varying from 2400-5000 psi). Assuming that concrete (or grout) strength does not vary significantly, however, it appears that the effect of concrete strength on bond performance may be ignored.

4)   Strand size.   Results of studies by Salmons [11] and Stocker and Sozen [12] have shown that average pullout bond stresses are not affected by variations in strand size from 1/4 to 1/2 inch diameter. Hanson and Karr [10] concluded that strand size had a considerable influence on average transfer bond stresses. In another report, transfer bond stresses for 0.6 inch diameter strand were found to be on average 20% greater than those obtained for strand sizes of 1/2 inch diameter or less [14].

5)   Concrete/Grout confinement.   Factors which influence the degree of confinement of concrete surrounding the strand, such as the amount of confining reinforcement, strand spacing, and concrete cover, have a significant impact on the bond stresses since they influence the cracking of concrete or grout around the strand. For the tests described in this report, the strands were grouted within rigid steel ducts which were considered to provide optimal confinement.

6)   Rate of loading.   Test results for strand released suddenly by flame or saw cutting, as compared to slow release, have shown up to a 20% reduction in transfer bond strength for 1/2 inch diameter strand and a 30% reduction for 0.6 inch diameter strand [14]. Reinhardt [15] found that the loading rate did not significantly affect pullout bond behavior of strands.

7)   Cyclic or alternating loads.   Trost et al. [16,17] conducted a very comprehensive study of bond performance of cement grouted prestressing strands in steel ducts. This report included results of cyclic load tests of four-0.6 inch diameter strand bundles as shown in Fig. 2.3. The cyclic loads were applied by stressing the tendon to a specified displacement (at the live end) and then unloading to the initial undisplaced position. This load cycle was repeated five times for each level of displacement. Figure 2.3 shows the bond stress values obtained at each level of displacement for each of the five load cycles. By comparing the average monotonic loading results (dashed line), to the cyclic response (solid lines), it can be seen that significant deterioration in bond capacity takes place even during the first load reversal. Furthermore, for large slips, the bond stress approaches a constant value associated with internal friction, independent of the number of cycles. Similar results have been obtained for normal reinforcement [18]. The question arises as to whether or not tendons bonded at deviators of externally post-tensioned bridges will be subjected to cyclic loads. This question is investigated in Section 2.2.3. As
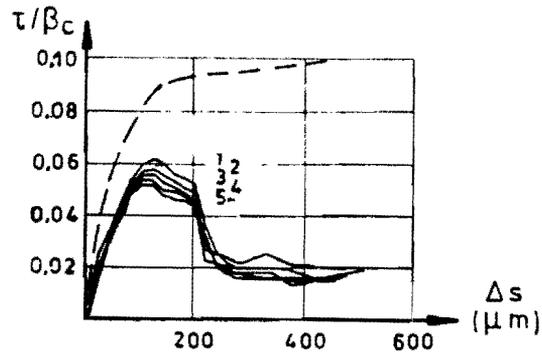
Test Series B-9 (4-0.6"Strands in the Middle of the Duct)
Fpu= 1770 Mpa (257 ksi)
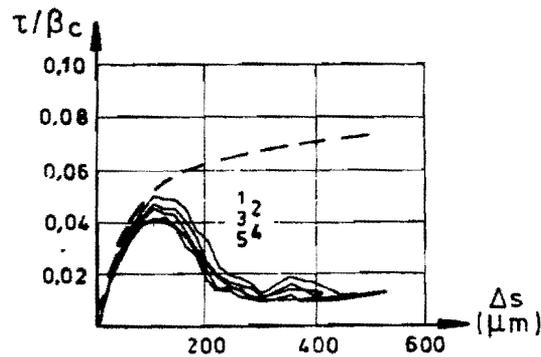
Test Series B-10 (4-0.6" Strands Adjacent to Duct wall)
Fpu= 1770 Mpa (257 ksi)

βc= Grout Cylinder Strength (Avg.= 55 MPa (8.0 ksi))

Δs= Loaded end slip

τ= Bond Stress (MPa)

Figure 2.3   Grouted tendon bond-slip performance under alternating tension [from Ref. 17 (Trost)].

outlined in Section 2.2.3, external tendon stress reversals are negligible for loads below either the joint or crack opening loads, or the factored design load (for both discretely bonded and unbonded external prestressing). Furthermore, tendons do not slip at deviators for the same load levels (see Section 2.2.3). Consequently, cyclic loading was not considered for the tests described in this report.

8)   Strand Slip.   Bond stresses occur wherever strains in the concrete and steel are not equal over a particular length of strand. After local loss of adhesion, the strain differential gives rise to relative local movement, or slip, between the steel and
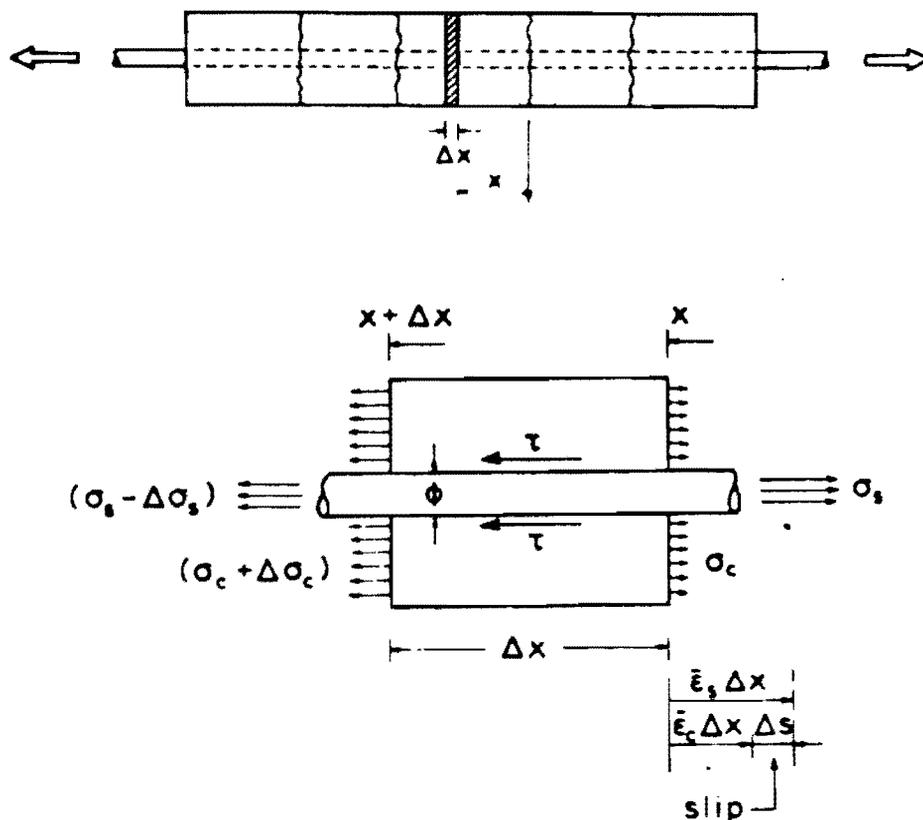
Figure 2.4   Strand slip due to differential strain (from Ref. 20).

concrete (Fig. 2.4). A unique relationship exists between local bond stress and local slip at every point along the embedded strand. Therefore, bond stress is always associated with slip. Furthermore, the magnitude of slip has been shown to have a significant influence on bond stress [16,17,19,20,21,22]. A bond-slip relationship for grouted multi-strand tendons is covered in Section 2.6.

2.2.3 Cyclic Loads. For normal design live loads, tension variations will occur in external tendons at deviators of externally post-tensioned bridges. In general, a differential in tendon stress (the difference in tendon stress on each side of the deviator) is developed as the live load is applied. The deviator is also subjected to alternating tension (from the difference in tendon stresses) as the liveload passes from one side of the deviator to the other. The increases in tendon stresses are negligible, however, for total loads up to the joint or crack opening loads (for both unbonded or discretely bonded external prestressing). Recent bridge model tests at The University of Texas investigated the strength and ductility of a three-span externally post-tensioned bridge model with both unbonded and discretely bonded external tendons [3,6]. At the critical joint location, tendon stress increases ranged from 3 to 4 ksi above initial stress levels for loads up to the factored design dead load plus live load. Maximum increases of only 3 ksi were measured at the decompression load level in a dry-jointed span. In addition, the external tendons did not slip at the deviators for the same load levels (for the unbonded tendon case, this means that the friction developed between the strand and duct was sufficient to prevent slip). It is important to note that the 1983 AASHTO factored design load includes a factor of safety of approximately 1.6 to 2.0, depending upon the relative ratio of dead load moments to live load plus impact moments. ie.

$$\text{Design Load} = 1.3 \times DL + 1.3 \times 1.67 \times (L+I)$$

where   DL   =   dead load

           L+I   =   live load plus impact

For short spans where the live load constitutes a large portion of the total load, the factor of safety is higher, while for long spans it would be lower. For normal unfactored service loads, tendon stress increases ranged from only 1 to 2 ksi in the bridge model tests. This means that for deviators located near the center of a simple span (the location of maximum live load moment and tendon stress increase) an alternating tendon stress increase of at most 2 ksi would occur as the live load vehicle passed from one side of the deviator location to the other. Although the bridge model results may not cover every design case, it appears that significant stress increases (and reversals) can only occur for very extreme overloads.

Despite the insignificant stress increases outlined above, the possibility of tendon fatigue may still exist for cyclic loading. Small ranges of tendon stress, combined with minimal tendon slip through the ducts, may potentially result in fretting fatigue failure at the deviator locations. Alternating loads may also cause progressive damage to the grout at the deviator. A parallel study is currently being conducted at Ferguson Laboratory to explore these topics.

For extreme overloads the external tendon will be subjected to significant tension loading at the deviator locations. For this ultimate case, however, a single load cycle is appropriate.

2.3 Previous Studies of Single-Strand Specimens

2.3.1 Introduction. One objective of this investigation was to provide data applicable to the specific flexural bond conditions which exist between the external tendon and deviator during ultimate loading (these bond conditions are outlined in detail in Section 3.1.2). Previous research for this specific case is limited. Fortunately, however, pullout tests of straight cement-grouted tendons (or strands) in steel ducts model the deviator bond conditions quite closely. Pullout test results for strands in concrete blocks are also pertinent. This section focuses primarily on the results of pullout tests of initially untensioned single-strand specimens which are bonded directly in concrete blocks or grouted inside steel conduits. Essential results from other single-strand tests with different bond conditions are also included for comparison. Single-strand tests represent an upper bound on the bond performance and are therefore important for evaluating test results of multi-strand cases. Pullout tests for multi-strand tendons in steel ducts are outlined in Section 2.4. Unless otherwise noted, 270 ksi seven-wire strand will hereafter be referred to simply as strand. First, a brief review of pullout test specimen response is presented.
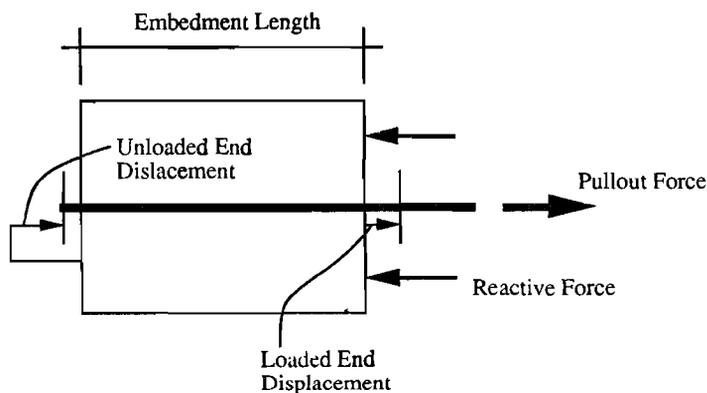
Figure 2.5 Typical pullout specimen.

2.3.2 Pullout Tests. In a typical bond pullout test, the strand (or bar) is embedded in a concrete block as shown in Fig. 2.5. The concrete block is held in place by a reaction plate at the end of the specimen where the strand is loaded. Tests with normal reinforcement have shown that confining effects of the reactive compression force can have a significant influence on the pullout response. Various specimens and testing arrangements have been developed to eliminate this effect (see Fig. 2.6). Since the strand is in tension and the concrete is in compression, high differential strains cause slip at the loaded end for low load levels or even immediately upon loading in most cases. Relative slip is commonly measured at the loaded end (or live end) and at the unloaded end (dead end). Slip is initiated at the loaded end and progresses towards the unloaded end as the tension load is

increased. General slip is defined as the point where slip on the unloaded end of the strand is sufficient to produce a measurable reading.

Test results are usually presented in terms of pullout force and loaded end slip. A problem arises, however, in the interpretation of these results. Stocker and Sozen [12] have shown that the distribution of differential strain, and corresponding slip, between the steel and the concrete is not linear along the bonded length. Furthermore, in general, the local bond stress (bond force per unit bonded area) is a non-linear function of local slip. Since the slip varies along the bonded length, the bond stress distribution is non-linear as is the distribution of the steel stress. In general, the variation in bond (and steel) stress is most pronounced for long embedment lengths and low load levels. For higher loads, and shorter bonded lengths, the stress distribution tends to become more uniform. In order to interpret test results when only pullout force and loaded end slip are measured, the distribution of bond stress and slip along the bonded length must be known or assumed. Most test results assume either a constant bond stress or a stress which varies from a maximum value at the loaded end to zero at the unloaded end (see Fig. 2.7). The overall bond-slip relationship, obtained in this manner, does not represent the true local bond-slip behavior but is only be valid for the assumed stress distribution and specific bonded length that is used (since the magnitude of the loaded end slip is the integration of the differential strain over the bonded length). Care must be taken when comparing test results based upon different bonded lengths or assumed stress distributions [12]. Furthermore, since bond stress generally increases with increasing slip (up to the point of maximum bond stress), it is important to know the value of slip for which the bond stress is quoted. The bond-slip
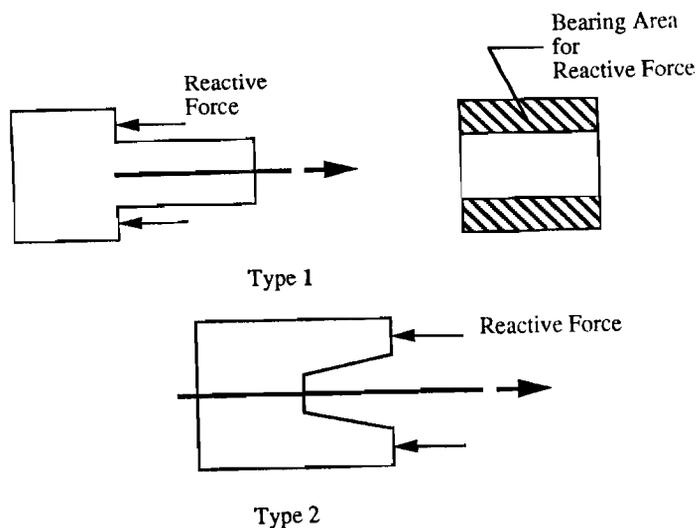
Figure 2.6 Modified pullout specimens.

response of grouted multi-strand tendons is outlined in Section 2.6.

In order to investigate the true local bond-slip relationship, very short (1 inch) bond lengths have been used for pullout specimens [12,23]. Testing short lengths assures essentially uniform slip and a constant bond stress which approaches the maximum bond that can be obtained. For longer embedments, the average bond stress is based on high adhesion stresses over a portion of the length, and lower stresses over portions where slip has occurred. Consequently, pullout tests on long strands give only the average bond stress and slip at the strand extremities. Specimens with long embedment lengths will yield lower average bond stresses than short bond specimens [19].

The drawback of the normal pullout test is that compression in the concrete prevents transverse tension cracking from occurring around the strand. This cracking has been shown to reduce the average bond stress that can be developed [19,24]. For tests of strands grouted in steel ducts, however, the duct isolates the bond region from the concrete and limits the compression that can be transmitted to the grout block around the strand. This compression is limited by the shear that can be transferred at the concrete-to-duct interface.

When interpreting the results of pullout tests it is necessary to determine the interfacial bond area of the prestressing strands or tendons. One method uses an equivalent strand (or tendon) diameter based on the strand (or tendon) area, as outlined below.

Figure 2.7   Bond and steel stress distributions along bonded length.

$$d_e = \sqrt{\frac{4}{\pi}A}$$

$$p_e = \pi d_e$$

$$U = p_e L$$

where d_e =   equivalent strand (or tendon) diameter

p_e = equivalent strand (or tendon) perimeter (circumference)
U = equivalent bond area
A = prestressing steel area
L = bonded length

For a 1/2 inch (nominal) diameter strand for example, the equivalent strand diameter is 0.44". For single strands, bond areas calculated using this method are approximately 40%

$$d_v = \sqrt{\tfrac{4}{\pi} \cdot A_v} = 1,13 \cdot \sqrt{A_v}$$

$$u_i = \pi \cdot d_v = 1,13 \cdot \pi \cdot \sqrt{A_v}$$
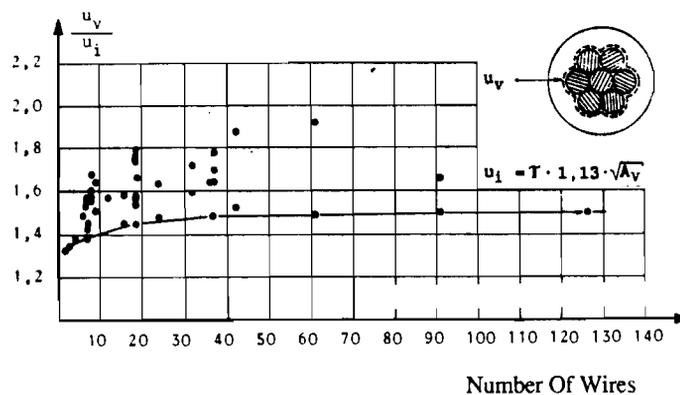
Uv= "Actual" Bond Cirumference
Ui= Equivalent Bond Circumference

Figure 2.8   Ratio of actual bond circumference to equivalent circumference (from Ref. 17).

less than the actual interfacial areas (see. Fig 2.8). Trost [16,17] used "actual" bond areas based on calculations which are outlined in Appendix A. Bond areas based on the nominal strand diameter typically yield values between these two extremes.

2.3.3 Burnett and Anis.   Burnett and Anis [25] performed pullout tests of initially untensioned 3/8 inch diameter prestressing strands which were anchored in uncracked concrete and grout blocks (see Fig. 2.9). Based on test results of single-strand specimens of constant grout quality and strand size, a pullout force-pullout displacement behavioral model was developed as shown in Fig. 2.10. The six behavioral modes shown in the figure are based upon varying embedment lengths. For long embedment lengths ($l_e > 150 \, d_b$), failure occurs by rupture of the strand without significant pullout displacement and prior to
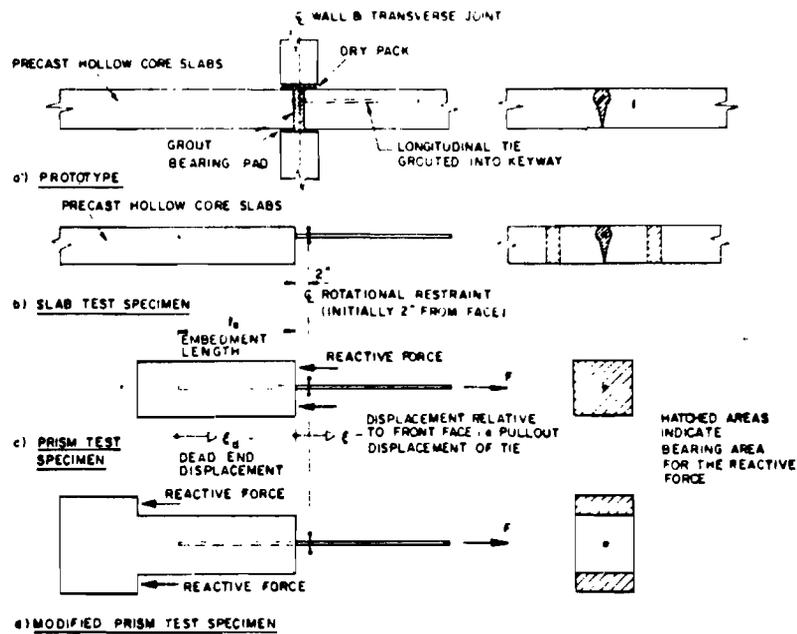
Figure 2.9   Pullout tests by Burnett (from Ref. 25).
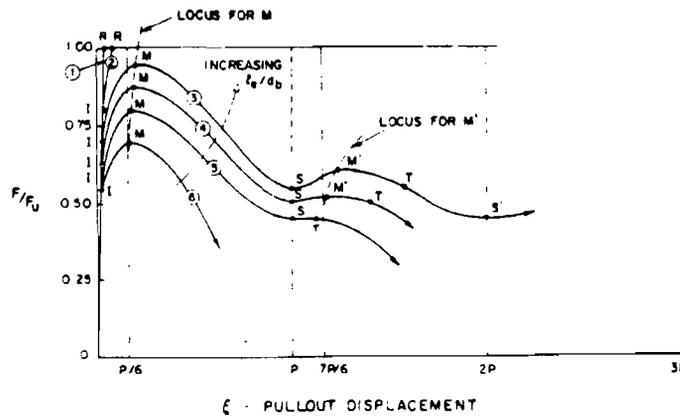
Figure 2.10   Pullout force vs. displacement by Burnett (from Ref. 25).

the initiation of general slip (Model 1). As embedment length decreases, relatively stable continuous pullout occurs after overall slip is initiated. The maximum pullout force is achieved at a pullout displacement equal to one-sixth of the strand pitch. This displacement, at point M, is independent of the strand embedment length and grout quality.

From stress measurements along the strand, it was observed that at the point of overall slip (point I), the distribution of tensile stress was essentially linear along the embedment length. Since the steel stress decreased linearly from the loaded end, the bond

stress was considered to be constant along the strand length engaged in resisting pullout (at the point of overall slip). By assuming the nominal bond stress to be proportional to the square root of the concrete cylinder strength, f_c', and the interfacial bond area, $(l_e p_b)$, proportional to $(l_e d_b)$, the following equation was proposed for the pre-slip pullout force, F_I.

$$F_I = K l_e p_b \sqrt{f_c'}$$

where K = 25 for 3/8 inch 270 ksi strand
       l_e = embedded length of strand
       p_b = nominal perimeter of 7-wire strand
       d_b = nominal strand diameter

The nominal strand perimeter was noted to be equal to 4/3 d_b. This value appears to have been quoted in error. The test results indicate that the nominal strand perimeter was taken as 4/3(πd_b). This appears to be an estimate of the actual strand perimeter (see Fig. 2.8).

For the 30 inch embedment length, with a constant bond stress distribution and a nominal strand surface area based on the nominal strand diameter, the 3/8 inch single-strand test results indicate an average nominal interfacial bond stress of 0.47 ksi at the onset of general slip and a maximum value of 0.60 ksi. These values are compared to other research results in Section 2.3.9.

2.3.4 Salmons and McCrate.   Salmons and McCrate investigated the use of untensioned prestressing strands as normal anchorage reinforcement between precast elements [11]. The bond behavior was studied to establish the load-embedment and load-deformation characteristics of the strand. Pullout tests were conducted for single, straight, 1/2 inch diameter strands with embedment lengths ranging from 5 to 45 inches (with three specimens for each length). In order to minimize compression effects in the concrete surrounding the single strands, and to eliminate confining effects of reactive forces on the loaded face, a special test specimen was developed (see Fig. 2.11). For single-strand pullout tests, strand displacement (slip) was measured at the loaded and unloaded end of each specimen. Since displacements were found to be dependent upon duration of the load, a closed loop hydraulic system was used to maintain a constant load while the displacements stabilized. Both initial and stable slip readings were obtained.

Test data was presented in terms of applied steel stress versus loaded end slip for varying embedment lengths and strand end conditions as shown in Fig. 2.12. Curves in the figure are based upon a polynomial fit of the bond pullout data only (all other failure modes were not included). The points shown at 4, 5, 10, 16, 20 inch etc, indicate the point where general slip commenced for the various embedment lengths. It was concluded that the relationship between loaded-end steel stress and slip was independent of the embedment length. For longer embedment lengths, however, the value of stress at general slip

STRAND

SUPPORT

SUPPORTS

LOAD
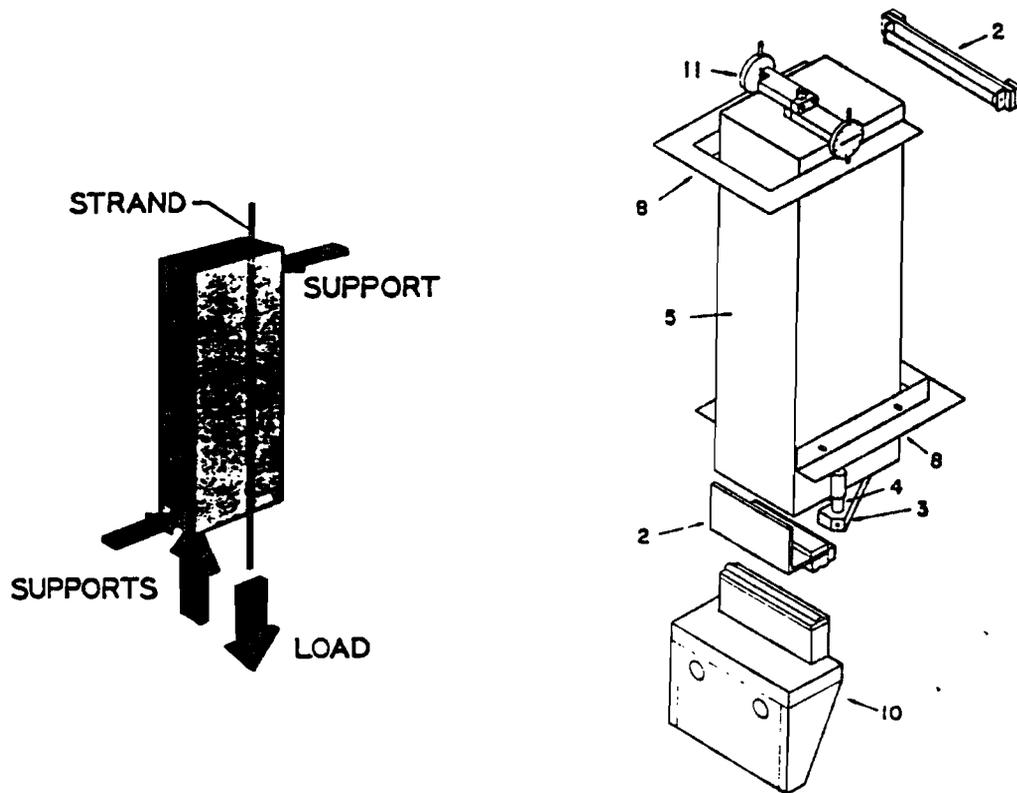
1 Strand Vice	5 Straight Specimen	9 Leveling Device
2 Support	6 Bent Specimen	10 Corbel
3 Equilateral Triangle	7 Clevis	11 Displacement Dial
4 Differential Transformer	8 Bracket	

Figure 2.11 Test apparatus used by Salmons and McCrate (from Ref. 11).
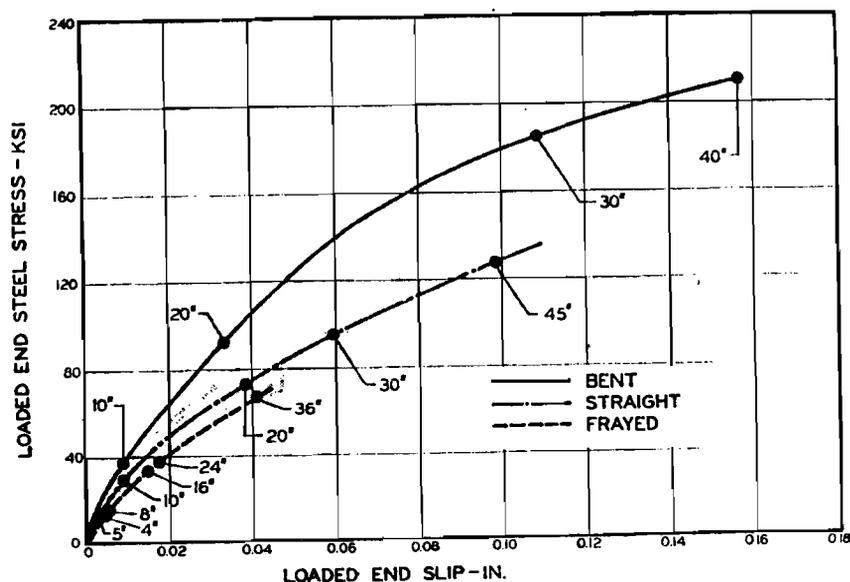
Figure 2.12 Steel stress vs. slip for Salmons and McCrate (from Ref. 11).

increased. Furthermore, the influence of strand diameter and concrete strength were also studied and shown to have a negligible effect when steel stress and slip were considered. The test data was also evaluated in terms of the nominal bond stress. The results in this case were much less meaningful than those based on loaded-end steel stress.

Strand test results were compared to pullout tests of high strength deformed reinforcing bars. Ferguson et al. [24] tested bars with yield strengths greater than 100 ksi which were enclosed in steel spirals. The steel stress-slip relationship of straight 1/2 inch diameter strand was shown to be similar to a #14 bar.

Based on the mean results of the 1/2 inch diameter strand tests for the 30 inch embedment the nominal bond stress was calculated to be 0.35 ksi at the point of general slip with a maximum value of 0.64 ksi. These values are also shown in Section 2.3.9.

2.3.5 Naus. Naus conducted pull-out tests of 1/2 inch diameter single strand specimens grouted inside 1-1/4 inch diameter smooth metal conduit [26]. The principal variables investigated were the level of prestressing (50, 60, and 70% of ultimate strand strength) and the type of grout material (shrinkage-compensating cement, polymer-silica cement, and commercial grout).

The straight strand conduit was cast in a concrete block which was contained within an outer six inch diameter cast iron pipe. The outer pipe was used as a mold during concreting and prevented concrete splitting during testing. Test specimen fabrication included: (1) placing three previously cast concrete blocks in a stressing bed, (2) positioning

the strand in the center of the conduit, (3) stressing the strand, and (4) grouting the strand. Seven days after grouting, strand tension was released and the strand was cut on either end of the specimen. Consequently, strand ends were unstressed during testing. Strand displacement was measured at the loaded end where a reaction plate was placed against the face of the specimen. The load-slip test results for the 29 inch embedment length are shown in Fig. 2.13 for conventional grout. The highest bond strength was achieved by the specimen with the lowest prestress level. No explanation was given for this effect. However, the release of the higher prestress prior to testing could have caused the greatest slip and subsequent damage to the adhesion developed by the grout. Despite this, the higher prestress should have also produced increased radial stresses and frictional forces.
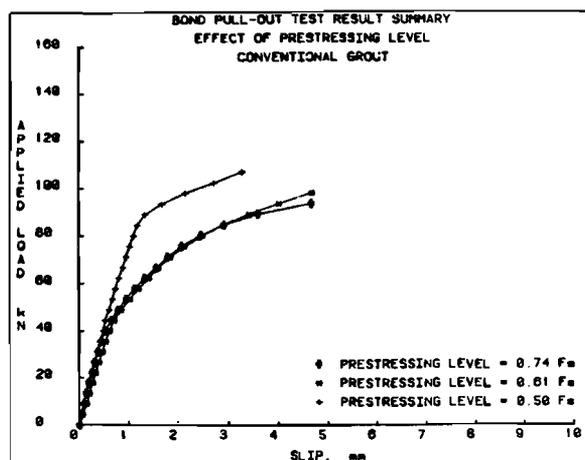
Figure 2.13   Load vs. slip for conventional grout [from Naus (Ref. 26)].

The test results indicated that:

1)   The bond developed by the polymer silica cement grout was superior to that developed by the other grout mixtures for all levels of prestressing.

2)   Both conventional grout and shrinkage compensating cement grout exhibited a reduction in bond strength for increasing levels of prestress.

Since slip was not measured at the unloaded end of the specimen, it is difficult to calculate a nominal bond stress value at the point of general slip. The test results do indicate a maximum bond stress value of 0.45 ksi (using the nominal area of the strand and the uniform stress distribution outlined previously).

2.3.6 Schupack and Mizuma.   Schupack and Mizuma investigated the bond characteristics of high strength, helically grooved, prestressing bars which are commonly used in Japan [27]. Pullout tests were conducted on 9.2 mm diameter helically grooved bars, and results were compared to tests of "equivalent" 250 ksi seven-wire strands (3/8 " or 7/16" diameter). The test specimens consisted of a single bar, or strand, embedded in a concrete cylinder as shown in Fig. 2.14. Displacement was measured at the unloaded end only. Based on the results of three tests for each strand size, the nominal interfacial bond stress, at general slip, was calculated to be 0.35 ksi for the 7/16" diameter strand and 0.44 ksi for the 3/8" strand. Maximum bond stresses were 1.01 ksi and 1.34 ksi (for the 7/16" and 3/8" diameter strands respectively). Bond stresses reported by the researchers were based on the
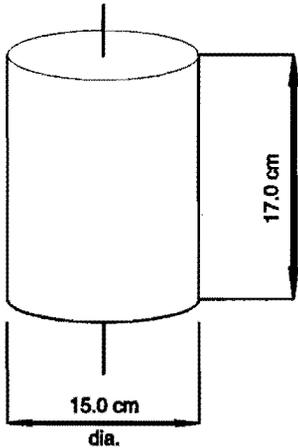
Test Specimen for Pull Out Test
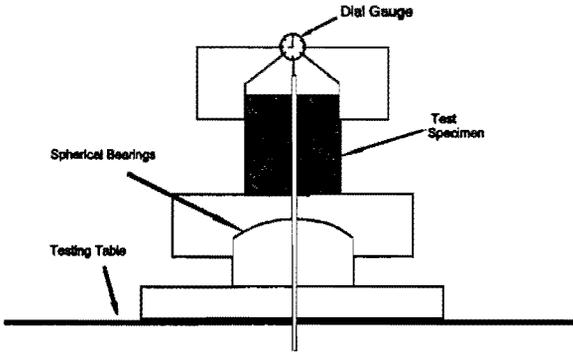
Test Setup for Pullout Test

Figure 2.14   Pullout tests by Schupack et al. (from Ref. 27).

actual calculated interfacial area. The values noted above have been adjusted to nominal surface area for comparison. These results were compared to pullout tests at the University of Illinois [12] for 7/16" diameter, 270 ksi strands. Based on an equivalent bond length, bond stresses for the Illinois tests were on average 0.41 ksi at the point of general slip, with a maximum value of 0.60 ksi (for tests which were stopped at 0.01 " tail-end slip). The values at general slip compare very favorably. These bond stresses are summarized in Section 2.3.9.

2.3.7 Stocker and Sozen.

Stocker and Sozen conducted a very comprehensive investigation of bond characteristics of prestressing strand in concrete [12]. The experimental program included simple pull-out tests of single-strand specimens with bonded lengths varying from 1.0 to 20 inches. Slip was measured at the unloaded end (tail-end) for bonded lengths less than two inches, and at both ends for longer lengths. Short bond lengths were used to investigate the local bond-slip relationship of the strand. Testing short bond lengths assured essentially uniform slip and a constant bond stress distribution. Average bond stress results for longer specimens, however, resulted in approximately the
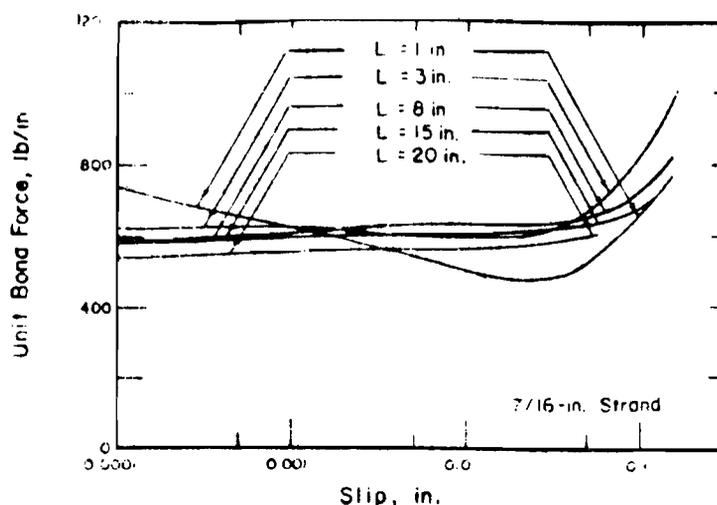
Figure 2.15   Unit bond force vs. tail-end slip for different bonded lengths [from Stocker and Sozen (Ref. 12)].

same unit bond force, or bond force per unit length (see Fig. 2.15). The left axis of the logarithmic slip scale does not indicate zero slip. It represents the smallest displacement that could be measured as slip progressed. The bond-slip relationship is essentially bi-linear up to a tail end displacement of 0.15 inch as shown in Fig 2.16. The average bond stresses for these tests have been outlined above (ie. Illinois tests).

2.3.8 Tests by VSL International.

At the request of VSL, Rostasy [28] conducted pullout tests of single 0.6 inch diameter strands embedded in concrete. The test specimens were similar to those used by Trost et al. However, the strands were not placed in steel
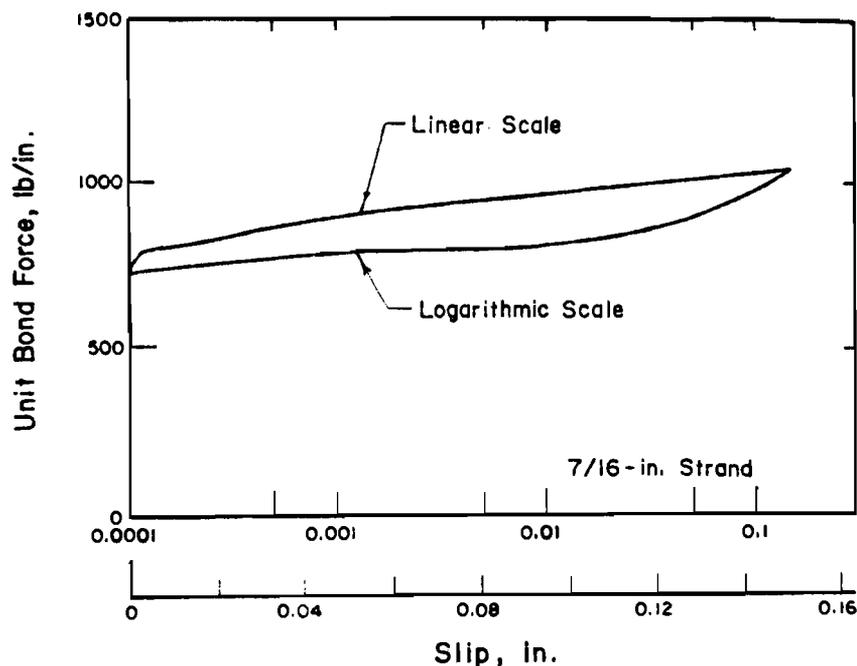
Figure 2.16   Bond-slip relationship for 7/16" strand with slip values plotted to linear and logarithmic scales [from Stocker and Sozen (Ref. 12)].

conduits (see Section 2.4.2). The following formula was proposed for the bond stress:

$$T_v = 0.09 \times \beta_w$$

where T_v =   concrete bond stress in kg/cm^2

β_w =   28 day concrete cylinder strength in kg/cm^2

(1kg/cm^2 = 98.06 KPa = 14.22 psi)

For example, for 5000 psi concrete, a bond stress of 0.45 ksi is obtained. This equation was based on a conservative lower bound estimate of the bond stress since the values were to be used in design. Consequently, the bond stress values obtained from the formula correspond closely to the general slip condition which is also a lower bound estimate of the ultimate bond capacity.

2.3.9 Summary. The single strand results for monotonic pullout tests are summarized in Table 2.1. The bond stresses are based on a uniform stress distribution along the bonded length. The nominal strand diameter was used to calculate the nominal perimeter and bond surface area.

A number of observations can be made regarding the test results presented in the table. Despite the wide variety of test conditions, (ie. bonded lengths and strand sizes) bond stress values are very uniform for the general slip case. The bond stresses at general

Table 2.1 Single Strand Bond Performance

Source	Strand Size (inches)	Bond Length (inches)	Concrete or Grout Strength (psi)	Bond Stress at General slip (ksi)	Maximum Bond Stress (ksi)
Burnett/Anis	3/8	30	3780	0.47	0.60
Salmons/McCrate	1/2	30	6010	0.35	0.64
Naus	1/2	29	-	-	0.45
Schupack/Mizuma	7/16 3/8	6.7 6.7	4680 5280	0.35(1) 0.44(1)	1.01(1) 1.34(1)
Stocker/Sozen	7/16	3-20	5280	0.41(3)	0.6(3)(4)
Osborne (2)	3/8	24	5830	-	0.43(3)
Braverman (2)	3/8	12	-	-	1.19(5)
VSL	0.6	-	5000	0.45	-

(1) Test results adjusted from "actual" bond area to nominal.
(2) Tests outlined in Section 2.4.
(3) Test results based on an estimate of the actual stand perimeter (4/3 nominal). Results adjusted to nominal perimeter.
(4) Test stopped at 0.1" tail-end slip.
(5) Maximum bond stress achieved at large slip (0.6")

slip vary by at most 14% from the mean value of 0.41 ksi (coefficient of variation of 0.125). The maximum bond stress values are influenced to a greater extent by the bonded length. In general, the tests with shorter bonded lengths (ie. Schupack/Mizuma and Braverman) exhibit higher ultimate bond stresses (as expected). If these two cases are not considered, the remaining maximum bond stress values compare very favorably. The results also indicate considerable reserve bond stress beyond the point of general slip for all cases. This reserve capacity is due to the mechanical bond resistance developed by the strand after general slip has occurred. This is an extremely important characteristic of strand bond performance (in contrast to smooth wires). It suggests that relatively stable pullout can be achieved with sufficient warning of distress. However, this observed characteristic may not be valid for cyclic loads.

2.4 Previous Studies of Multi-Strand Tendons

2.4.1 Introduction. The most direct way to investigate the bond performance of multi-strand tendons is to test full-scale specimens. Although these tests are more difficult and expensive than single-strand tests, they are the only way to evaluate the complex bond conditions which exist for various types of tendons and steel ducts. In general, for a single-strand pullout test, bond failure will occur at the strand-grout interface. For a multi-strand

tendon, on the other hand, failure may also occur at the duct-grout surface, depending upon the ratio of the tendon to duct areas and type of duct that is tested. Furthermore, the bond performance is also influenced to a greater extent by the geometry, compactness, and location of the tendon in the duct. For curved tendons, the tight grouping of strands and lateral pressure due to curvature may also reduce the ability of the grout to penetrate the grouping. This section presents the results of pullout tests of initially untensioned tendons which were grouted in steel ducts.

2.4.2 Trost. Trost investigated the bond performance of initially untensioned prestressing tendons which were cement grouted in straight corrugated steel ducts [16,17]. This study included pullout tests of four different seven-wire strand tendons ranging from 3 to 19 strands, as outlined in Table 2.2.
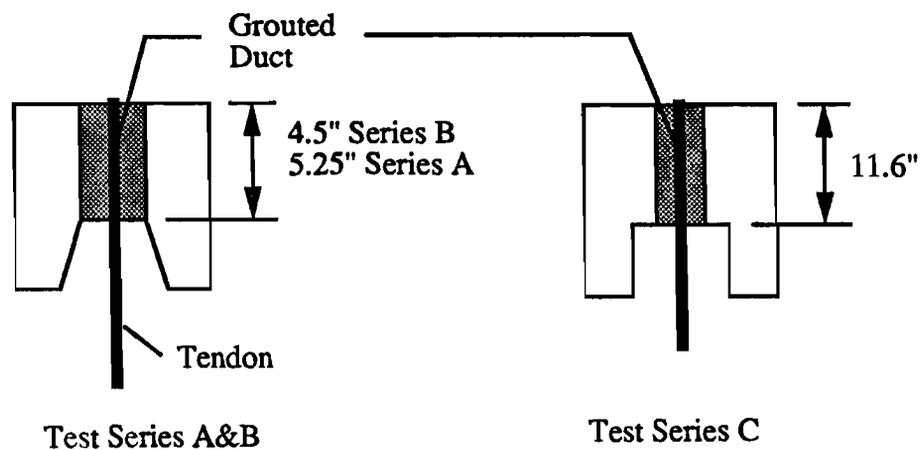
Figure 2.17 Pullout specimens tested by Trost (from Ref. 17).
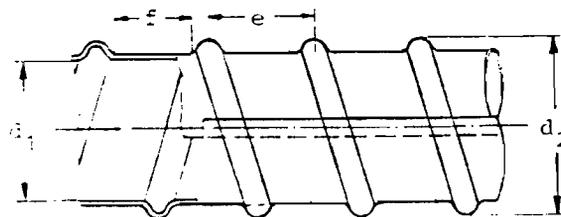
Figure 2.18 Steel duct detail for tests by Trost (from REf. 17).

Test specimens and duct details are shown in Figs. 2.17 and 2.18. The loading apparatus for test series A and B is shown in Fig. 2.19. This apparatus was capable of both monotonic and cyclic loading. The results reported here are for the monotonic case only. For series A and B, slip was measured at the loaded and unloaded ends of the specimen. For test series C, specimens were anchored by a reaction plate and the tendon was pulled

Table 2.2 Tendon Tests by Trost

Test Series	A-9	A-10	C-4	B
Strand Pattern				
Strands/Size	4-0.6"	4-0.6"	19-0.6"	3-0.6"
Steel Area (in^2)	0.864	0.864	4.104	0.648
Equivalent Steel Diameter(in)	1.05	1.05	2.28	0.908
Equivalent Bond Circumference(in)	3.3	3.3	7.16	2.85
Actual Bond Circumference(1) (in)	6.3	7.56	14.36	4.55
Bonded Length(in)	5.25	5.25	11.6	4.5
Equivalent Bond Area (in^2)	17.3	17.3	83.1	13.0
Actual Bond Area(in^2) (1)	33.1	39.7	166.7	20.5
Number of Tests	4	4	3	1
Duct Diameter (inside/outside) (in)	1.77/1.96	1.77/1.96	3.54/3.85	1.57/1.77
Steel Area/ Duct Area - %	35	35	41	33
Test Details	Tendon in Center of Duct	Tendon Against Duct Wall	Tendon in Center of Duct	Tendon in Center of Duct

(1) Actual bond perimeter is based on approximate calculation outlined in Appendix A.
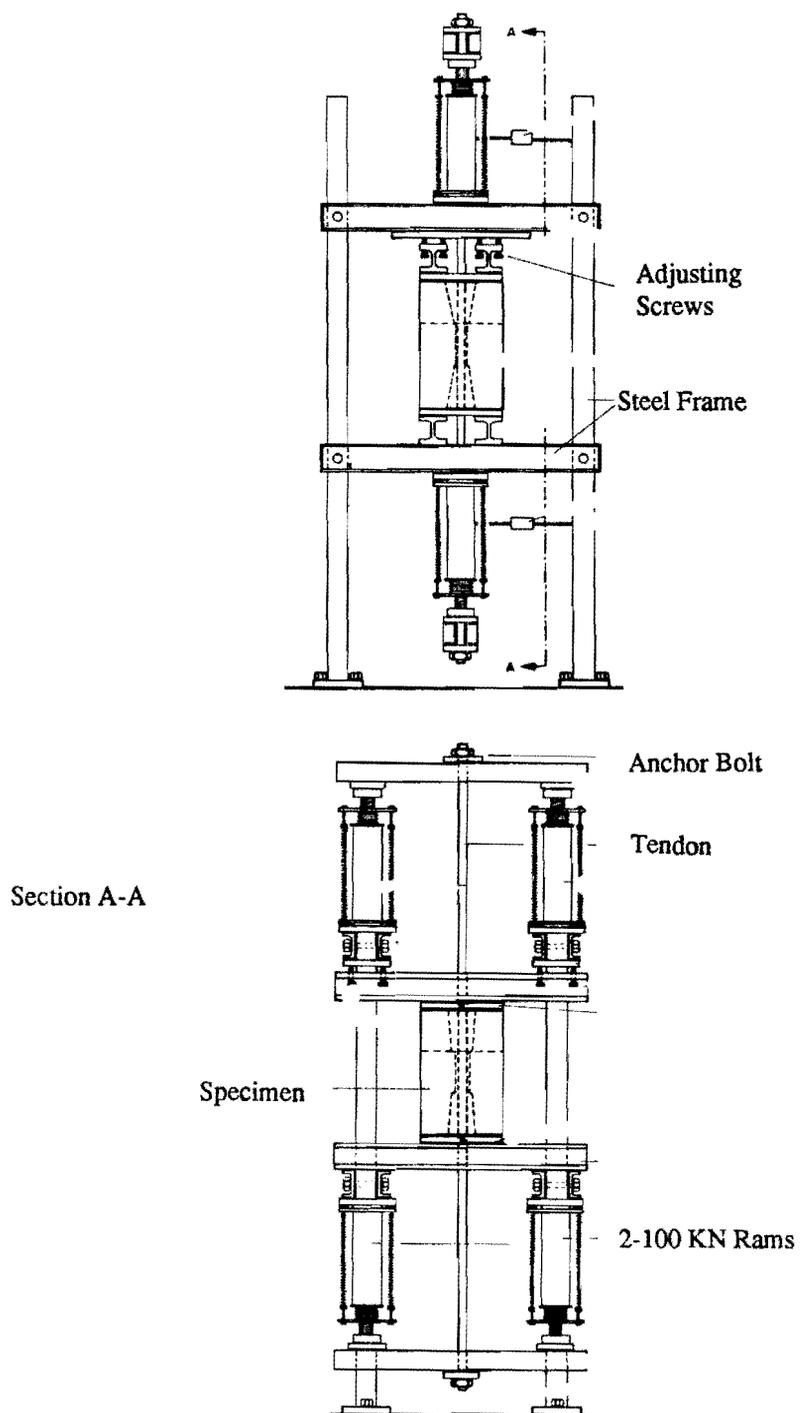
Figure 2.19   Test apparatus for Series A & B [from Trost (Ref. 17)].

through the grout by a moving grip as shown in Fig. 2.20. Tendon slip was measured at the unloaded end of the specimen only for test series C. For all cases, specimens were loaded at a rate of 2.0 Kn per second and the tests were stopped when slip at the unloaded end reached 2 mm (0.08").

Load-slip responses for test series A are shown in Fig. 2.21. Trost concluded that bond developed by the tendon against the duct wall was on average 68% of the value obtained for tests with the tendon in the center of the duct. The eccentric tendon also exhibited greater slip. In both cases, relatively stable pullout occurred. Bond stresses shown in the figures are based on a uniform bond stress distribution using the calculated "actual" bond areas (see Appendix A). These results are also shown in Table 2.3.

Table 2.3 Test Results for Trost

Test	Average Grout Strength (psi)	Average Bond Stress at 0.1mm unloaded end slip (1) (ksi)	Average Bond Stress at 0.5mm unloaded end slip (1) (ksi)
A-9 (4-0.6")	8090	0.64	0.81
A-10 (4-0.6")	8225	0.42	0.58
C-4 (19-0.6")	5180	0.52	-
B (3-0.6)	7370	0.81	1.20

(1) Based on "actual" calculated bond area (see Appendix A)
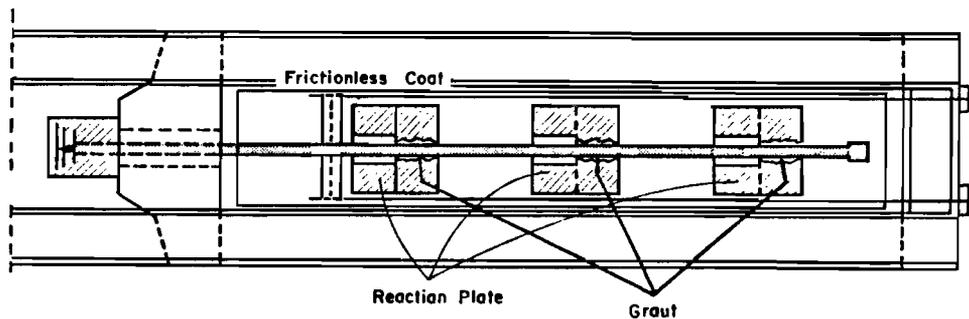
Figure 2.20 Test apparatus for series C [from Trost (Ref. 17)].

38
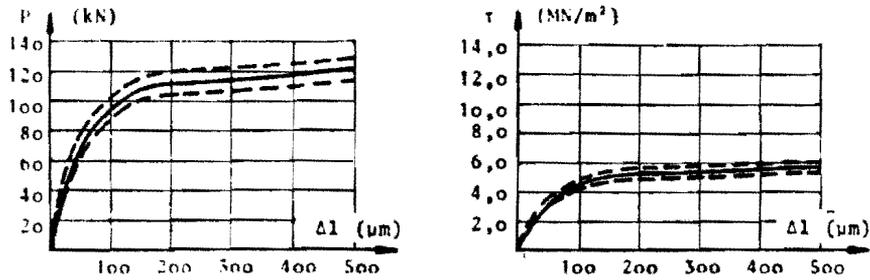
Test Series A-9 (4-0.6"Strands in the Center of the Duct)
Fpu= 1770 Mpa (257 ksi)
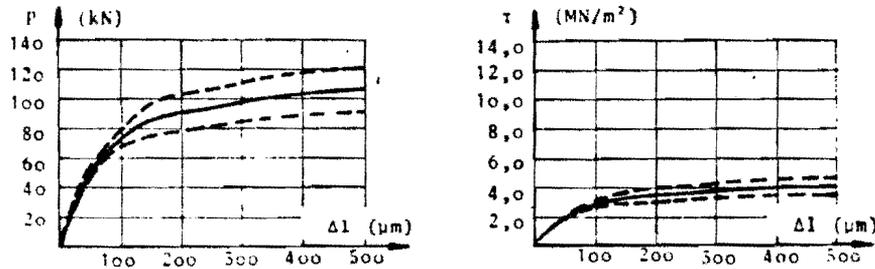
Test Series A-10 (4-0.6" Strands Adjacent to Duct Wall)
Fpu= 1770 Mpa (257 ksi)

Δl = Unloaded end slip

τ = Bond Stress (MPa)

P= Pullout Load (KN)

Figure 2.21   Grouted tendon bond-slip performance under monotonic loading for test series A [from Trost (Ref. 17)].

The results of test series C are shown in Fig. 2.22. For these tests, the mode of failure is of particular interest. At relatively insignificant unloaded- end displacements (0.1-0.3 mm), bursting cracks formed in the grout and the bond failed suddenly (for all three tests). Stable pullout could not be achieved.

Series IV 19-0.6" Strands
Fpu=1770 Mpa (257 ksi)
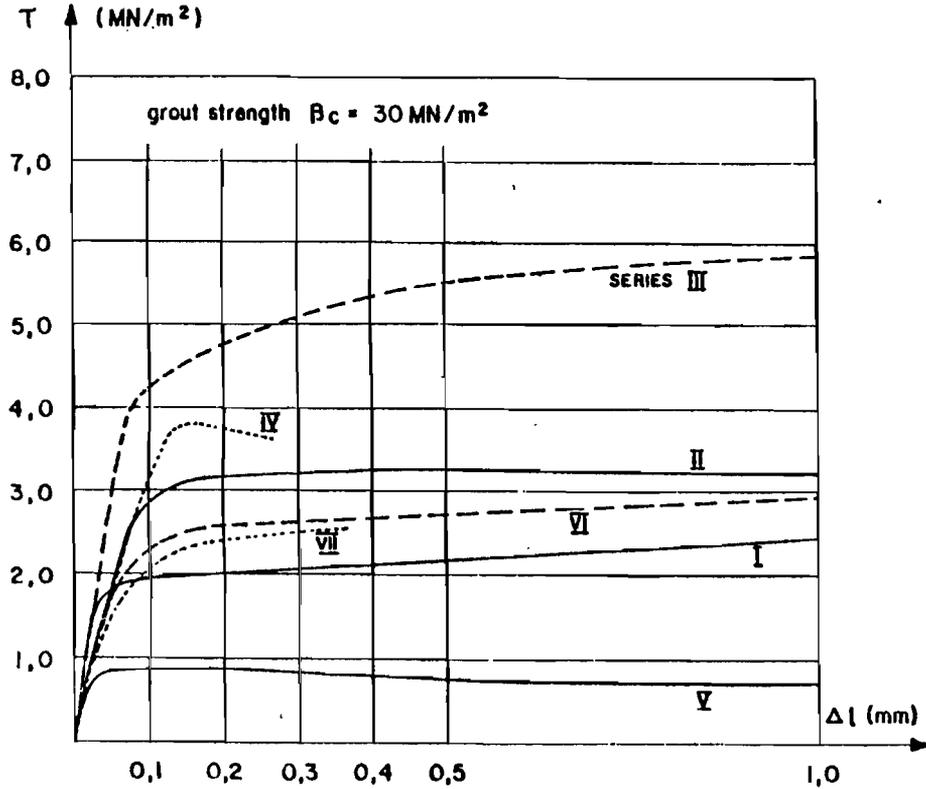
Figure 2.22   Grouted tendon bond-slip performance under monotonic loading for test series C-IV [from Trost (Ref. 17)].

2.4.3 Osborne.   Osborne conducted 13 pullout tests of unstressed 3/8 inch strand bundles grouted inside straight 2 inch diameter steel pipes [29]. The principal variable investigated was the ratio of the tendon area to the duct area. Tendons were composed of 1, 3, 5, 7, and 11 strands with corresponding tendon areas ranging from 3 to 30 percent of the duct cross-sectional area. The tendons were positioned in the center of the ducts for all tests. Slip of a single strand was measured at the top (loaded end) and middle of the specimen using slip wires attached to the strand and at the unloaded end using a dial gauge. Test results were presented in terms of nominal bond stress and unloaded end slip.

Osborne observed that the maximum bond stress between the strand and the grout was obtained for a ratio of tendon area to duct area of approximately 0.14. When the tendon area exceeded 18 percent of the duct area (ie. 7 and 11 strand tendons), bond failure occurred between the duct and the grout and the bond stress was reduced significantly (the grout pulled away from the duct surface). Maximum bond stresses for the three and five strand tendons were 0.52 ksi and 0.69 ksi respectively. These stresses were based on tendon perimeters which were taken to be 4/3 of the nominal value (an estimate of the actual bond area).

2.4.4 Braverman. Braverman [30] conducted pullout tests similar to those of Osborne. Tendons containing 1, 3, and 5-3/8 inch strands were tested in 1-1/2 inch diameter smooth ducts with a 12 inch embedment length. The tendon areas correspond to 5, 14, and 24% of the duct cross-sectional area. Strand instrumentation was similar to Osborne's tests.

For the three strand case, the maximum bond stress was 1.1 ksi (average of two tests). This stress was calculated using tendon bond areas based on the nominal strand perimeter multiplied by the number of strands (ie. without consideration of strand bundling). The five strand tendon failed at the duct-grout interface at a significantly reduced load.

2.4.5 Related Tests. Private engineering firms have conducted specific bond pullout and load transfer tests of large tendons grouted in steel or plastic ducts. These tests are required prior to the use of the tendons in grouted rock anchors, nuclear containment structures or large bridges. Some of these tests are briefly outlined below.

a) Test by Shupack and Johnston [31]. The bond development length of a curved post-tensioning tendon was investigated. The tendon, containing 54-1/2 inch strands, was positioned in a flexible 5-1/2 inch diameter duct which was cast inside a curved concrete beam. After stressing and grouting, the tendon stress was released and the bond transfer length was determined by measuring the change in concrete strain along the tendon. The transfer length was approximately 10 feet. The average bond stress, corresponding to this transfer length, has been calculated to be 0.19 ksi [28]. This stress was based on a very conservative estimate of the bond area. (ie. the equivalent strand perimeter multiplied by the number of strands). Examination of cut tendon sections indicated good grout penetration.

b) Test by Losinger (VSL International) [32]. A pullout test was conducted for a rock anchor containing 52-0.6 inch strands. The tendon was grouted inside a straight 273 mm (10.7") diameter smooth steel tube with a bonded length of 10m (32.8 ft). The duct was cast in a concrete block which covered only 4m (13.1 ft.) of the pipe length. At a load of 874 tonnes (1926 kips), the tendon elongated by 1/2 inch and the grout block displaced one inch out of the steel pipe. Considering the failure mode, the average bond stress obtained at the duct-grout interface is calculated to be 0.15 ksi.

During testing, strain gauges were used to monitor stresses in 10 of the 52 strands. The maximum stress variation in the gauged strands was 7%.

c) Tests by VSL [28]. Under the supervision of Rostasy, VSL conducted a pullout test of a tendon containing 16-1/2 inch strands. The tendon was grouted within a ribbed polyethylene duct (3.15" I.D./3.75" O.D.). At a load of 225 tonnes (496 kips) the grout failed. The bond stress was calculated to be 0.22 ksi (using a conservative bond area equal to the equivalent strand perimeter multiplied by the number of strands). The bond developed at the ribbed duct interface was 0.46 ksi. It was concluded that the polyethylene pipe could effectively transfer the prestress force to the concrete section. VSL had similar tests conducted in the United States for the Sunshine Skyway Bridge [33]. From these and other tests it was concluded that transfer of bond force at the duct interface was rarely a problem, except possibly for smooth steel pipes.

2.5 Limitations of Previous Research

Previous studies outlined above have not completely addressed three particular aspects of the bond conditions which exist between external tendons and deviator pipes. First, these tendons are commonly bonded at the deviators through curved rather than straight steel ducts. The adequacy of the bond mechanism for curved ducts has not been investigated in previous studies. In addition, no pullout tests have been conducted on tendons which have been stressed prior to grouting. Although transfer bond and beam flexural bond tests model this aspect quite accurately, these tests are typically conducted on single strands embedded in concrete only. Very few transfer bond tests have been conducted for multi-strand tendons stressed prior to grouting in steel ducts [similar to Reference 31]. For curved steel ducts, this aspect may be important since the stressed tendon will impose radial forces through the duct which could affect the bond transfer mechanism. In addition, for tendons stressed prior to grouting, the ability of the grout to penetrate the compressed strand bundle is a concern which has not been investigated. Finally, other than tests of small tendons conducted by Trost, previous studies have used strands or tendons which are positioned in the center of the straight duct rather than adjacent to the duct wall. For the case where the tendon is adjacent to the duct wall in the curved regions of the deviator, the bond conditions are more adverse. The tests described herein are a preliminary investigation of these specific bond conditions which exist at deviators.

2.6 Bond-Slip Relationship of Grouted Multi-strand Tendons

2.6.1 Background. The local bond stress and local slip between steel and concrete is of fundamental importance for many aspects of the behavior of reinforced or prestressed concrete elements. The majority of the research in this area has focused on normal

reinforcement in reinforced concrete [22,34,35,36]. The available body of research for prestressing strand is much more limited. As outlined in Sections 2.3 and 2.4, most studies have investigated pullout bond performance of strands (or tendons) rather than local bond-slip behavior. Applied force and slip measurements of pullout tests do not represent the true local bond-slip relationship of the strand (see Section 2.3.2). These results are valid only for the bonded length that was tested and provide averaged bond-slip behavior. The study by Stocker and Sozen [12], however, is one exception (see Section 2.3.7). They investigated the local bond-slip relationship of single strands in concrete by testing short bonded lengths (which assured essentially uniform slip and a constant bond stress distribution). Evans and Johnston [37] also studied the local bond-slip performance of individual prestressing wires. A preliminary bond-slip relationship was developed for 2, 5, and 7 mm wires based on results of transfer bond tests where wire slip was measured using X-Ray techniques (see Fig. 2.23).
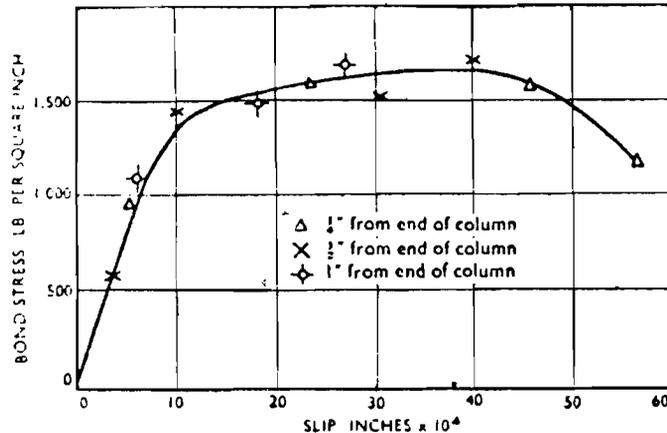
Figure 2.23   Bond-slip relationship for smooth 7mm prestressing wires (from Ref. 37).

The limited data available has been used to verify that bond-slip behavior of a multi-strand tendon takes the same qualitative form as that of a normal reinforcing bar. Martins [38] proposed a bond-slip model for grouted multi-strand tendons which was based on the type used for normal reinforcement. The characteristic numerical values of the relationship, however, were taken from pullout tests of multi-strand tendons. This model is outlined below. Consequently, the lack of specific information has made it necessary to use the results of pullout tests, using various bonded lengths, to establish the bond-slip behavior of multi-strand tendons.

2.6.2 Theoretical Bond-Slip Relationships. A number of different local bond-slip relationships have been proposed for normal reinforcement under monotonic loading. Tassios and Koroneos [39] suggested the multi-linear relationship shown in Fig 2.24. The descending portion of the curve represents the point where sufficient slip has occurred to rupture the bond. For ribbed bars, a residual bond stress is maintained after slip.
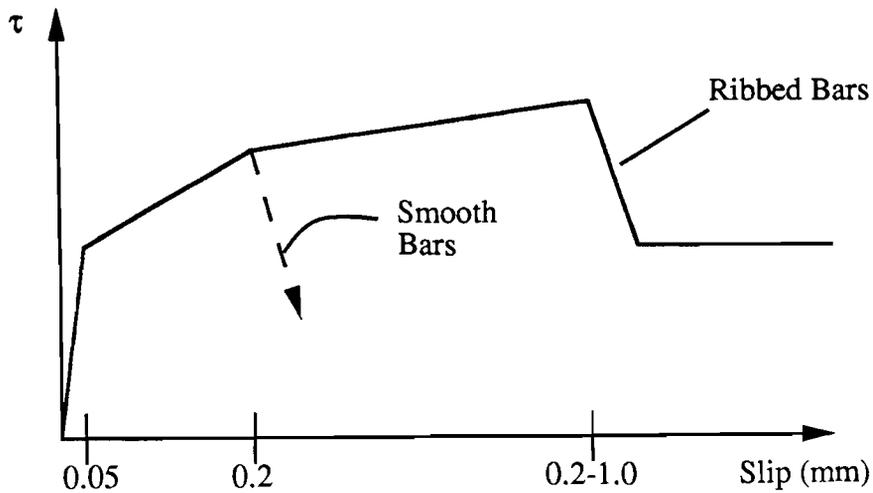
Figure 2.24   General form of bond-slip model proposed by Tassios (from Ref. 39).
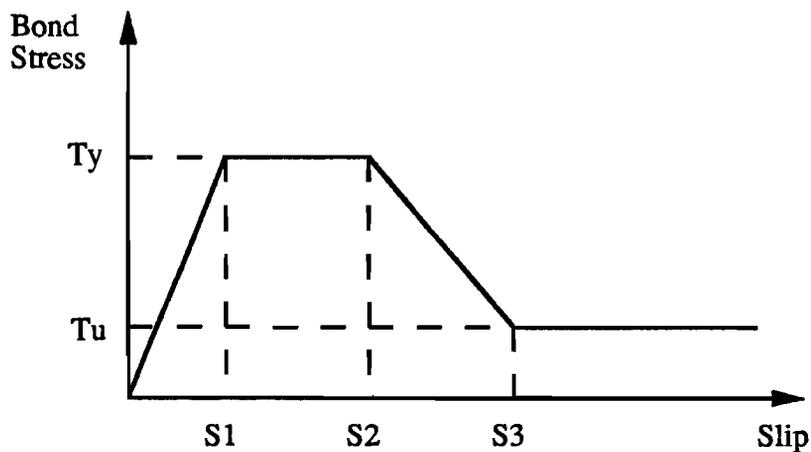
Figure 2.25   Bond slip model for normal reinforcement proposed by Yankelevsky (from Ref. 40).

Yankelevsky [40] presented a bond-slip model of the form shown in Fig. 2.25. The model was used for a finite element representation of experimental monotonic pullout tests of #8 reinforcing bars. Values of loaded end stress and slip predicted by the model compared very well with experimental results.

Giuriani investigated the local bond-slip behavior of ribbed bars [22]. Figure 2.26 shows the results of his pullout tests of specimens with short bonded lengths for relatively large values of slip. The C.E.B recently proposed the bond-slip relation shown in Fig. 2.27 for normal reinforcement [41].
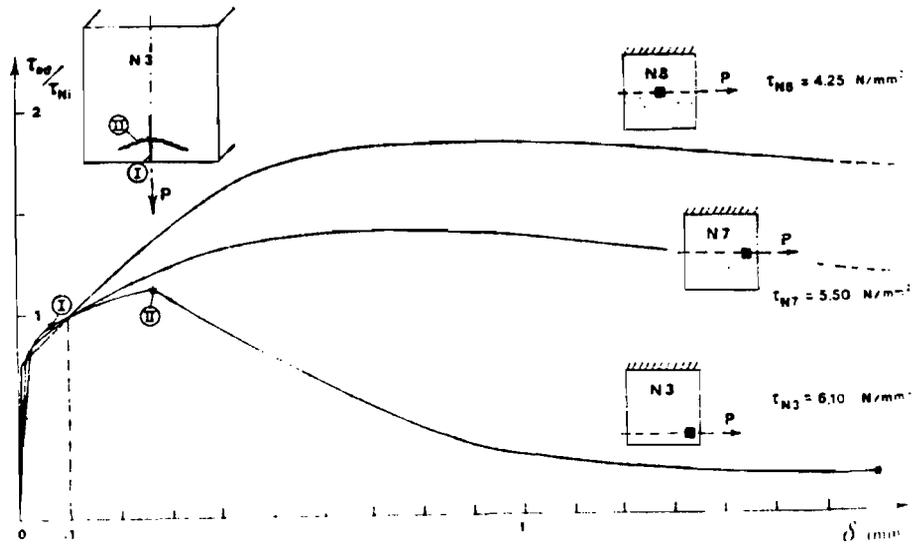
Figure 2.26   Bond-slip behavior of ribbed bars [from Giuriani (Ref. 22)].
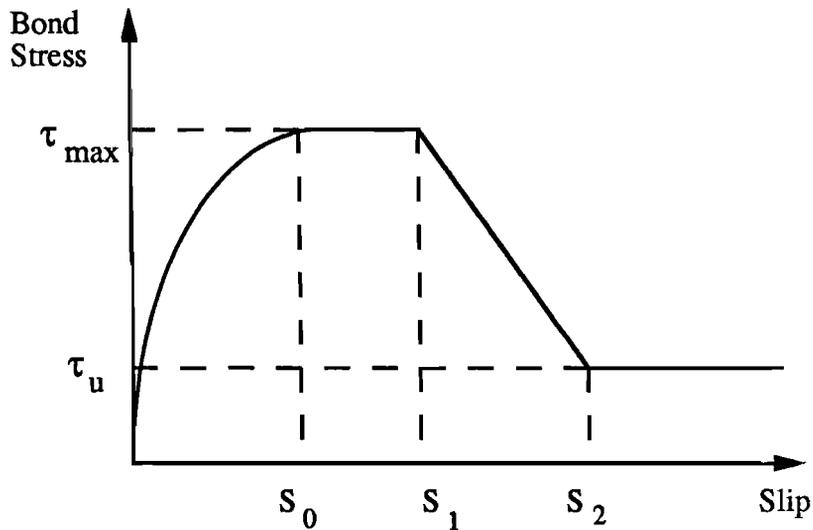
Figure 2.27   Proposed bond-slip relationship for reinforcing bar under monotonic loading [from C.E.B. (Ref. 41)].

2.6.3 Bond-Slip Model for Grouted Multi-Strand Tendons.   After studying a number of different models,   including those outlined above,   Martins proposed the bond-slip relation for grouted multi-strand tendons shown in Fig. 2.28 [38].   The general form of this relationship was based not only on the models cited above,   but also,   more importantly,   on the results of Trost's [17] alternating tension pullout tests of tendons containing 4-0.6" strands.   These cyclic tests were described briefly in Section 2.2.2 and the tendon

τ - Bond Stress
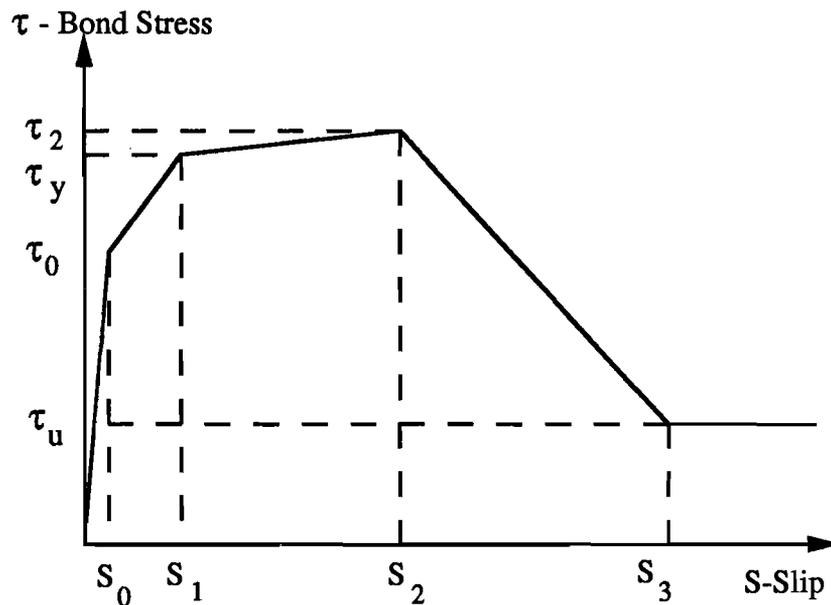
Figure 2.28   Proposed bond-slip relationship for grouted multistrand tendons in steel ducts [from Martins (Ref. 38)].

arrangements are the same as test Series A-9 and A-10 which are shown in Table 2.2. As illustrated in Fig. 2.29, the cyclic response has the same form as the proposed monotonic responses outlined above. Once the general form of the relationship was determined, Martins concluded that the only numerical results that could be found in the literature for this type of response were those of Trost. Consequently, the approximate numerical values shown in Table 2.4 were taken essentially from the experimental results of Trost (see Fig. 2.29). Ultimate shear values at τ_2 were increased by comparing the cyclic response (solid lines) to the monotonic response (dashed line). The value of bond stress at τ_2, however, appears to be greater than the values obtained from the monotonic tests. Foure and Martins [42] used an identical idealization for modelling the tendon slip and ultimate flexural behavior of externally post-tensioned bridges.

The following is a brief summary of the bond-slip model outlined above: (1) The values of tendon slip are based on Trost's measurements of loaded end slip for cyclically loaded specimens with a bonded length of 5.25 inches. (2) The degrading bond response is based on a cyclic load test. As shown in Fig. 2.29, the monotonic response is much more stable than the cyclic response. However, the cyclic response values are conservative. (3) Bond stresses at τ_2 were assumed to be greater than cyclic response values.
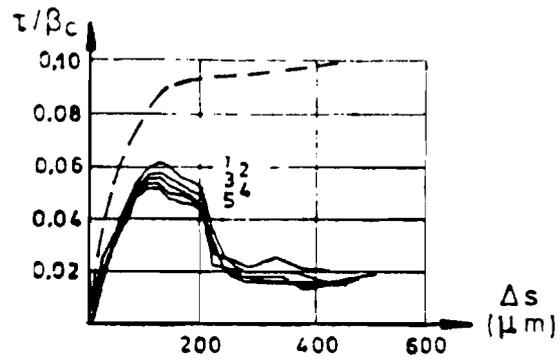
Test Series B-9 (4-0.6"Strands in the Middle of the Duct)
Fpu= 1770 Mpa (257 ksi)
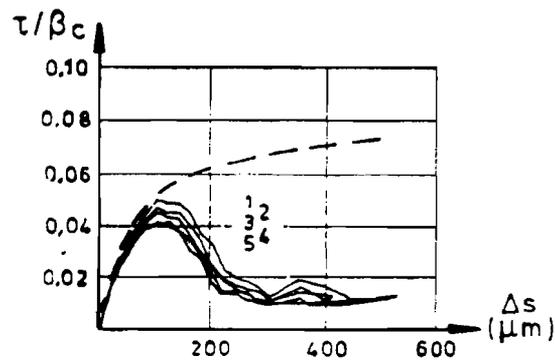
Test Series B-10 (4-0.6" Strands Adjacent to Duct wall)
Fpu= 1770 Mpa (257 ksi)

βc= Grout Cylinder Strength (Avg.= 55 MPa (8.0 ksi))

Δs= Loaded end slip

τ= Bond Stress (MPa)

Figure 2.29 Grouted tendon bond-slip performance under alternating tension [from Trost (Ref. 17)].

Table 2.4   Parameters for Establishing the Bond-Slip Relationship of Grouted Multi-Strand Tendons (From Ref. 38)

Parameter	Good Conditions of Injection (1)	Normal Conditions of Injection (2)
S_0	0.005-0.030 mm (0.0002-0.0012 in)	0.02-0.035 mm (0.0008-0.0014 in)
τ_0	0.8-1.7 MPa (0.12-0.25 ksi)	0.6-1.5 MPa (0.09-0.22 ksi)
S_1	0.09-0.1 mm (0.0035-0.004 in)	0.07-0.1 mm (0.0028-0.004 in)
τ_y	3.5-3.8 MPa (0.51-0.55 ksi)	2.7-2.8 MPa (0.39-0.41 ksi)
S_2	0.14-0.18 mm (0.006-0.007 in)	0.09-0.15 mm (0.0035-0.006 in)
τ_2	5.3-7.8 MPa (0.77-1.13 ksi)	3.9-4.6 MPa (0.56-0.67 ksi)
S_3	0.28-0.4 mm (0.01-0.016 in)	0.215-0.3 mm (0.008-0.012 in)
τ_u	1.1 MPa (0.16 ksi)	1.0 MPa (0.15 ksi)

(1)   Tendon centered in the middle of the duct (see Test Series A-9 in Table 2.2). Grout surrounding all the strands.

(2)   Eccentric tendon in the duct. Difficult to inject grout around all the strands adjacent to the duct wall. (see Test Series A-10 in Table 2.2).

CHAPTER 3

Experimental Program and Test Results

3.1 Tendon-Deviator Tests

3.1.1 Introduction. This test series consisted of modified monotonic pullout tests of multi-strand tendons grouted in curved and straight, smooth steel ducts. The tendons were positioned against the duct wall and were stressed prior to grouting. Full-scale specimens were used to provide an accurate representation of the specific bond conditions at the deviator. The tendon bond stress-slip behavior was investigated for three angles of tendon deviation and two ratios of prestressing tendon area to duct cross-sectional area. The primary objectives of the test program were to determine the level of effective bond stress developed through the deviator and to establish the bond-slip performance of the tendon. A secondary objective was to determine frictional losses through curved ducts during stressing of the tendon.

3.1.2 General Information. The bond mechanism between an external tendon and a deviator duct is influenced by the following factors (including those discussed in Chapter 2):

1) Ratio of prestressing tendon area to duct cross-sectional area.

2) Tendon radius and duct deviation angle.

3) Location of the tendon in the duct (ie. in the center of the duct or adjacent to the duct wall).

4) Bonded length of the tendon.

5) Type of duct and duct surface properties.

6) Degree of strand entanglement through the duct (see definition outlined below).

7) Tendon stress level prior to grouting.

8) Type of grout and grout strength.

Strands are considered to be entangled when they do not run parallel to one another through the duct. Entanglement may consist of strands either crossing one another or spiralling around the tendon bundle. During post-tensioning in long-span structures, strands in a tendon are usually pulled through the duct as a group. For large tendons it is difficult to keep the strands parallel as they are threaded through the duct.

Since the number of specimens which could be tested in this series was limited, only two factors were chosen as variables to be investigated. The remaining factors were either held constant or kept within an acceptable range of variation.

The principal variables investigated were: 1) the deviation angle of the curved ducts and, 2) the ratio of prestressing tendon area to duct cross-sectional area. The limited number of tests did not permit a complete evaluation of these test variables. Nevertheless, the tests did investigate specific tendon bond conditions at deviators typical of those in existing U.S. structures. As detailed below, a total of six specimens were tested with tendon deviations of 0, 6, and 12 degrees and ratios of tendon area to duct area of 0.145 and 0.25. The following section provides background information on the design and development of the test specimens.

3.1.3 Development of Test Specimens

3.1.3.1 Survey of Existing U.S. Structures. A number of external tendon bridges were reviewed to determine typical tendon-deviator dimensions. Three specific bridges, which provided a good representation of the range of dimensions found in existing U.S. structures, were investigated in detail. The pertinent tendon-deviator details of these prototype structures are shown in Table 3.1. The full scale specimens used in the tests were based primarily on these representative prototypes.

As shown in Table 3.1, the maximum tendon deviation angle is approximately ten degrees and the ratio of tendon prestressing steel area to duct cross-sectional area ranges from 0.20 to 0.33. The longitudinal dimension of the deviation blocks (ie. bonded length) typically varies from 15-36 inches. For all structures, actual steel duct radii were usually much greater than specified minimum values. The minimum duct radius was used only rarely for extreme deviation angles. For example, the Long Key and Seven Mile bridges used ducts with radii ranging from 7-20 feet or more (depending on the deviation angle of the tendons).

3.1.3.2 Variables Considered.

a) Duct and Tendon Size. The minimum duct cross-sectional area for a multiple-strand post-tensioning tendon is specified as two times the area of the tendon [43,44]. For external tendon structures, however, it is common practice to use duct areas of 2-1/2 to 3 times the tendon area [2]. For the tests described here, 3 inch nominal diameter (3-1/2" O.D. - 3.068" I.D.) duct pipe was donated by Prescon Corporation of San Antonio. This galvanized steel pipe was prebent to specified deviation angles and radii (galvanized pipe is also commonly used in existing structures). Since the pipe diameter was set, it was only necessary to select tendon sizes using available 1/2 inch diameter strand. After considering the ratios of tendon area to duct area for the existing structures outlined above, and limitations of the test apparatus, the tendons shown in Table 3.2 were selected.

Table 3.1 Prototype Bridge Details

	Long Key Bridge	San Antonio Y Project	Seven Mile Bridge
Maximum Vertical Tendon Deviation Angle (deg)(1)	8.2	4.8	9.5
Tendon 1/ Duct 1	19-1/2" strands/ 3-3/8" (I.D.)(3)	19-0.6"/ 4.03" (I.D.)(2)	19-1/2"/ 4.03" (I.D.)
Ratio of Area: Tendon 1/ Duct 1	0.325	0.324	0.23
Tendon 2/ Duct 2	12-1/2"/ 3-3/8" (I.D.)(3)	12-0.6"/ 3.55" (I.D.)(4)	27-1/2"/ 4.03" (I.D.)
Ratio of Area: Tendon 2/ Duct 2	0.205	0.263	0.32
Tendon 3/ Duct 3	–	9-0.6"/ 3.55" (I.D.)	–
Ratio of Area: Tendon 3/Duct 3	–	0.197	–
Minimum Radius of Curvature	6 ft. - 7 in.	10 ft.	6 ft. - 7 in.
Deviator Block Length (in)	16-20	36	15

(1) Combined effect of vertical and horizontal deviation would not change these values significantly.

(2) 4" Nominal Schedule 40 Pipe - I.D. = 4.026"

(3) Design drawings indicate 3-3/8" pipe which is not readily available for Schedule 40. 3-1/2" I.D. pipe or Schedule 80 pipe probably used.

(4) 3-1/2" Nominal Schedule 40 Pipe - I.D. = 3.548"

The 12 strand tendon provided a ratio of tendon area to duct area which was approximately in the middle of the range of values obtained for existing structures. Furthermore, this tendon size was compatible with existing hardware. The second tendon, although outside the range of existing tendon-duct area ratios, was selected to obtain a prestressing steel area sufficiently different from that of Tendon A.

b) Tendon Deviation Angle. Rigid metal deviator ducts are bent to a radius compatible with the geometry of the external tendon profile. In order to ensure that the tendon does not bear on the edge of the deviator pipe at the face of the deviator block, the duct is bent to a radius which provides a larger deviation angle than that of the tendon. The difference between the tendon and duct deviation angle is typically one or two degrees [2]. Tendon deviation angles of 0, 6.0, and 12.0 degrees were selected to be used with available ducts with deviation angles of 0, 8.0, and 13.5 degrees, respectively. This provided a minimum "overbend" of 1.5 degrees. These deviation angles also cover the range of values

Table 3.2 Tendon Sizes for Test Specimens

Parameter	Tendon A	Tendon B
Tendon Size	12-1/2" strands	7-1/2" strands
Tendon Area (in^2)	1.836	1.071
Duct I.D. (in)	3.068	3.068
Duct Area (in^2)	7.393	7.393
Tendon Area/ Duct Area	0.25	0.145

in existing structures and were compatible with available hardware. Only vertical tendon deviations were used in the tests. The combined effect of vertical and horizontal deviations can always be resolved to a single principal deviation in a given plane.

As shown in Fig. 3.1 (see Section 3.1.3.3), tendons were horizontal on one side of the deviator block, while on the other face the tendons were deviated at the required angle. This was the most common detail used in the existing bridges. The duct overbend was placed on the deviated side of the block. On the other side of the block, the duct projected out horizontally to match the horizontal tendon.

c) Duct Radius of Curvature. Neither AASHTO nor PTI specify a minimum radius of curvature for post-tensioning ducts [43,44,45]. For U.S. practice, a minimum radius of 10 feet has been recommended for external tendons at deviators (for tendon sizes up to 19-0.6" diameter strands) [2]. The French Federal Transportation Administration specifies a minimum
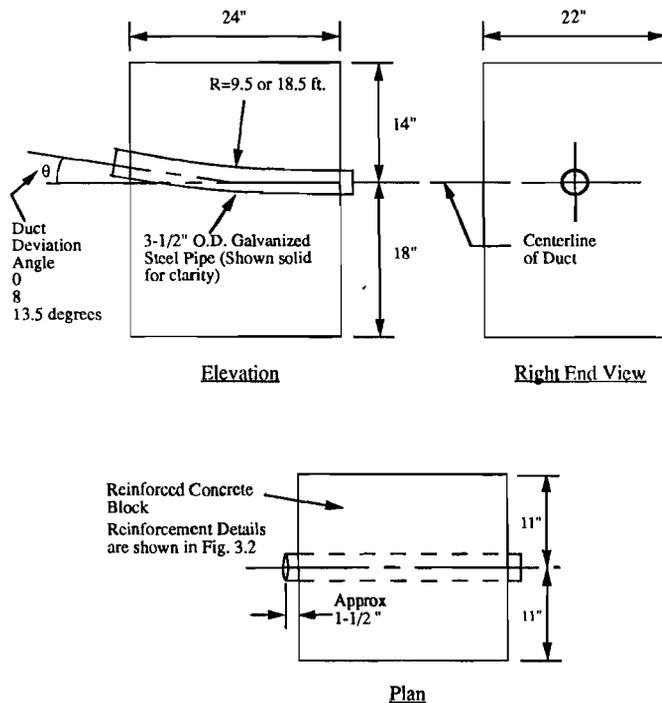
Figure 3.1 Deviator Block Details.

external duct radius of 3.0 meters (9.8 feet) for small tendons, and 4.0 meters (13.1 feet) for larger tendons (ie. more than 19-0.6"diameter strands) [2]. For design, the duct radius is selected to achieve the required deviation angle (plus overbend) within the length of the deviator block. For a deviator of constant length, this means that duct radius must vary to achieve different deviation angles. For the 8.0, and 13.5 degree ducts used in the tests, the pre-bent duct radii were 18 ft.- 6 in. and 9 ft.- 6 in. respectively (the ducts were bent on circular curves). As outlined below, these values were compatible with the constant length of the deviator block used in the tests.

d) Deviator Length (Bonded Length).   Using the duct radii and tendon deviation angles outlined above, the required deviator length was calculated using the following geometric relationship:

$$L = 2R\sin(\theta/2)$$

where   R   =   Radius of curvature of duct

L   =   Deviator block length (approximately equal to duct length for small deviation angles)

θ =   Deviation angle of tendon (degrees)

For the specified tendon deviation angle of 6.0 degrees and R= 18.5 feet, the calculated deviator length is 23.2 inches. Similarly, using the 12.0 degree angle and R= 9.5 feet, the length is 23.8 inches. A deviator length of 24.0 inches was selected to satisfy the geometric requirements of the existing ducts. To keep the bonded length of the tendon equal for all tests, the duct radius necessarily had to vary to obtain different deviation angles. This was considered to be acceptable since the most important test criteria was a constant bonded length.

It is important to note that the 24 inch bonded length was not ideal for determining the bond stress-slip behavior of the tendons. A shorter specimen would have resulted in a more uniform bond stress and slip distribution along the length of the tendon. This could not be avoided, however, since a shorter bonded length would have required a very small duct radius. For example, for a bonded length of 12 inches (similar to the 19-0.6" strand tendon tests by Trost [17] outlined in Section 2.4.2), and a deviation angle of 12 degrees, the required duct radius would be 4 ft.-8 in. For this case, the radius and bonded length would not represent typical values for existing structures. Furthermore, it may be difficult to fabricate full-scale specimens with these sharp curvatures without buckling the smooth duct surface. The longer bonded length was selected to provide a more realistic model of existing structures. This also made it possible to use the duct material that was supplied.

e) Level of Prestress.   When external tendon ducts are grouted in post-tensioned bridges, the maximum tendon stress level is 70% of the ultimate strength of the strands (ie. after jacking and release). The stress level varies along the tendon length due to friction losses. For the tests described herein, the tendons were stressed to 50% of ultimate strength prior to grouting. This stress level is discussed in Section 3.1.8.

f) Location of Tendon in the Duct.   For the curved deviator specimens outlined below, the tendon was compressed against the top side of the duct after stressing. The lateral pressure due to tendon curvature resulted in a very tight strand grouping. For the straight specimens, the tendon was also located near the top of the duct. In this case, however, the strand bundle was not compressed against the duct because minimal contact pressure existed between the tendon and duct surface.

3.1.3.3 Description of Test Specimens.   Dimensions and details of the concrete deviator block specimens are shown in Fig. 3.1. Test specimen details are summarized in Table 3.3.

Table 3.3 Test Specimen Details

Specimen No.	Tendon Deviation Angle (deg)	Tendon Size	Tendon Area/ Duct Area	Bonded Length (in.)
1A-12-12°	12.0	12-1/2"	0.25	24
1B-7-12°	12.0	7-1/2"	0.145	24
2A-12-6°	6.0	12-1/2"	0.25	24
2B-7-6°	6.0	7-1/2"	0.145	24
3A-12-0°	0	12-1/2"	0.25	24
3B-7-0°	0	7-1/2"	0.145	24

The test specimens are designated by a label that includes the number of strands (7 or 12) and deviation angle for the tendon (0, 6, or 12 degrees). For example, Test 1A-12-12° refers to the specimen with 12 strands and a 12 degree deviation angle (the A designation also indicates a 12 strand tendon as shown in Table 3.2.

3.1.4 Materials

3.1.4.1 Prestressing Strand.   Seven-wire low relaxation strand with a nominal diameter of 1/2 inch was used for all multi-strand tendons. The strand conformed to ASTM A416 specifications (stress-relieved strand) and had a specified minimum ultimate strength

of 270 ksi. Two spools of strand and all associated hardware were donated by Prescon Corporation of San Antonio, Texas. The mill reports for the strand indicated a modulus of elasticity of 28,400 ksi. An effective elastic modulus was determined by performing a tension test on a sample of strand with strain gauges mounted on all six exterior wires [47]. Test results indicated an elastic modulus of 28,000 ksi. This value was used to provide a calibration between electronically measured strains and strand stresses. Only clean bright strand with negligible rust was used in the test specimens.

3.1.4.2 Duct.   Three inch nominal diameter Schedule 40 steel pipe (3-1/2" O.D.- 3.068" I.D.) was used for tendon ducts. The pipe was galvanized and bent to specified radii and deviation angles (for a particular length). The pipe surface was smooth on both the inside and outside surfaces.

3.1.4.3 Grout.   The cement grout mix was developed from Texas State Department of Highways and Public Transportation Standard Specifications as follows:

- 1 bag Portland Cement(94 lbs.), Type III (substituted for Type I or II)

- 5-1/2 U.S. gallons water

- 0.94 lbs Interplast-N expansion admixture (1% of cement by weight)

To accelerate the testing schedule, high early strength cement (Type III) was substituted for the standard Type I or II cement. This substitution is permitted by the TSDHPT, Post-Tensioning Institute [44], and AASHTO (1983) Specifications (trial mixes are recommended, however). The water-cement ratio for the mix design outlined above is 0.49. This value is higher than the maximum ratio of 0.45 recommended by the Post-Tensioning Institute and AASHTO. Two trial grout mixes indicated that a water-cement ratio of 0.48 was acceptable for the Type III cement (the lowest ratio that could be pumped effectively). Since grout fluidity was a more important criteria than early age strength, the higher water-cement ratio was used. Tendon grouting procedures and grout strengths are outlined in detail in Section 3.1.6.4.

3.1.4.4 Concrete and Non-Prestressed Reinforcement.   Concrete for the deviator block specimens was supplied by a commercial concrete supplier. The mix was designed using a maximum aggregate size of 3/8 to provide a 28-day compressive strength of 5000 psi. To reduce costs, casting was scheduled to coincide with other projects using equal or higher design concrete strengths and the same aggregate size. This strength variation was accepted since the deviator block concrete was overdesigned to ensure bond failure at the tendon-grout interface. Actual concrete strengths were determined from compression tests of 6 x 12 inch concrete cylinders. These results are presented in Table 3.4. All specimens were cast a minimum of 28 days prior to testing.

Table 3.4 Concrete Strengths

Specimen	28-Day Concrete Compressive Strength (psi)*
1A-12-12^P	7045
1B-7-12^P	7045
2A-12-6^P	8200
2B-7-6^P	8200
3A-12-0^P	8060
3B-7-0^P	8060

* Average of three cylinder tests

Non-prestressed reinforcement used in the concrete deviator block specimens is shown in Fig. 3.2. Normal reinforcement for the concrete deviator block was designed to accommodate forces induced by tendon stressing and during load testing. Excessive reinforcement was provided to eliminate the possibility of deviator block failure, or significant displacements, prior to bond failure between the tendon and the grout. ASTM A615 Grade 60 reinforcement was used throughout.
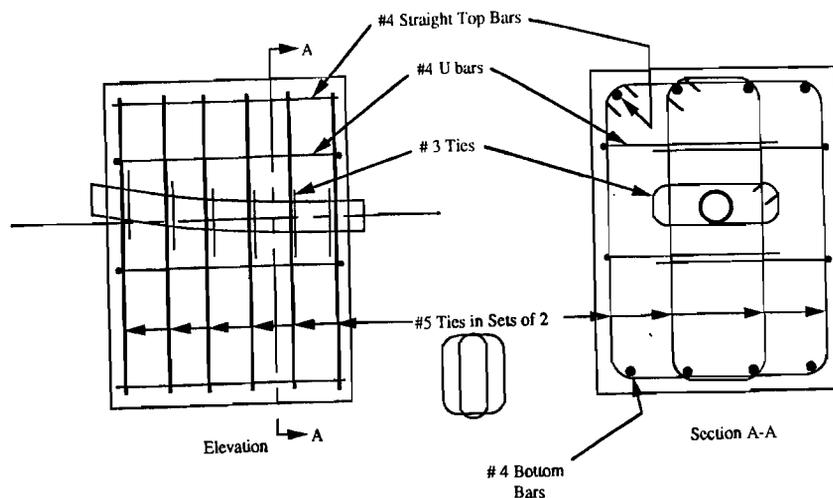
Figure 3.2 Deviator Block Reinforcement Details.

3.1.5 Fabrication of Deviator Block Specimens.

3.1.5.1 General.   This section covers the fabrication of the deviator block specimen. Tendon stressing and grouting procedures are outlined in Section 3.1.6.
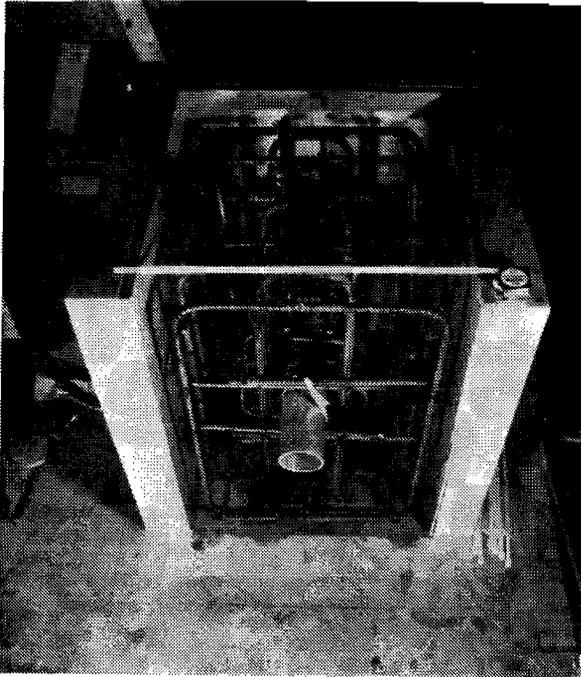
Figure 3.3   Deviator Block Formwork.   Figure 3.4   Typical End Section.
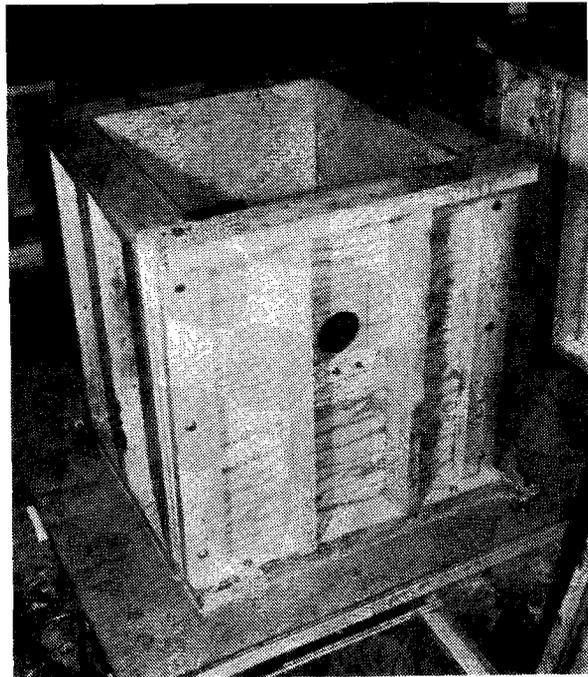
3.1.5.2 Formwork and Concreting.   Two forms were used for rapid construction of the block specimens. Figure 3.3 shows one form prior to placing the end section over the duct. A typical end section, with a hole to accommodate the duct, is also shown in Fig. 3.4. The duct was tied to all transverse ties and was attached to the forms at the ends to prevent it from shifting during concrete placement. Extreme care was taken to ensure that the duct was placed with the correct vertical and horizontal alignment. Ends of the ducts were also covered to prevent contamination of the interior bond surface. After the forms were closed and sealed, the concrete was placed. Concrete was delivered from the truck using a bucket hoisted by an overhead crane, and was vibrated in three equal lifts to avoid consolidation problems. Two specimens were cast at the same time as six 6 x 12 inch test cylinders. About two hours after concrete placement, the forms were covered with wet burlap which and plastic sheets which were kept in place for approximately 24 hours. Formwork was usually stripped the day after casting.

58

3.1.6 Test Setup

The test setup was developed from an existing prestress bed located on the elevated testing slab at FSEL. The bed consisted of two bulkheads which were located at the north and south ends of the test slab, as shown in Fig. 3.5. The bulkheads were anchored to the test slab, and compression struts were located between the two ends to create a self reacting frame. As shown in Fig. 3.6, a 500-ton stressing ram was positioned at the south end of the bed.

3.1.6.1 General Layout. The test setup was constructed by placing two reaction frames within the prestressing bed near the north bulkhead, as shown in Figure 3.7. The reaction frames were used to provide longitudinal (ie.North-South) restraint for the deviator specimens during stressing and testing. As shown in Figure 3.8, the south reaction frame consisted of two beams which were anchored to the test floor with four 3-inch diameter bolts. The bolts were post-tensioned to the test floor. The north reaction beam was positioned to provide support between the north bulkhead and the deviator block. Potential transverse (ie. East-West) and torsional forces were negligible. However, the wide reaction beams on the north and south ends of the specimen provided effective transverse and torsional restraint in any case. The deviator specimen was prevented from overturning by the longitudinal reaction frames and the hold-down beam (which also provided vertical restraint). The existing bulkheads were used to anchor the tendons as outlined below.
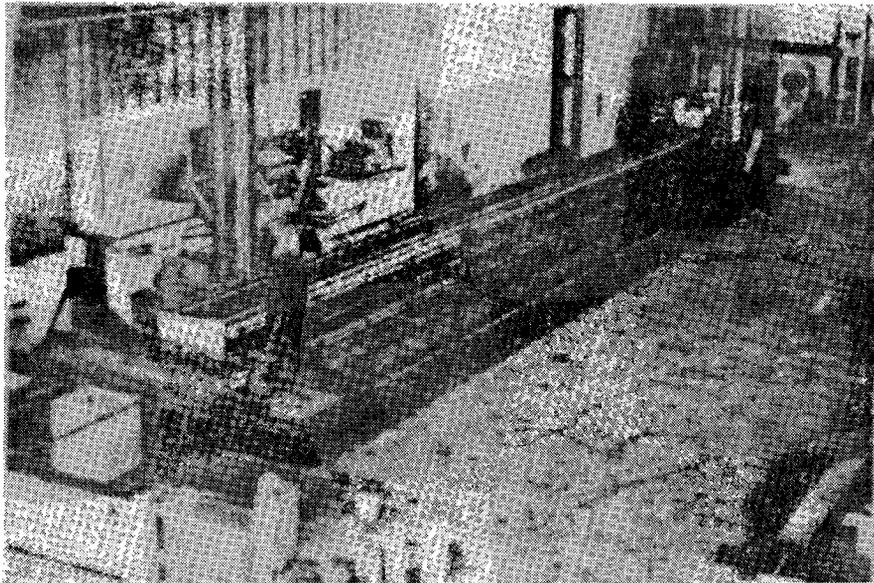
Figure 3.5   Existing Prestress Bed.
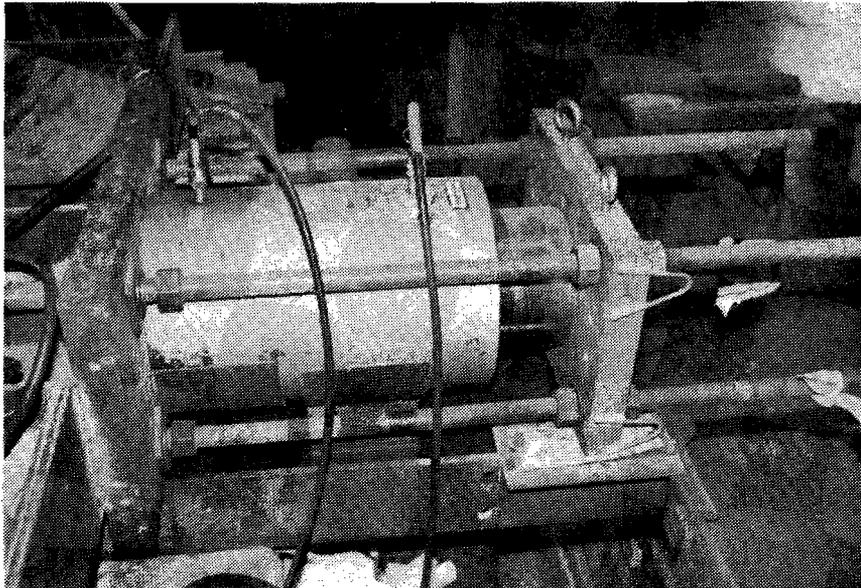
Figure 3.6 500-Ton Stressing Ram at South End of Bed.

A large steel frame was located at the north bulkhead as illustrated in Fig. 3.7. Each tendon was anchored at the frame using a steel plate and Freyssinet type multi-strand anchor which was bolted to the extreme north edge (see Fig. 3.9). The north anchorage detail is also shown in Fig. 3.10. The anchorage device was positioned along the centerline of the prestress bed. As indicated in Fig. 3.7 , tendons were deviated on the north side of the deviator block only. The required deviation angles were achieved by changing the location of the anchorage plate on the end frame. Beveled pipe sections were also fabricated and welded to the anchor plates to accommodate the required angles. At the south end, the tendons was horizontal and was anchored at a plate near the south bulkhead as shown in Fig. 3.11. A large 27-K5 Freyssinet type anchor head was used to distribute forces over the anchor plate. The stressing operation also took place at this end. After the tendon was preloaded (see Section 3.1.6.3), the south anchor plate was displaced using four 1-3/4 inch diameter rods which were connected to the stressing ram as shown in Fig. 3.12.

3.1.6.2 Safety.   One of the concerns governing the design of the test setup was the safety of the testing personnel. Since the energy stored in the stressed tendon presented a potentially dangerous situation, several specific measures were taken to mitigate possible dangers. A system was designed to contain the tendon in the event that a strand was to break. The external tendon was enclosed in a 3-1/2 inch diameter high strength polyethylene pipe. The pipe was anchored to the test floor using steel cables which were looped around the pipe (see Fig. 3.13). Large concrete barriers were positioned behind the north anchor zone. The bulkhead provided effective containment at the south end. Finally, and most importantly, the strands were stressed to only 50% of their ultimate strength (this
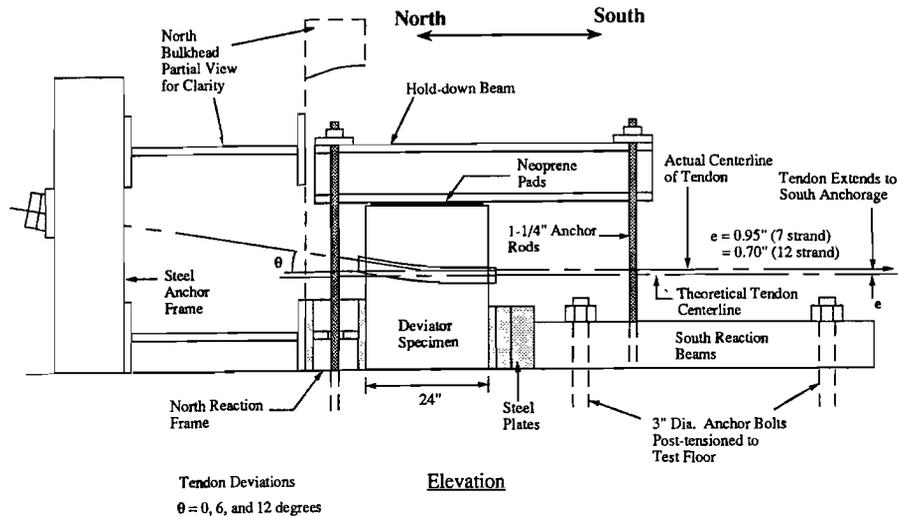
Figure 3.7   General View of Test Set-Up.

stress level is discussed in Sections 3.1.6.3 and 3.1.6.5).

3.1.6.3 Tendon Stressing Procedure.

Prior to stressing the strands, the deviator block was placed in the test frame and the duct was positioned accurately along the centerline of the prestressing bed using a survey instrument. The prestressing operation was accomplished in two stages. In the first stage, strands were stressed individually to an initial preload level of 1.5 kips (9.8 ksi) per strand. The strands were pulled through the anchorages and deviator duct one at a time. The preload was applied with a mono-strand ram at the south anchor plate using a special stressing chair. The anchor wedges were then driven into the anchor head with a 2 - lb. hammer prior to inserting the next strand. This was done to prevent strand entanglement and binding in the curved region of the

Figure 3.8   Post-Tensioning Anchor Bolts for South Reaction Frame.

deviator. Since strand entanglement has been shown to influence friction (and bond) at the deviator [46], care was taken to place the strands parallel to one another. Strands on the top of the tendon bundle were stressed first while bottom strands were stressed last. This stressing procedure was especially critical since the strands were compressed along the top

of the curved duct after preloading (for the curved duct cases). By stressing the strands from the "top down", entanglement and binding were eliminated. A similar technique was used by Hoang in tendon-deviator friction tests [46]. Hoang tested the friction of the polyethylene duct against the rigid steel duct through the deviator region (ie. French double duct system). The tendon was not bonded to the deviator duct in these tests. The application of the preload was used to ensure uniform initial tension in all strands and to seat the wedges. This also provided taut strands for application of strain gauges and an epoxy collar which was formed around the strand (see Section 3.1.7). Preload tension was monitored with a pressure transducer which was connected to the mono-strand ram. For Test 1A-12-12°, the preload was also checked by strain gauges which were applied prior to initial stressing (see Section 3.1.7). For the remaining tests, gauges were placed after the preload was applied.
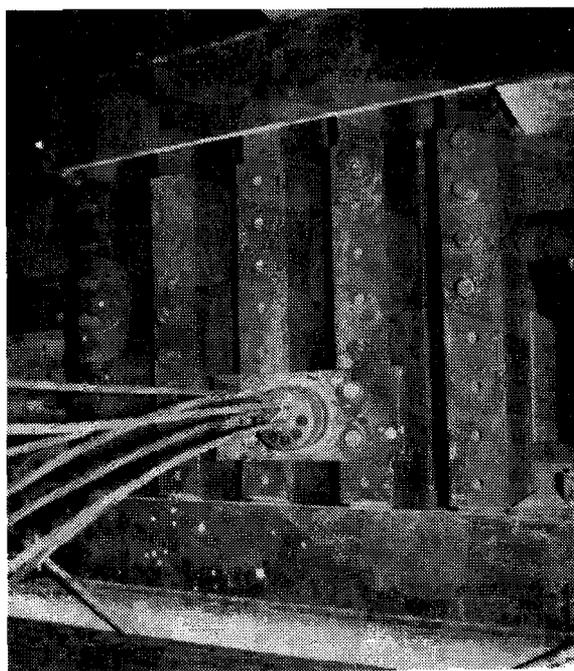
Figure 3.9   Tendon Anchorage at North End.

Prior to the second stressing stage, five strain gauges were attached on both sides of the deviator block to five different strands of the tendon (see Section 3.1.7). In the second stage of stressing, all strands were tensioned together to a total stress of 135 ksi ($0.5f_{pu}$) using the 500 ton ram at the south (live) end of the prestressing bed. The total stress was the sum of the preload stress and the second stage stress. After tensioning, the end plate that was used to pull the strands was secured with locknuts. During stressing, applied load and tendon tension were monitored as follows: (1) using a pressure transducer and strain indicator box calibrated with the 500 ton Ram, (2) with strain gauge readings from a Hewlett-Packard/IBM PC data acquisition system (see Section 3.1.7), and (3) measuring strand elongations (ie. movement of the live-end anchor plate (after stressing only)). By comparing these values it was determined that large unquantifiable friction losses were inherent in the prestressing bed. The strand strain gauge readings, however, provided very accurate measurements of strand stress on both sides of the deviator block.

3.1.6.4 Grouting Procedure.   A grouting procedure was developed from recommendations by Schupack [48,49]. Typical tendon grouting specifications suggest that grouting be continued and grout continuously wasted until entrapped air is removed and the duct is completely filled with grout. It is also recommended that the valve at the outlet end

62

be closed immediately after the duct is completely filled with grout [44]. Schupack suggests that closing the valve immediately after grouting is not correct and states that,

There is only one way that free expansion can be effective: permit free expansion of the grout by leaving the high points open (with a grout tube standpipe). This allows the expansion to push out bleed water and laitance that tends to rise in the sedimentation or bleeding process.

Schupack also recommended that an extension tube (standpipe), which could be closed off one hour or so after grouting, be placed at the high end. Schupacks' recommendations were followed for the tests herein. It was expected that this procedure would reduce grout bleeding. It is possible that closing the grout tubes immediately after grouting may explain some of

Figure 3.10   North Anchorage Detail (from Ref. 2).

the grouting problems observed by Osborne [29]. Osborne found that inadequate grout expansion caused the grout block to pull away from the duct interface for large tendon tests.

Tendon ducts were grouted the day after post-tensioning. Prior to grouting, hard styrofoam "forms" were placed around the strand bundle in both ends of the duct pipe and were sealed with silicone (see Fig. 3.14). The styrofoam was inserted in the duct on each end of the specimen to maintain a constant 24 inch bonded length. A hard, stiff styrofoam was used to provide effective confinement of the grout. Injection and outlet ports consisting of 3/8 inch (I.D.) steel tubes with ball valves were placed at both ends of the duct. At the low end (South) the ports were horizontal as shown in Fig. 3.14. The port on the high end (North) was similar except that a vertical standpipe was attached. The grout was mixed and pumped using a commercial grouting machine with an electric mixer and screw pump. Prior to connecting the grout hose to the south injection port, grout was wasted until a uniform grout quality was obtained. During grouting, pumping was continued and grout was wasted at the outlet end to eliminate air and water pockets. At this point, the lower valve was

Figure 3.11   Tendon Anchorage at South End.

closed and the valve at the high end was kept open for one hour as outlined above. For test 1A-12-12°, a valve was not used at the outlet end. The polyethylene tubing was clamped one hour after grouting. With the exception of the recommendations by Schupack, the grouting procedures outlined in Reference 44 were followed.

Actual grout strengths were determined from compression tests of standard 2 inch mortar cubes formed in standard sealed molds. Six grout cubes were fabricated for each specimen. As discussed previously, high early strength cement was used in the grout. This was done to permit testing the deviator bond specimens 72 hours after grouting. Grout cubes were tested in a Forney 600 kip cylinder-testing machine. The rate of loading was approximately 8000 pounds per minute. The three day compressive strengths of the grout cubes are summarized in Table 3.5.

For specimen 1B, the low grout strengths were the result of excessive water in the grout mix. Extremely high temperatures resulted in an unpumpable mix using the standard water-cement ratio of 0.48. For subsequent tests in hot weather, the standard water-cement ratio of 0.48 was used. A pumpable grout mixture was obtained by cooling the water to approximately 40°F prior to mixing. Examination of the specimens after grouting showed excellent grout quality.

3.1.6.5 Loading Concept.   To perform a standard pullout test, it would have been necessary to apply load to the tendon using the ram at the south end of the prestressing bed. This procedure could not be used since the applied load would be distributed between the

Table 3.5 Grout Cube Strengths

Specimen	Grout Strength at Start of Test(3 days) (psi)*
1A-12-12^P	2710
1B-7-12^P	1550**
2A-12-6^P	2590
2B-7-6^P	2530
3A-12-0^P	2555
3B-7-0^P	2760

*   Average of six tests
**   Water cement ratio increased to 0.55 (see below)
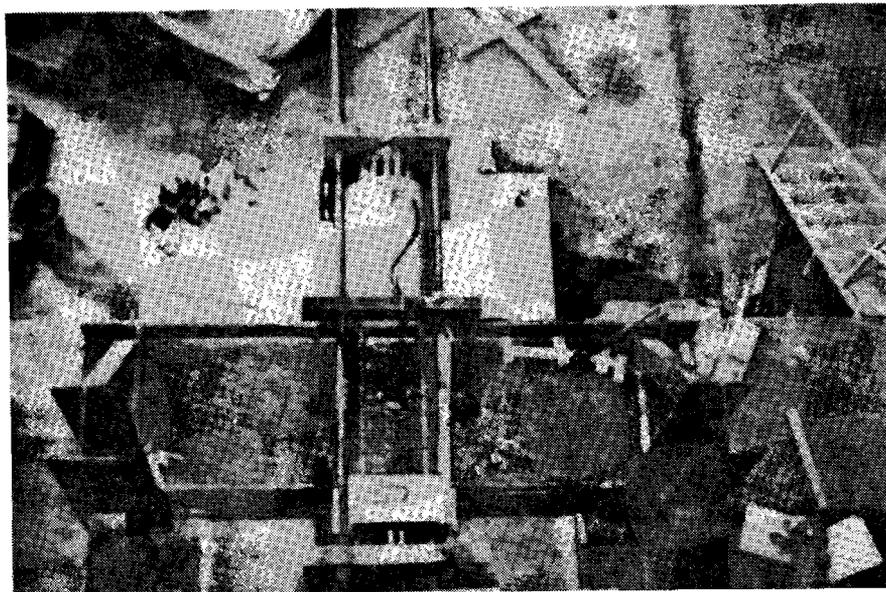
Figure 3.12   Stressing Ram Connected to South Anchor Plate.

prestress bed supports and south reaction frame (which also provided longitudinal restraint to the specimen). Consequently, it would not be possible to ensure that all of the applied load was transmitted to the specimen (ie. to the tendon-grout bond). Furthermore, since the tendons were already stressed to 0.5 f_{pu}, the application of additional stress could have presented a potentially dangerous situation (depending on the bond capacity of the grout). It was decided that the specimen would be loaded by reducing the tendon stress on the

south side of the specimen. This was achieved by applying load to the ram until the locknuts just became loose (ie. when the applied load became equal to the existing force in the tendon (A_{ps}x0.5f_{pu})). The nuts were then loosened and pressure in the stressing ram was reduced, thereby reducing stress in all strands on the south end simultaneously and applying load to the deviator specimen. This meant that the load applied to the deviator was the difference between the tendon force on the north side of the specimen and the reduced tendon force on the south side (see Fig. 3.15). This method ensured that all of the applied load was transferred to the deviator specimen. A safe test procedure was also achieved.

Figure 3.13   Tendon Restraint.

Figure 3.14   Grout Injection Details.

Despite this, however, the loading concept did not accurately model actual tendon pullout conditions. As outlined previously, tendon forces increase above the initial prestress level as overloads are applied to an externally post-tensioned structure. This increases the radial forces and friction through the curved duct. For the tests herein, tendon forces (and friction through the duct) were reduced as the tests progressed. The total force difference across the deviator is the sum of friction and bond components. By measuring the friction component during stressing, and the total force difference during testing,   the net bond component can be determined. Furthermore, the friction component for any tendon stress level can also be calculated quite accurately. Consequently, the test results can still be used

to estimate the total potential force difference across the deviator for the actual case (ie. by adding the calculated friction component and the bond component from the tests). Alternatively, the test results can be used directly since they provide a lower bound estimate of the maximum tendon stress differential that can be achieved across the deviator.

3.1.7 Instrumentation

Primarily electronic instrumentation equipment was used during testing, although some measurements were checked with mechanical devices. The most important measured quantities were the tendon forces and relative displacements between the tendon and grout on both sides of the deviator specimen. This section outlines the philosophy behind the various measurements and specifies the locations of the instrumentation devices.

3.1.7.1 Force Measurement (Strain Gauges). For the 12-strand tendon tests, five electronic resistance type strain gauges were applied to the tendon on both sides of the deviator specimen (10 gauges in total). The seven-strand tests used four gauges per side. Gauges were positioned on different strands and were distributed as much as possible around the tendon perimeter. An attempt was also made to apply gauges to the same strands on each side of the deviator. For the larger tendon, however, this was not always possible. For a particular strand, strain gauges were attached to a single wire and were orientated parallel to the axis of the wire. Relatively wide gauges (Micro Measurements Type EA-06-062AP-120 Option LE) were selected to facilitate alignment of the gauge on the strand .

By placing the gauges adjacent to an epoxy collar which was cast and hardened around the tendon, very uniform strain readings were obtained. The epoxy collar is discussed in Section 3.1.7.2. Typical gauge locations are shown in Fig. 3.16. Strain gauges were used during stressing and load testing to monitor strand stress (and tendon force) differences across the deviator. Readings were taken after initial preload stressing (Test 1A-12-12° only), and throughout final tensioning and load testing.

3.1.7.2 Displacements (Linear Potentiometers and Dial Gauges). A total of nine linear potentiometers were used to measure displacements of the south reaction beam, deviator block, grout block, and the tendon (see Fig. 3.16). The manufacturer's literature specified infinite accuracy for the potentiometers. However, realistic accuracy was estimated to be ± 0.0005 inch. Dial gauges of similar accuracy were used to check deviator block displacements in the first two tests only. The tendon displacements were measured on the loaded and the unloaded end of the deviator specimen (ie. the south and north sides respectively). Grout displacement was measured at the loaded end only. As shown in Fig. 3.17, an epoxy collar or sleeve was used to attach potentiometers directly to the tendon. The collar was cast by placing a polyethylene pipe form around the strand bundle and pouring liquid epoxy into the sealed mold. Since the tendon was not completely tensioned, the epoxy flowed between the strands and bonded the strands of the tendon together at that point. This forced the strands in the tendon to displace as a unit. Consequently,

displacements were measured for the entire tendon and not for a particular strand. The development and fabrication of the epoxy collar is presented in detail by Arrellaga [47]. For the case of bond failure between the tendon and grout block, the correct displacement (slip) between the strand and grout was measured directly. It was not necessary to make corrections for rigid body displacements of the deviator block since the potentiometers were connected to the tendon and the grout block did not move in the duct. On the other hand, the potentiometer measuring grout displacement was anchored on the south reaction frame. Consequently, grout block displacements were measured relative to movements of the deviator block. In the event that the grout block and tendon displaced as a unit (ie. no slip between the tendon and grout), actual tendon displacement was corrected for relative movements of the deviator block. In this case, actual tendon displacement was simply equal to actual grout block displacement at the loaded end. Since failure occurred at the duct-grout interface, however, actual tendon displacements were not particularly important. Tendon displacements were also corrected for elastic shortening of the tendon which occurred between the point of attachment of the potentiometers on the collar and the face of the specimen (the point of slip measurement).

Pn= Tendon force on North side

= P cos θ

Note: Cos θ = 0.99 for θ = 6 Degrees
    Cos θ = 0.98 for θ = 12 Degrees

Ps= Tendon force on South side

ΔP= Pn-Ps = Load Applied to Deviator
(Force difference across Deviator)

Figure 3.15   Tendon Force Difference Across Deviator.

3.1.7.3 Other Instrumentation and Data Acquisition.   A 10,000 psi pressure transducer was used to monitor pressure in the 500-ton stressing ram. Data from the pressure transducer, strain gauges, and linear potentiometers were read electronically with a Hewlett-Packard scanner. Data acquisition software and an IBM AT computer were used to control the scanning functions. The scanning software was also used to check the entire system prior to each test.

3.1.8 Test Procedure

3.1.8.1 General.   Figure 3.18 shows the general test setup and a specimen ready for testing. The following is a summary of the overall test procedure:

1) The deviator specimen was positioned in the test setup.

2) The strands were pulled through the duct, preloaded, and anchored one at a time.

3) Strain gauges and the epoxy collars were attached to the tendon. (For test 1A-12-12° only, gauges were placed prior to preloading the tendon).

4) All strands were stressed simultaneously to $0.5f_{pu}$ (135 ksi) using the 500-ton ram and anchor plate setup at the south end of the prestress bed. Strain gauge readings were taken at 10 kip load increments using the data acquisition equipment. Tests results from this first phase of the test were used to determine stress losses through the deviator due to friction.
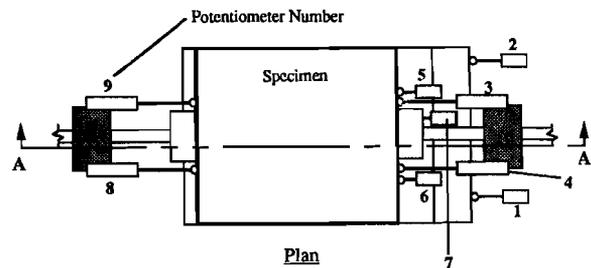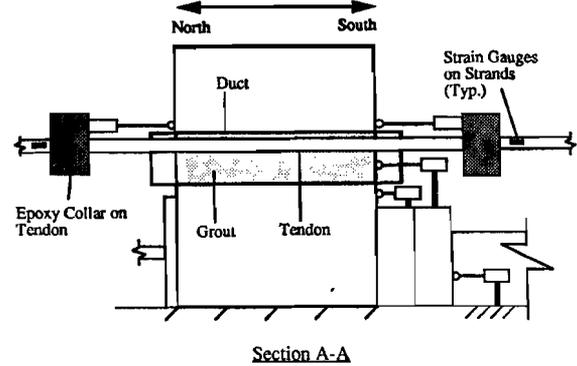
5) The tendons were grouted.

6) Three days after grouting, the ram was loaded again until the locking nuts were loose. The nuts were loosened and pressure in the ram was reduced at a specified rate providing a transfer of load to the deviator specimen (see Section 3.1.8.2). This was the second and final phase of the test which investigated the bond stress-slip behavior of the grouted tendons.

Figure 3.16 General Layout of Instrumentation.

3.1.8.2 Loading. As outlined in Section 3.1.6.5, the specimen was loaded by reducing the tendon stress on the south side of the specimen. The load applied to the deviator was the difference between the tendon force on the north side and the reduced tendon force on the south side. The deviator was loaded monotonically in 10 kip load increments at a rate of approximately 20 kips/min or 1.5 Kn/sec. This loading rate was similar to that used by Trost (ie. 2.0 Kn/sec) [17]. An electronic pump was used to reduce the ram pressure at a uniform rate (In Test 1A-12-12°, pressure was reduced manually with a hand pump). At each 10 kip load step, strain gauges, potentiometers, and pressure transducers were scanned with the data acquisition system, and data was stored in the computer. Tendon forces were measured from the strain gauge readings on each side of the
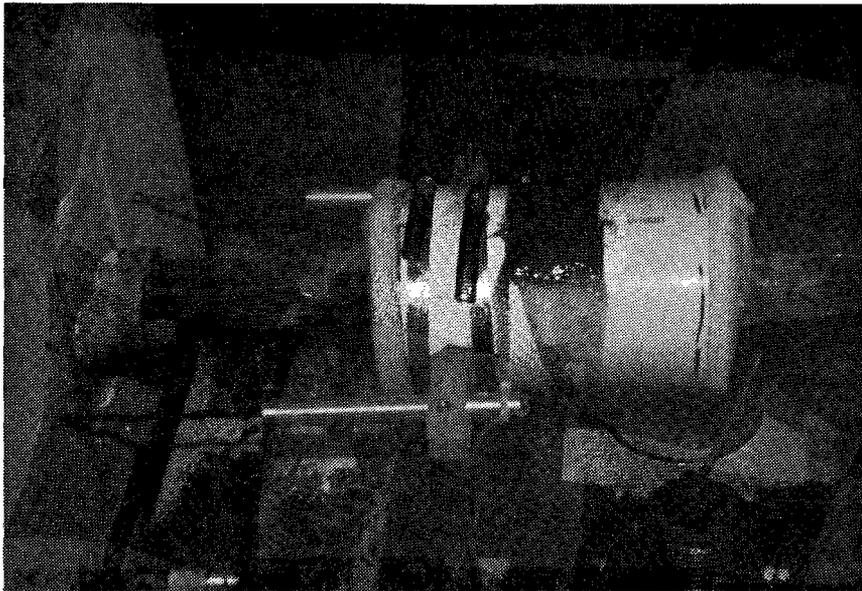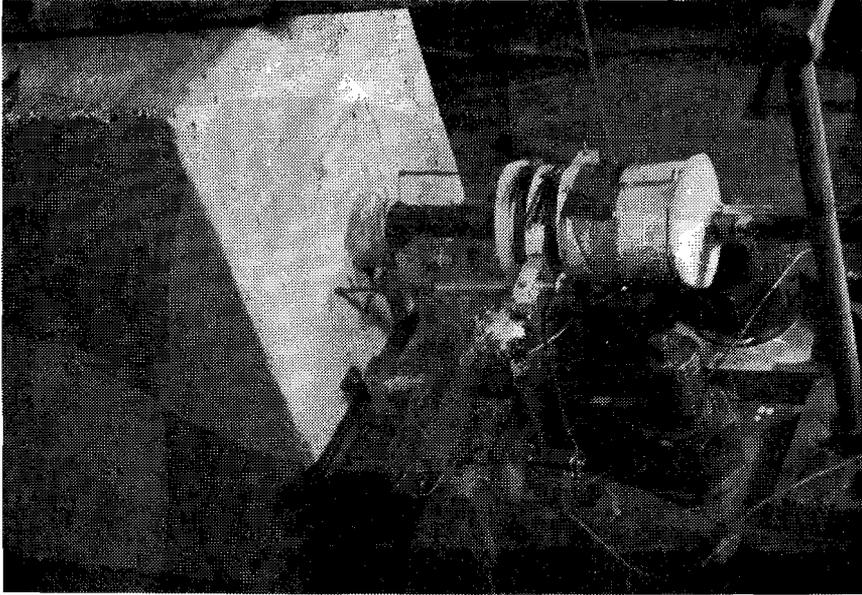
Figure 3.17   Epoxy Collar Formed on Tendon.

70

deviator specimen. Tendon force was taken as the average of four and five gauge readings for the 7 and 12-strand tests, respectively. Since strain gauges were placed adjacent to the epoxy collars, measured strain values in different gauges were very uniform (on one side of the specimen). The maximum variation in strain readings was between 1% and 3%. For test 1A-12-12°, the variation in strain readings was slightly higher since strain gauges were placed prior to positioning the epoxy collar. Testing was discontinued when the tendon force on the south side of the deviator was reduced to zero.

3.1.9 Tendon-Deviator Test Results

3.1.9.1 Introduction. Test results presented in this section are divided into two groups. The first series contains results of the tendon-friction portion of each test determined during the initial post-tensioning operations. This series refers to the results of the curved duct specimens only (Tests 1A-12-12°, 1B-7-12°, 2A-12-6°, and 2B-7-6°). The second series includes results from all six bond stress-slip tests.
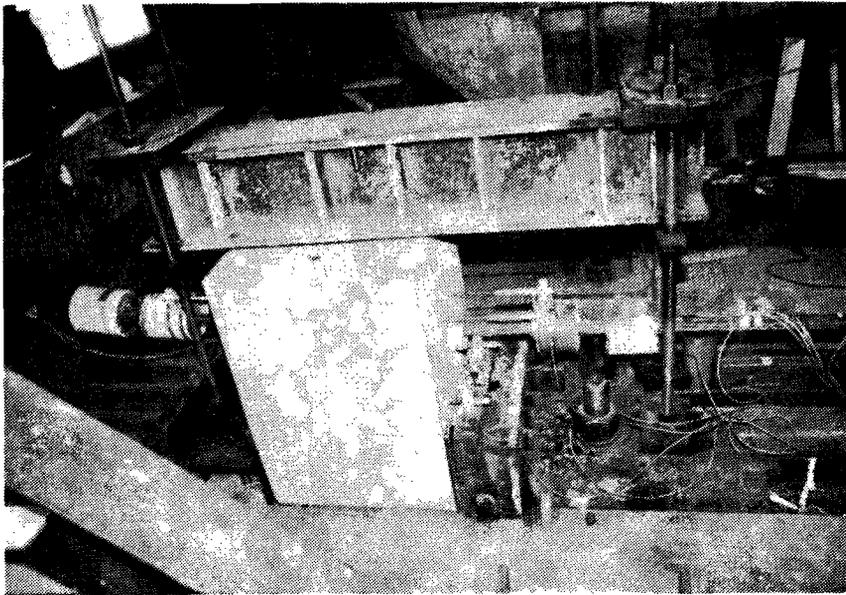
Figure 3.18   General Test Setup with Specimen in Position.

3.1.9.2 Tendon-Deviator Friction Tests. By measuring the tendon forces on each side of the deviators during stressing, friction losses through the curved ducts were determined. From these results, the coefficient of curvature friction for the smooth galvanized duct was calculated as outlined below.

For a prestressing tendon stressed on a curve, the theoretical relationship between the active and passive forces is given by the following formula:

where

BOND STRESS VS. TENDON SLIP
SPECIMEN 1A-12-12
12 STRAND TENDON - 12 DEGREE DEVIATION
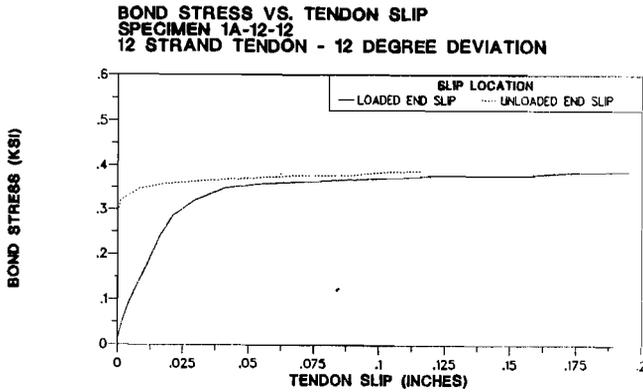
Figure 3.19 Bond Stress-Slip Response for
Specimen 1A-12-12°.

FORCE DIFFERENCE ACROSS DEVIATOR VS. TENDON SLIP
SPECIMEN 1A-12-12
12 STRAND TENDON - 12 DEGREE DEVIATION

Figure 3.20 Pullout Force-Slip Response for
Specimen 1A-12-12°.

$$F_p = F_a e^{-(\mu\alpha + KL)}$$

F_a	=	the tendon force (or stress) on the active (stressed) side
F_p	=	the tendon force (or stress) on the passive side
α	=	the cumulative angular deviation of the tendon (in radians)
μ	=	the coefficient of curvature friction
K	=	the coefficient of wobble friction
L	=	Length of tendon in the duct

Since the deviator duct is rigid and the contact length of the tendon is very short, the value of KL can be considered to be negligible. This means that the value of the coefficient of curvature friction, μ, can be calculated as follows.

$$\mu = -\frac{1}{\alpha} \ln(\frac{F_p}{F_a})$$

Table 3.6 summarizes calculated values of the coefficient of curvature friction for the four tests. The values in the table were calculated at a tendon stress level of $F_a = 0.5f_{pu}$. The ratio of passive tendon force to active force, F_p/F_a, represents the percentage reduction in force due to friction through the deviator duct. These values are also provided in the table.

The coefficient of friction values vary considerably. This variation is largely due to the relatively small deviation angle used in the tests. As shown in Table 3.7, the value of the coefficient of friction is very sensitive to changes in the value of F_p/F_a when small deviation angles are used. Table 3.7 gives a comparison of typical deviator values (top two lines) in contrast to what might be considered more normal total angle changes and losses for internal tendons in a girder (lower two lines). As shown for the structure with internal tendons, the total deviation angle change over the length of the tendon is much greater than the values used in the tests. Furthermore, total friction losses are higher and the ratio of passive to active force is therefore reduced. In this hypothetical case, the variation in

Table 3.6   Coefficients of Curvature Friction

Specimen	Deviation Angle (α)	Duct Radius (ft)	Coefficient of Friction μ	F_p/F_a	Percentage Friction Loss $(1-F_p/F_a)$
1A-12-12°	12°	9.5	0.19	0.96	4%
1B-7-12°	12°	9.5	0.28	0.94	6%
2A-12-6°	6°	18.5	0.26	0.97	3%
2B-7-6°	6°	18.5	0.12	0.99	1%
			Avg.= 0.21		

the friction coefficient is considerably less (see Table 3.7). Similar observations were made by Hoang [46]. For the rigid galvanized ducts used in these tests, The Post-Tensioning Institute [44] recommends a value of 0.20 for the curvature friction coefficient. This value compares very favorably with the average value of 0.21 obtained from the tests described here.

Since all sources of tendon-duct misalignment were eliminated

Table 3.7 Variation of Friction Coefficient

F_p/F_a	Change in F_p/F_a	Total Deviation Angle	Coefficient of Friction	Change in the Coefficient of Friction
0.97	-	12°	0.145	-
0.96	-1.0%	12°	0.195	+34%
0.80	-	100°	0.128	-
0.792	-1.0%	100°	0.134	+4.5%

in the tests, the results could be considered to be for an ideal case. Care was taken to avoid the following sources of error: (1) entangled strands, (2) contact between the tendon and deviator pipe on both ends of the specimen, and (3) pivoting of the duct around the axis joining the points of exit from the deviator block. Tendons in typical structures may contain entangled strand bundles and misaligned deviator ducts. For these cases, friction losses through the deviator may be somewhat higher than the results presented here.

The percentage friction losses are more consistent than the coefficient of friction values. Friction loss through the 12 degree duct is approximately 5% while the loss for the 6 degree duct is 2%.

Change in stress across the deviator due to friction also represents the maximum tendon stress increase that can be achieved by an unbonded tendon for ultimate load

BOND STRESS VS. TENDON SLIP
SPECIMEN 1B-7-12
7 STRAND TENDON - 12 DEGREE DEVIATION
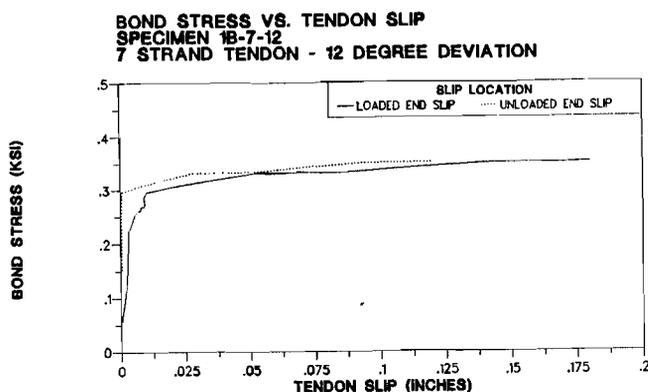
Figure 3.21 Bond Stress-Slip Response for Specimen 1B-7-12°.

FORCE DIFFERENCE ACROSS DEVIATOR VS. TENDON SLIP
SPECIMEN 1B-7-12
7 STRAND TENDON - 12 DEGREE DEVIATION
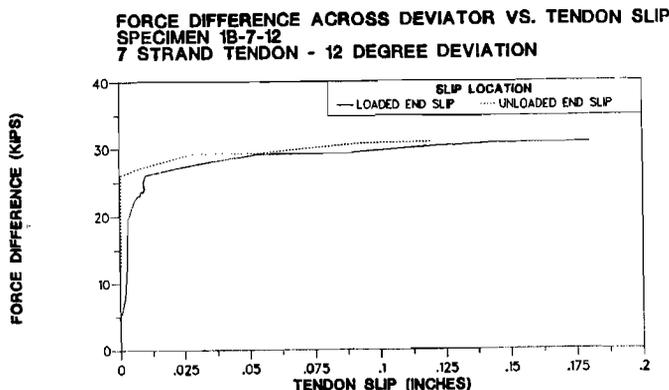
Figure 3.22 Pullout Force-Slip Response for Specimen 1B-7-12°.

conditions (for a single deviator). In an actual structure, a number of deviators exist along the span length. In this case the potential stress increase in the tendon would be the sum of the friction values in successive deviators from the point of interest to the end of the span. This is an ideal case, however, since it does not consider the effect of tendon slip at deviators. As loads are applied to the structure, tension variation in the tendon at particular section will be greater than the friction developed at an adjacent deviator. The tendon will slip through the deviator, and tension will be transferred along the span length to the next deviator. A detailed investigation of this subject was presented by Virlogeux [50].

3.1.9.3 Tendon-Deviator Bond Stress-Slip Tests.

A. Introduction. This section presents the results of six modified pullout tests of multi-strand tendons grouted in curved and straight rigid steel ducts. Tests results indicated that the general behavior of specimens with curved ducts was significantly different from that of straight ducts. General observations for these two groups are presented separately in the following sections. Comparison and evaluation of test data is provided in Chapter 4.

Data obtained from the tests are presented in terms of applied load (pullout load) and displacement (slip) of the tendon at the unloaded and loaded ends of the specimen. The results are also presented in terms of calculated nominal bond stress values. In this chapter bond stresses are computed using an interfacial area based on an equivalent tendon perimeter as outlined in Section 2.3.2. A uniform bond stress distribution along the bonded length is also assumed. Alternative methods for calculating bond stress values are discussed in Chapter 4. Tendon displacements are corrected for elastic shortening in the tendon between the point where potentiometers were attached to the collar and the face of the deviator specimen (the point of slip measurement).

BOND STRESS VS. TENDON SLIP
SPECIMEN 2A-12-6
12 STRAND TENDON - 6 DEGREE DEVIATION

Figure 3.23 Bond Stress-Slip Response for Specimen 2A-12-6°.

FORCE DIFFERENCE ACROSS DEVIATOR VS. TENDON SLIP
SPECIMEN 2A-12-6
12 STRAND TENDON - 6 DEGREE DEVIATION
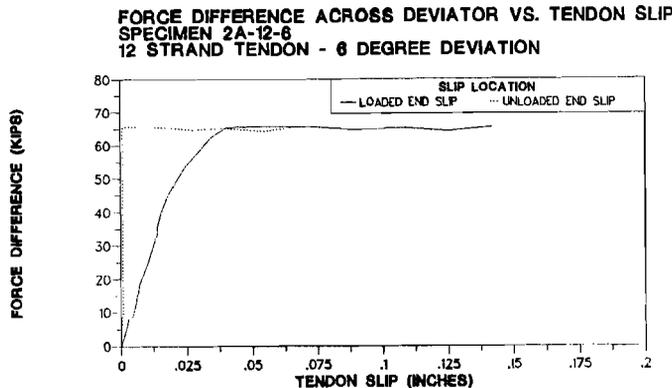
Figure 3.24 Pullout Force-Slip Response for Specimen 2A-12-6°.

For curved ducts, as discussed in Section 3.1.6.5, the total force difference across the deviator is the sum of the friction and bond force components. For the tests described here, tendon forces (and friction through the duct) were reduced as the test progressed. Consequently, the contribution of friction to the total force measured across the deviator was also reduced. In general, however, the test results indicated that the friction component was small compared to the bond component, even for higher tendon force levels. Nevertheless, the net bond component at each stress level was determined and used in the test results presented here. The net bond component was the total force difference measured during testing less the friction force which was calculated using the results of Section 3.1.9.2.

B. Test Results for Deviators with Curved Ducts. A general description of the test results is presented in this section. Comparison and evaluation of data is provided in Chapter 4. For all four test specimens with curved ducts, bond failure and slip occurred at the interface between the tendon and grout. The grout did not move relative to the deviator duct, and no displacement occurred between the duct and deviator block. Bond stress-slip and pullout force-slip relationships for these specimens are shown in Figs. 3.19 through 3.26. As illustrated in the figures, the general shape of the bond stress-slip curves for specimens 1A-12-12°, 1B-7-12°, and 2A-12-6° were quite consistent. Specimen 2B-7-6° exhibited somewhat different behavior. Results of the first three tests are outlined below. The behavior of specimen 2B-7-6° is discussed later in this section.

As outlined in Section 3.1.6.5, load was applied to the deviator by reducing the stress in all strands on the south side of the specimen. The load applied to the deviator was the difference between the tendon force on the north side of the specimen and the reduced tendon force on the south side. This load was effectively applied at the south end of the

BOND STRESS VS. TENDON SLIP
SPECIMEN 2B-7-6
7 STRAND TENDON - 6 DEGREE DEVIATION

SLIP LOCATION
— LOADED END SLIP   ···· UNLOADED END SLIP

BOND STRESS (KSI)

TENDON SLIP (INCHES)
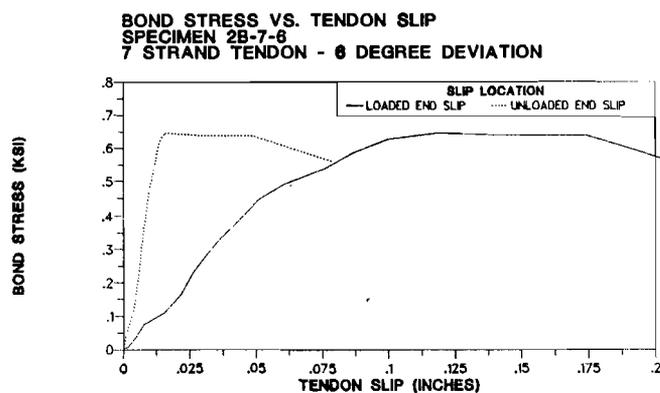
Figure 3.25   Bond   Stress-Slip   Response   for Specimen 2B-7-6°.

FORCE DIFFERENCE ACROSS DEVIATOR VS. TENDON SLIP
SPECIMEN 2B-7-6
7 STRAND TENDON - 6 DEGREE DEVIATION

SLIP LOCATION
— LOADED END SLIP   ···· UNLOADED END SLIP

FORCE DIFFERENCE (KIPS)

TENDON SLIP (INCHES)
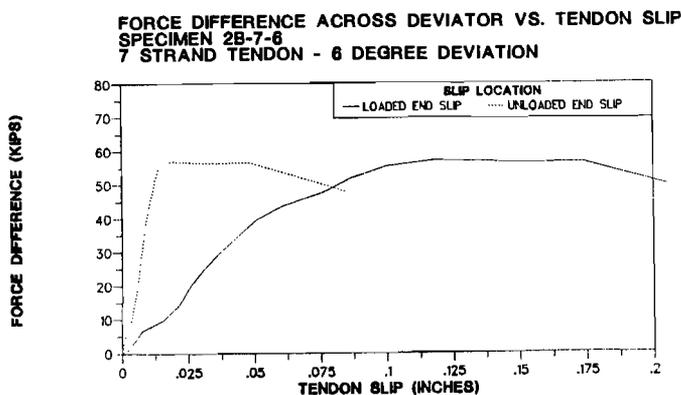
Figure 3.26   Pullout   Force-Slip   Response   for Specimen 2B-7-6°.

specimen as illustrated previously in Fig. 3.15. Consequently, the loaded end (live end) and unloaded end (dead end) of the specimen correspond to the south and north sides respectively.

For the three tests outlined above, tendon slip at the loaded end started immediately upon initial unloading at the live (south) end. Due to the relatively long bonded length, however, the unloaded end (north) did not exhibit measurable slip until much higher loads. As expected, tendon slip progressed from the loaded end to the unloaded end as the pullout load (force difference between the two ends) increased. The differential slip between the loaded and unloaded ends also increased as load was applied (force differential increased). When slip had progressed to the unloaded end (ie. general slip condition), the pullout load generally reached its maximum value and the rate of slip increased significantly. The bond-slip curve resembles an elasto-plastic response curve. The bonded tendon was pulled out with approximately constant load after slip had extended over the total bonded length. The test results are similar to the "stick-slip" behavior of an ideal friction mechanism.

General slip was regarded as the point where slip at the unloaded end was sufficient to produce a measurable reading. Bond stress values at 0.004" (0.1mm) unloaded-end slip are shown in Table 3.8. The unloaded end slip of 0.004 inches conforms to the results presented by Trost [17] and is approximately the point of general slip. Maximum bond stress values are also shown in the table. The ratio of maximum bond stress values to bond stress at general slip ranged from 1.02 to 1.18. These results indicate only minimal reserve bond strength beyond the point of general slip. The tests were conducted using tendons with strands positioned "as parallel as possible" prior to stressing. Actual structures, which might contain tendons with entangled strands, would likely achieve greater bond strengths. Tendon with entangled strands should also exhibit greater reserve bond strength beyond the

BOND STRESS VS. TENDON SLIP
SPECIMEN 3A-12-0
12 STRAND TENDON - NO DEVIATION

SLIP LOCATION
— LOADED END SLIP   ---- UNLOADED END SLIP

BOND STRESS (KSI)

TENDON SLIP (INCHES)
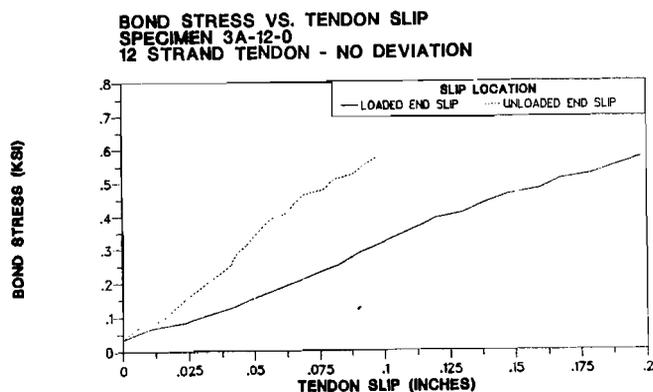
Figure 3.27   Bond   Stress-Slip   Response   for
Specimen 3A-12-0°.

FORCE DIFFERENCE ACROSS DEVIATOR VS. TENDON SLIP
SPECIMEN 3A-12-0
12 STRAND TENDON - NO DEVIATION

SLIP LOCATION
— LOADED END SLIP   ---- UNLOADED END SLIP

FORCE DIFFERENCE (KIPS)

TENDON SLIP (INCHES)
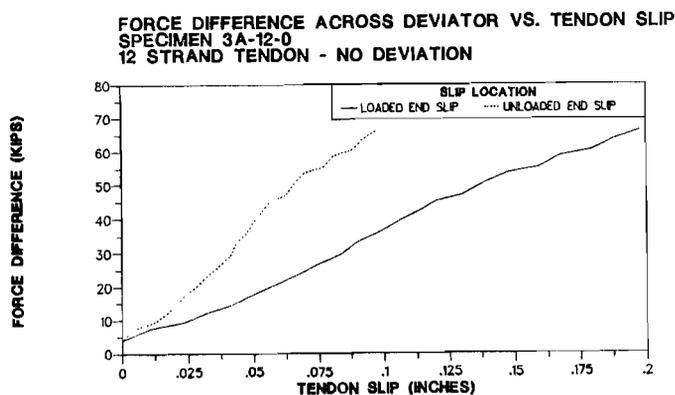
Figure 3.28   Pullout   Force-Slip   Response   for
Specimen 3A-12-0°.

point of general slip due to greater mechanical interlock and interference.

Table 3.8 Bond Stresses For
Specimens with Curved Ducts

Specimen	Bond Stress at 0.004" Unloaded End Slip (ksi) (1)	Maximum Bond Stress (ksi)(1)
1A-12-12°	0.33	0.39
1B-7-12°	0.31	0.35
2A-12-6°	0.56	0.57
2B-7-6°	0.16(2)	0.64

(1) Bond stress based on equivalent tendon perimeter.
(2) General slip commenced earlier than for other 3 tests.

The measured loaded-end slip at the transition points in the bond-slip curves was also very uniform for three of the tests. The transition point can be defined as the point where the increase in bond stress for a given increment of slip becomes negligible. Loaded-end slip was of the order of 0.04-0.05" for the transition points in the three tests outlined previously (see Figs. 3.19 through 3.24). Slip values at the unloaded end were also very consistent. Very stable pullout was achieved for all cases; maximum bond stresses were maintained up to high levels of tendon slip.

Specimen 2B-7-6° exhibited different behavior. The unloaded end started to slip at the onset of loading. When the maximum bond stress was achieved, loaded-end slip was considerably greater than that of the other specimens with curved ducts. Despite this, however, stable pullout was observed.

As shown in Table 3.8, bond stresses varied considerably more than the tendon slip values. The lowest bond stress value for specimen 1B-7-12° was most likely the result of poor grout strength. For this test the grout strength was significantly lower than that of the

other three specimens (see Table 3.5). However, the bond stress was close to the value obtained for specimen 1A-12-12°. For test 2B-7-6°, the unloaded end slipped earlier than for any of the other tests. Consequently, bond stress at general slip was significantly lower.

Bond stress differences between the 6 and 12 degree deviation specimens are more difficult to evaluate. Tendons with smaller deviation angles exhibited significantly higher bond strengths. As shown in Chapter 4, however, the differences between the two cases are less when the results are interpreted in terms of pullout force. One possible explanation for this apparently contradicting trend could be the limited number of tests and the large scatter that can be expected for bond tests. The tests results may simply reflect this scatter (especially when the pullout force values are compared, as outlined in Chapter 4). This would indicate that the duct deviation angle may not be a significant factor in the bond developed at the deviators, especially for such small differences in angle. (However, tendons passing through straight ducts may exhibit significantly different

BOND STRESS VS. TENDON SLIP
SPECIMEN 3B-7-0
7 STRAND TENDON - NO DEVIATION

Figure 3.29 Bond Stress-Slip Response for Specimen 3B-7-0°.

FORCE DIFFERENCE ACROSS DEVIATOR VS. TENDON SLIP
SPECIMEN 3B-7-0
7 STRAND TENDON - NO DEVIATION

Figure 3.30 Pullout Force-Slip Response for Specimen 3B-7-0°.

behavior as outlined below). Considering the limited number of tests, any conclusions must be regarded with caution. Differences in bond capacity could also be the result of variations in grout quality. For the 12 degree tendon, the grout column extended over a greater height than the 6 degree case. Since the potential for grout bleeding becomes more pronounced as the height of grout increases, it could be expected that a longer portion of the bonded length at the top of the 12 degree tendon would be subjected to bleeding. This would reduce the effective bond area. However, inspection of the grout at the inlet and outlet ends of the specimen revealed excellent grout penetration for all specimens. One final explanation for this trend is suggested. The 6 degree tests used a duct which had an

78

angular overbend which was greater than the 12 degree case (2 degrees vs. 1.5 degrees). Although the difference is small, the space between the top of the tendon and duct wall was somewhat greater for the 6 degree case over a longer portion of the bonded length (at the deviated side of the specimen). Grout penetration and effective bond area might be enhanced for the 6 degree case.

C. Test Results for Deviators with Straight Ducts. For the deviator specimens with straight ducts, net bond stress values were obtained directly since no friction existed. The bond stress-slip and pullout force-slip behavior for the two specimens with a straight duct are shown in Figs. 3.27 through 3.30. In both tests, bond failure and slip occurred at the duct-grout interface (the duct did not displace through the concrete deviator block). As shown in Fig. 3.30, the tendon did not slip relative to the grout at the loaded end of the specimen. Although grout displacement was not measured at the unloaded end, it appeared that the tendon slipped through the grout at the unloaded end of the specimen. Differential strain developed along the bonded length of the tendon as a result of this slip.

Table 3.9 Bond Stresses for Specimens with Straight Ducts

Specimen	Bond Stress at 0.004" Unloaded End Slip (ksi)(1)	Maximum Bond Stress (ksi)(1)
3A-12-0°	0.04	0.63
3B-7-0°	0	0.42

(1) Bond stress based on equivalent tendon perimeter.

For both tests, significant bond stresses were achieved only after large displacements had occurred. Bond stresses at low displacement levels were much lower than values obtained from the curved duct specimens. The observed bond stress values outlined in Table 3.9 are based on the same stress distribution and general slip criteria outlined earlier.

Maximum bond stresses shown in the table are comparable to values obtained for specimens with curved ducts. The mode of failure, however, was different. Bond failure occurred suddenly when the grout core slipped in the deviator pipe. This failure is illustrated clearly in Fig. 3.30. As outlined in Chapter 4, bond failure for the curved-duct specimens was much more progressive.

3.2 Dismantled Bridge Span Tests

3.2.1 Introduction.   As outlined in Chapter 1, this report is part of a larger study which investigated the effects of improved bonding of external tendons in externally post-tensioned bridges. Part of this larger study included testing of a three-span externally post-tensioned precast segmental box-girder bridge model. This scale model is shown in Fig. 3.31. After the test program was completed, the three spans were separated by cutting the continuity tendons over the pier segments. The spans were then removed from the laboratory as individual intact units (segments remained under compression from external post-tensioning). The external tendons were anchored at the ends of each dismantled span and were bonded at all deviator locations along the span length. The test series described here consisted of successively cutting the external tendons and monitoring stress differences across the diaphragm (deviator) locations where the tendons were bonded. The objective of the test program was to determine the level of bond stress developed through the diaphragms.
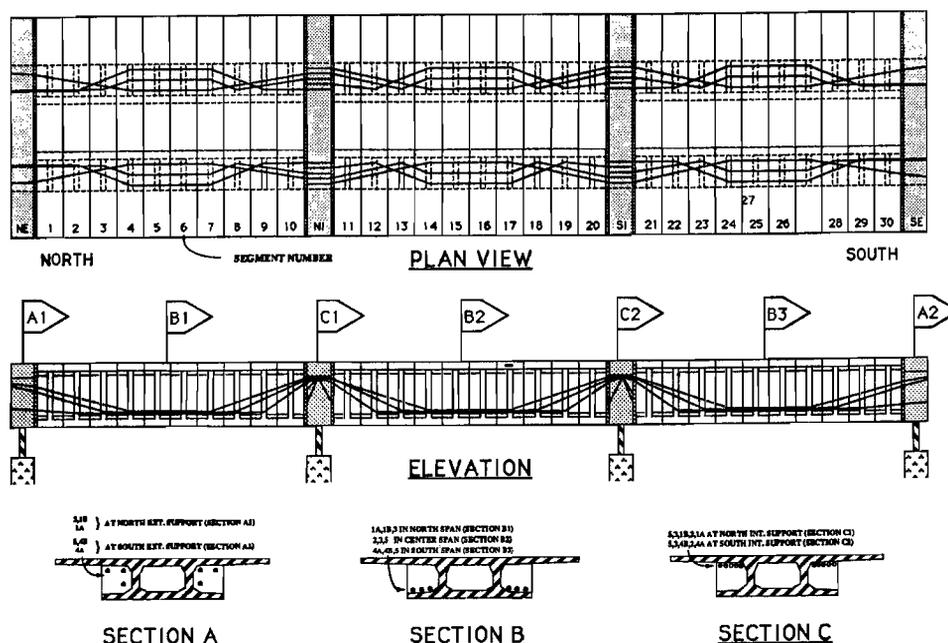
Figure 3.31   Schematic of Post-Tensioning Layout in Bridge Model (from Ref. 3).

3.2.2. Background.   For the test program outlined above , the bridge spans were subjected to several ultimate flexural load cycles [3,6]. During these tests, the external tendons slipped through the grout at higher load levels. Despite this however, a post-mortem investigation of the grouted tendons did not indicate cracking or deterioration of the grout [6]. The external tendons and concrete segments were in relatively good condition after testing was completed. Strain gauges and lead wires were also in position on each side of a number of the deviators in each span (see Section 3.2.5).

3.2.3 Description of Dismantled Spans (Test specimens).

The North and South spans which were tested in this facet of the complete program are shown in Figs. 3.32 and 3.33. To maintain the integrity of the spans after testing, only the 5-strand tendons (ie. Tendons 1A, 1B, 4A, and 4B) were cut. The 2-strand tendons (ie. Tendons 3 and 5) were not easily accessible and were not cut. The tendons were bonded at all diaphragm (deviator) locations (as part of the original test program). Pertinent tendon-deviator details in the bridge model are outlined below.

Prestressing steel used in the bridge model was 3/8" diameter Grade 270 low relaxation strand. The strand had a measured ultimate strength of 279 ksi and a specified elastic modulus of 28,400 ksi. Strand tests indicated an apparent modulus of 30,300 ksi [3].

As shown in Figure 3.31, tendons 1A, 1B, 4A, and 4B were deviated vertically at two points along the span length. These tendons were also deviated horizontally at four locations in each span. Deviation angles for these tendons, at diaphragms where the test results were obtained, are shown in Table 3.10.

Grout used in the external tendon ducts conformed to Texas State Department of Highways and Public Transportation specifications (see Section 3.1.3.2). Ducts at all diaphragm (deviator) locations consisted of 1-1/2" diameter galvanized electrical conduit. Between deviator locations, the tendons were enclosed in high-density polyethylene tubing which was spliced to the ducts on each side of every diaphragm. All deviators consisted of five- inch thick solid diaphragms. The duct extension beyond the face of the deviator varied from approximately 1/2" to 1". The duct extension increases the effective bond area at the duct-grout (and tendon-grout) interface. However, for the tests described here, the bonded length at each deviator was simply taken to be equal to be five inches (the width of the diaphragm).

3.2.4 Instrumentation and Test Setup.

The general layout of the test specimen and data acquisition equipment is shown in Fig. 3.34. Electrical resistance strain gauges were used to measure strain in the external tendons during testing. These gauges had been placed at a number of positions along the span length and used during the original test program. The layout of the gauges is shown in Fig. 3.35. The tendon force was determined from the average of two gauge readings at each location. Signals from the strain gauges were read electronically with a Hewlett-Packard scanner driven by an IBM XT computer. Tendon slip was not measured during the tests.

3.2.5 Test Procedure.

The following is a summary of the testing procedure:

(1)   A "zero state" reading of all strain gauges was taken.

(2)   The specified tendon was cut with a power grinder in the middle of the span (ie. between segments 5 and 6 as shown in Fig. 3.36). The corresponding tendon on the other side of the bridge was then cut at the same location.

SECTION

Y top =6.60"

Y bot =9.40"

h   h

NEPS

Tendon 1A

Tendon 1B   Tendon 3

NIPS

X (FT)
FROM ℄ NEPS

0

ELEVATION
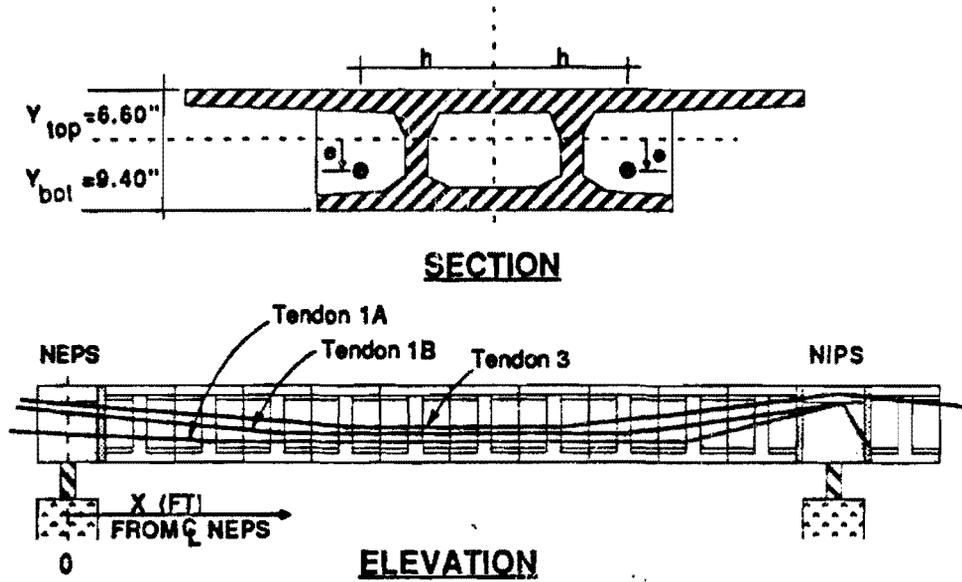
TENDON 1A : 2 x (5-3/8" dia. Grade 270 Strands)

x (ft)	-1	0	4.625	9.125	15.875	20.375	25	26
e (in)	2.9	3.4	5.65	6.23	6.23	5.65	-2.67	3.15
h (in)	15	15	15	22	22	15	14	15.25

TENDON 1B : 2 x (5-3/8" dia. Grade 270 Strands)

x (ft)	-1	0	6.875	9.125	15.875	18.125	25	26
e (in)	-2.48	-2.1	5.65	5.94	5.94	5.65	-2.61	3.15
h (in)	15	15	15	18.5	18.5	15	18.25	20.75

TENDON 3 : 2 x (2-3/8" dia. Grade 270 Strands)

x (ft)	-1	0	9.125	15.875	25	31.875	Continues
e (in)	-2.6	-2.1	5.65	5.65	-2.86	5.65	In Center Span
h (in)	21.5	21.5	15	15	20.38	15	

Figure 3.32   North Span Tendon Layout (from Ref. 3).

SECTION

ELEVATION
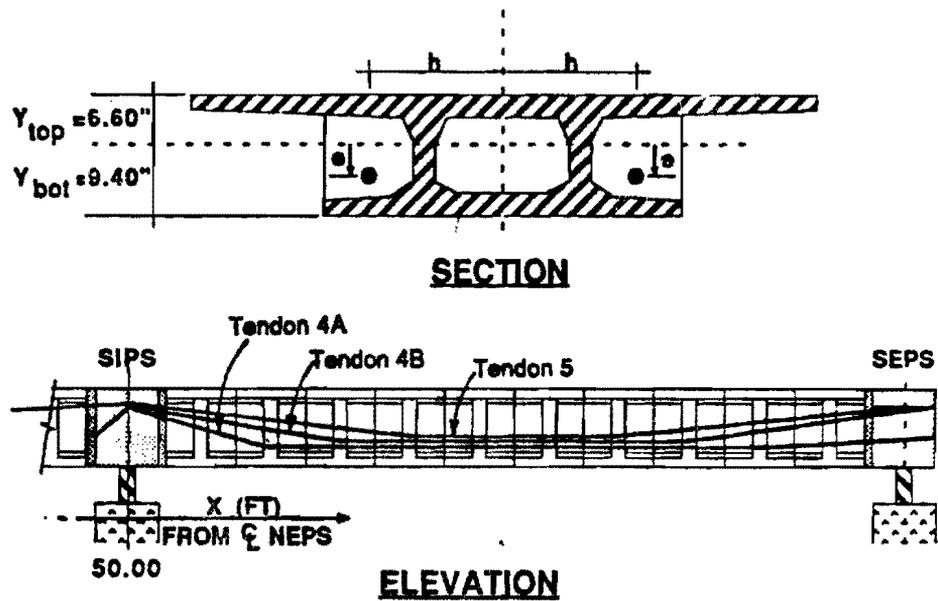
TENDON 4A : 2 x (5-3/8" dia. Grade 270 Strands)

x (ft)	49	50	54.625	59.125	65.875	70.375	75	76
e (in)	3.15	-2.67	5.65	6.23	6.23	5.65	3.4	2.9
h (in)	15.25	14	15	22	22	15	15	15

TENDON 4B : 2 x (5-3/8" dia Grade 270 Strands)

x (ft)	49	50	56.875	59.125	65.875	68.125	75	76
e (in)	3.15	-2.81	5.65	5.94	5.94	5.65	-2.1	-2.48
h (in)	20.75	18.25	15	18.5	18.5	15	15	15

TENDON 5 : 2 x (2-3/8" dia. Grade 270 Strands)

x (ft)	Continues	40.875	50	59.125	65.875	75	76
e (in)	In Center Span	5.65	-2.95	5.65	5.65	-2.1	-2.6
h (in)		15	22.5	15	15	21.5	21.5

SOUTH EXTERIOR SPAN

Figure 3.33   South Span Tendon Layout (from Ref. 3.).
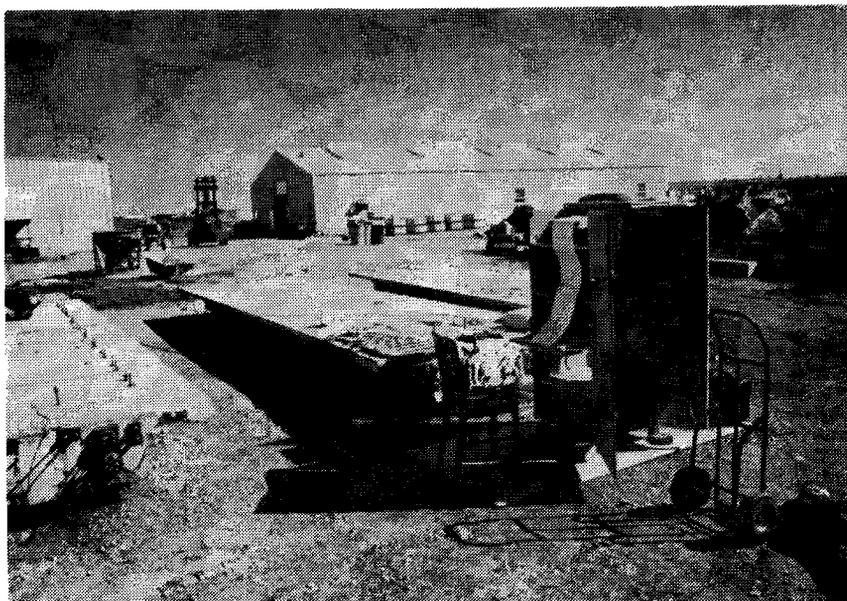
Figure 3.34 Dismantled Span Test Layout.

This was done to ensure that the tendon force could not be redistributed to the other side of the segment. It also eliminated the effects of flexural displacement on tendon stresses by balancing the forces on both sides of the segment.

(3) The instrumentation was scanned to measure the change in stress in the tendons at each location.

(4) The tendon was cut in the segment adjacent to midspan (ie. between segments 4 and 5 as shown in Figure 3.36). The corresponding tendon was also cut on the other side of the bridge.

(5) The instrumentation was scanned to measure changes in tendon stress. The bond force developed in the diaphragm of each segment was determined as outlined in Fig 3.36.

(6) This procedure was repeated for each successive segment towards the end of the span. An identical procedure was used for cutting tendons towards the other end of the span.

3.2.6 Dismantled-Span Test Results. The total bond developed at the deviator could be calculated directly when tendon stresses were obtained on both sides of the diaphragm before and after cutting the tendon. In some cases, however, gauges failed in segments where gauges were cut. For these cases, stress changes could not be obtained

T-(1,2)-(1A.W1)
(1A.W2)
-(1A.E1)
-(1A.E2)
(1B.W1)
(1B.W2)
-(3.W1)
-(3.W2)

T-(5,6)-(1A.W1)
(1A.W2)
-(1A.E1)
-(1A.E2)
(1B.W1)
(1B.W2)
-(3.W1)
-(3.W2)

T-(9,10)-(1A.W1)
(1A.W2)
-(1A.E1)
-(1A.E2)
(1B.W1)
(1B.W2)
-(3.W1)
-(3.W2)

T-(11,12)-(2.W1)
-(2.W2)
-(2.E1)
-(2.E2)
-(3.W1)
-(3.W2)
-(5.W1)
-(5.W2)

T-(15,16)-(2.W1)
-(2.W2)
-(2.E1)
-(2.E2)
-(3.W1)
-(3.W2)
-(5.W1)
-(5.W2)

T-(19,20)-(2.W1)
-(2.W2)
-(2.E1)
-(2.E2)
-(3.W1)
-(3.W2)
-(5.W1)
-(5.W2)

T-(21,22)-(4A.W1)
-(4A.W2)
-(4A.E1)
-(4A.E2)
(4B.W1)
(4B.W2)
-(5.W1)
-(5.W2)

T-(25,26)-(4A.W1)
-(4A.W2)
-(4A.E1)
-(4A.E2)
(4B.W1)
(4B.W2)
-(5.W1)
-(5.W2)

T-(29,30)-(4A.W1)
-(4A.W2)
-(4A.E1)
-(4B.E2)
-(4B.W1)
-(4B.W2)
-(5.W1)
(5.W2)

Segment Number

1 2 3 4 5 6 7 8 9 10 NI 11 12 13 14 15 16 17 18 19 20 SI 21 22 23 24 25 26 27 28 29 30

T-(3,4)-(1A.W1)
(1A.W2)
(1B.W1)
-(1B.W2
-(3.W1)
-(3.W2)

T-(4,5)-(1A.W1)
(1A.W2)
(1B.W1)
-(1B.W2
-(3.W1)
-(3.W2)

T-(7,8)-(1A.W1)
(1A.W2)
(1B.W1)
-(1B.W2
-(3.W1)
-(3.W2)

T-(NI,11)-(2.W1)
-(2.W2)
-(3.W1)
-(3.W2)
-(5.W1)
-(5.W2)

T-(20,SI)-(2.W1)
-(2.W2)
-(3.W1)
-(3.W2)
-(5.W1)
-(5.W2)

T-(23,24)-(4A.W1)
(4A.W2)
(4B.W1)
(4B.W2)
-(5.W1)
-(5.W2)

T-(26,27)-(4A.W1)
(4A.W2)
(4B.W1)
(4B.W2)
-(5.W1)
-(5.W2)

T-(27,28)-(4A.W1)
(4A.W2)
(4B.W1)
(4B.W2)
-(5.W1)
-(5.W2)

North Span - Tested

Interior Span - Not Tested

South Span - Tested

25'

25'

25'

For Example:

T-(9,10)-(1A.W1) represents Strain Gauge No.1 at Joint (9,10) on Tendon 1A on the West Side

Figure 3.35   Instrumentation Layout for Strain Gauges.

After Cutting the Tendon Between Segments 5 & 6 :
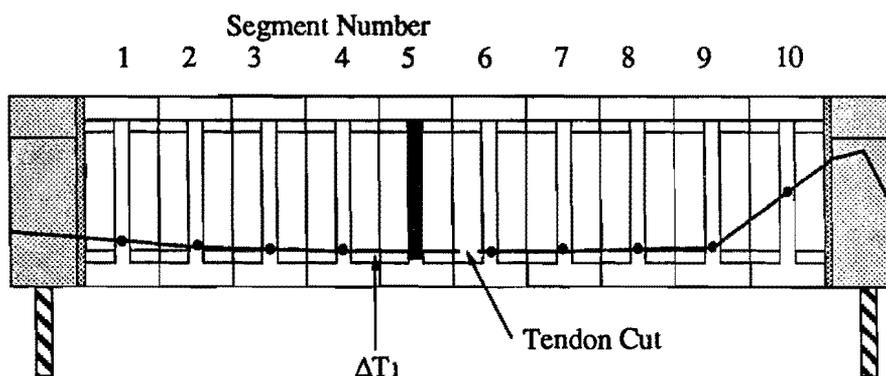
After Cutting the Tendon Between Segments 4 & 5 :
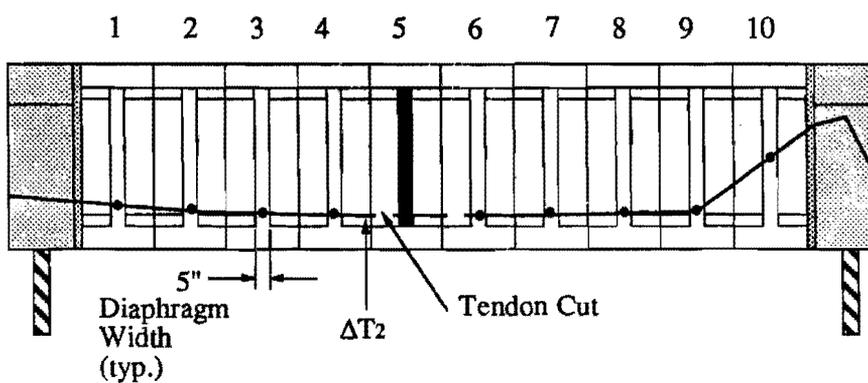
ΔT_1 = Measured change in tendon stress after first cut
(from initial zero reading)

ΔT_2 = Measured change in tendon stress after second cut
(from initial zero reading)

$(\Delta T_2 - \Delta T_1)$ Aps = Bond force developed through shaded diaphragm

Where Aps = Tendon Area

Figure 3.36   Calculation of Bond Force by Cutting the External Tendons (adapted from Ref. 6).

after cutting the tendon. Despite this, good results were obtained for eight cases where gauges did not fail after cutting the tendons. These results are shown in Table 3.10. The bond stresses indicated in the table are based on an equivalent tendon diameter and a uniform bond stress distribution along the five inch bonded length. Bond stress results were taken directly from tendon stress measurements regardless of the deviation angle of the tendons. No consideration was given to the friction component of the bond force (for deviated tendons) since it was considered to be a small portion of the total force developed across the deviator.

Table 3.10 Bond Stress Across Diaphragms

Case	Location of Deviator	Tendon	Tendon Deviation Angles (Vertical/ Horizontal) Degrees	Stress Difference Per Strand Across Diaphragm (ksi)(1)	Force Difference Across Diaphragm (kips)	Nominal Bond Stress (ksi)
1	South Span Segment 26	4B	0/0	7.0	3.0	0.26
2	South Span Segment 27	4B	0/7.4	20.0	8.5	0.73
3	North Span Segment 5	1A	0/0	23.1	9.8	0.85
4	North Span Segment 4	1A	0/7.4	17.9	7.6	0.66
5	North Span Segment 5	1B	0/0	24.7	10.5	0.91
6	North Span Segment 4	1B	0/7.4	11.0	4.7	0.40
7	South Span Segment 26	4A	0/0	7.0	3.0	0.26
8	South Span Segment 27	4A	0/7.4	13.0	5.5	0.48
Average				15.5	6.6	0.57

(1) 5 strand tendon

After tendons were cut, large differential stresses were applied across the deviator adjacent to the cut (especially for segments located near midspan where all of the test results were obtained). Stresses in the tendons prior to cutting ranged from 135-170 ksi per strand. After the tendons were cut, stresses transferred to the deviator adjacent to the cut were considerably greater than the expected bond capacity. Although the tendon slip was not measured, it is likely that the tendons slipped through the grout at these locations and a large portion of the stress differential was transferred along the span to adjacent deviators. Despite this extremely severe loading condition, bond did not fail completely at the deviator adjacent to the cut. In fact, tests results indicate that considerable bond capacity was maintained even after the tendon had slipped. This means that bond stresses from the tests correspond to ultimate bond capacities that can be achieved at high levels of tendon slip. This is important since it shows that significant bond can be maintained at deviators even after severe overloads have been experienced.

3.3 Remedial Bonding Tests for Tendons at Pass-Through Locations

3.3.1 Introduction.   As outlined previously, the overall project 1209 study at The University of Texas investigated the effects of improved bonding of external tendons for externally post-tensioned bridges [6]. The scope of this study included the testing of a three-span externally post-tensioned box-girder bridge model. External tendons in this structure were bonded to the structure by cement grout at all diaphragm and pier locations where the tendons were deviated. At all other diaphragm locations the tendons were passed through the diaphragm (prior to remedial bonding). Similar pass-through details are also common at intermediate diaphragms in existing structures. This test series consisted of a preliminary study to investigate methods for bonding the external tendons at these pass-through locations. The primary objective of the tests series described here was to recommend methods for remedial bonding of external tendons. Preliminary results from the bridge model tests indicate that bonding the tendons at pass-through locations in diaphragms will increase the strength and ductility of a segmental box-girder bridge with external tendons [6].

In an actual structure, two aspects of remedial bonding of external tendons must be considered. The first concerns bond between the tendon and grout. The possibility of bond failure between the grout and inside face of the duct is also pertinent. This aspect was investigated in the full-scale bond tests outlined in Section 3.1. The second aspect concerns the bond between the deviator duct and concrete diaphragm. In order to simulate cast-in-place behavior, a very rigid linkage between the pass-through duct and the diaphragm is desirable. Bond developed between the duct and the diaphragm should also be sufficient to ensure bond failure at the tendon-grout or grout-duct interface for ultimate load conditions.

3.3.2 Background.   Provisions were made in the bridge model to permit bonding of external tendons at all diaphragm pass-through locations. As shown in Fig. 3.37, during
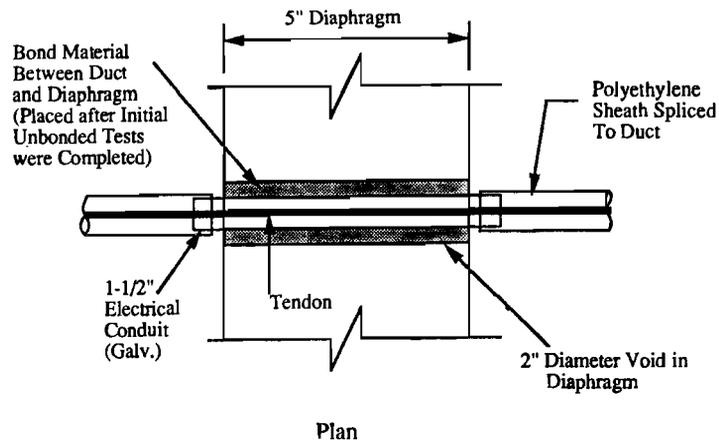
Figure 3.37 Duct-Deviator Detail in Bridge Model.

initial construction a piece of 1-1/2" diameter metal conduit was passed through an oversized 2" diameter hole that was formed in the diaphragm during casting of the segments. Polyethylene sheathing was spliced to the electrical conduit on both sides of the diaphragm to form a continuous sheath for the external tendon. The tendon sheath was grouted after stressing. At this stage there was no effective bond between the tendon and concrete at these diaphragm pass-through locations. At a later stage of testing it was desirable to effectively bond the metal duct to the concrete diaphragm. The original detail was designed to permit remedial bonding of the duct to the diaphragm by injecting an adhesive material into the void between the metal conduit and concrete (see Fig. 3.37). Prior to performing remedial bonding on the bridge model, a series of satellite tests were conducted to investigate the bond performance of a number of adhesive injection materials. These tests are outlined below.

3.3.3 Fabrication of Bond Test Specimens

3.3.3.1 General. Test specimens were similar to the pass-through detail used in the bridge model. They consisted of a 1-1/2 inch diameter metal duct (electrical conduit) placed inside a 2 inch diameter blockout in a precast concrete block as shown in Fig. 3.38. The precast concrete block was 5 inches thick (the same thickness as the diaphragms in the model bridge). Six ducts were placed in each concrete block and were positioned in the middle of the blockouts using styrofoam wedges. To permit the injection of the bond material, polyethylene injection and outlet tubes were placed in each end of the specimens. The injection tube was placed below the duct on one side of the specimen and the outlet tube was positioned above the duct on the other side. Spaces between the duct and concrete at the end of the specimens were then sealed with either silicone or epoxy as outlined in Section 3.3.3.2. After the sealing material had hardened, specimens were ready for injection of bond material between the metal duct and concrete block.
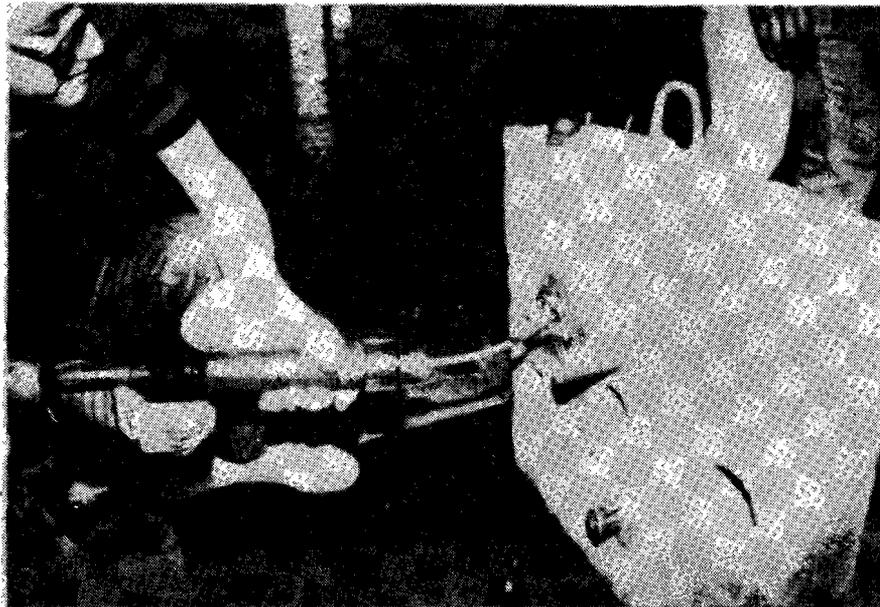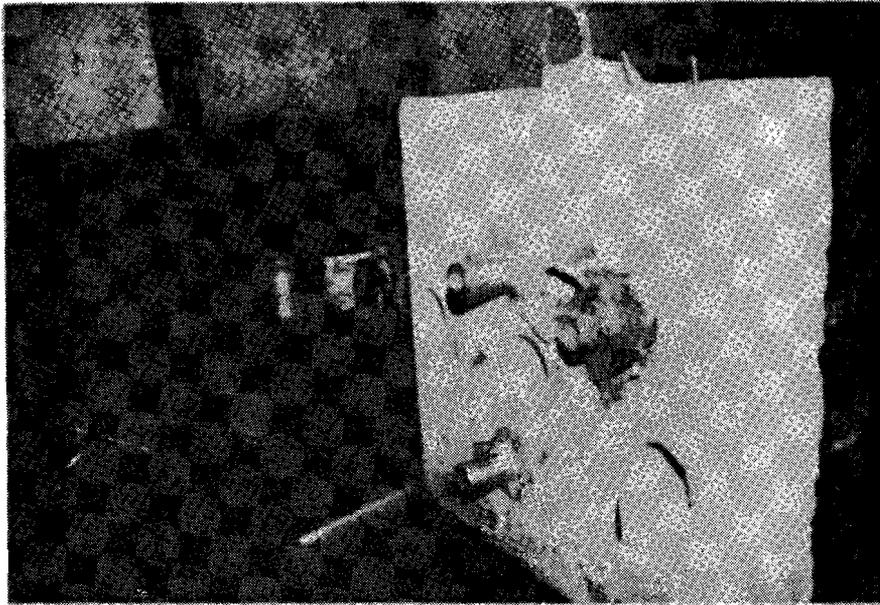
Figure 3.38   Bond Specimens.

3.3.3.2 Injection of Specimen. The primary variables in the test program were the type of sealing agent and type of bond material. Three epoxy materials and two grout mixes were investigated. The sealing agents consisted of either silicone or epoxy. Injection materials used in the tests are outlined below.

A) Specimens Sealed with Silicone.

1) Cement grout with a water cement ratio of 0.5. (Aside from the water cement ratio the grout was similar to that outlined in Section 3.1.3.2).

2) Cement grout with a water-cement ratio of 0.4.

B) Specimens Sealed with Epoxy.

1) Cement grout with a water cement-ratio of 0.4.

2) Texas State Department of Highways Type A-103 epoxy adhesive with 50% magnesium filler material (by weight). The A-103 epoxy is identical to Type V (Special) epoxy adhesive which is commonly used by TSDHPT for bonding segment joints. The epoxy was manufactured by Industrial Coatings Specialties Corporation.

3) HILTI-Crack Injection Epoxy (Type EP-IS650) without filler material.

4) Type A-103 Epoxy adhesive with 50% sand filler (by weight).

Type A-103 epoxy was also used to seal the specimens.

Mixing and application of epoxy resins was carried out according to the manufacturers' specifications. A hand injection gun was used to force epoxy into the void space. Injection was stopped when no air was visible in the flow of epoxy at the outlet nozzle. The injection and outlet ports were not sealed after injection. Cement grout was pumped into the void space with a commercial grout machine which used compressed air to force the flow. General grouting procedures were similar to those outlined in Section 3.1.6.4., however, injection ports were not closed off after grouting. Bond specimens were cured for seven days prior to testing. A total of 18 specimens were fabricated and tested.

3.3.4 Test Procedure. Specimens were loaded to failure in a 600 kip test machine. The specimen was supported on steel plates, and load was applied to the metal conduit which extended from the concrete block. Since the concrete block contained six specimens, it was necessary to shift the block after each test to align a new specimen under the loading head. Applied load was measured directly from the calibrated test machine. Displacement of the steel ducts was not measured.

3.3.5 Bond Specimen Test Results. Three tests were conducted for each type of injection mix. The simple average of the test results for each specimen type are shown in Fig. 3.39. For all tests, bond failure occurred at the interface between the metal duct and injection material. Load typically increased until the duct started to slip through the bond material. Test results were based on the maximum force developed by bond during testing.

DEVIATOR BOND FORCE

1- CEMENT GROUT w/c=0.5
2- CEMENT GROUT w/c=0.4   ⎱ SILICONE SEAL

3- CEMENT GROUT w/c=0.4
4- A103 EPOXY AND 50% MAGNESIUM
5- HILTI CRACK INJECTION EPOXY   EPOXY SEAL
6- A103 EPOXY AND 50% SAND
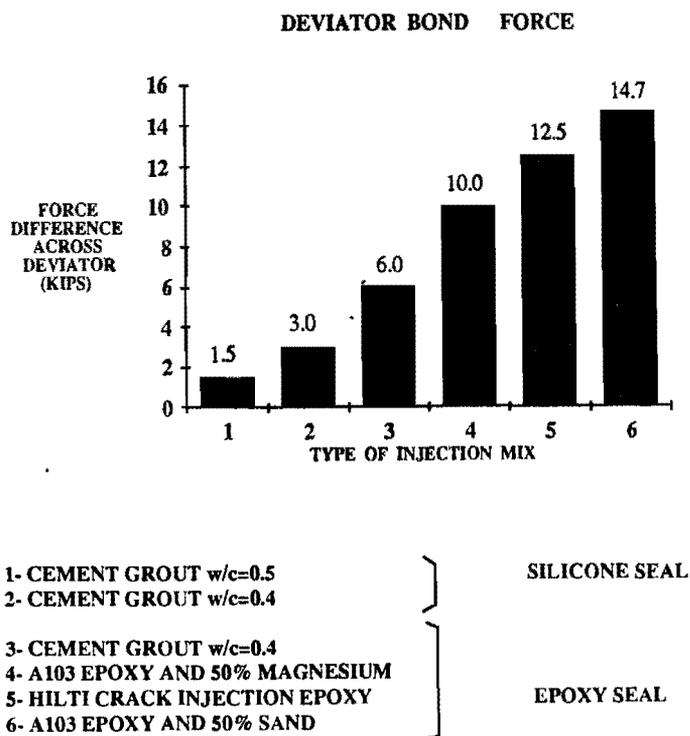
Figure 3.39   Bond Specimen Test Results.

The epoxy adhesive specimens developed significantly greater bond strength than grouted specimens. It appears that epoxy adhesive materials are most suitable for achieving a rigid linkage between the duct and diaphragm. A comparison can be made between results for the epoxy adhesives shown in Fig. 3.39 and those outlined previously in Table 3.10 (tendon-grout bond tests). The bond developed between the duct and diaphragm by the A-103 epoxy and sand mixture is greater than the bond between the tendon and grout for all cases. This epoxy mix will ensure bond failure at the tendon-grout (or grout-duct) interface for ultimate load conditions.

CHAPTER 4

Comparison And Evaluation of Test Results

4.1 Tendon-Deviator Bond Stress-Slip Tests

4.1.1 Introduction. This section contains the evaluation and comparison of the tendon-deviator bond stress-slip test results. The initial sections present a general discussion of specimen performance and deal with the effects of the primary variables on the test results. The influence of the tendon deviation angle and the ratio of tendon area to duct cross-sectional area are discussed. Bond stress and slip results are also compared to values obtained in other related studies. In subsequent sections, a bond stress-slip model is developed for multi-strand tendons grouted in smooth steel ducts. This model is also compared to a similar relationship proposed by Martins [38]. Implications of the test results on ultimate behavior are discussed in Section 4.4.

As outlined in Chapter 3, the bond mechanism between the external tendon and deviator duct is affected by a large number of interdependent variables. Although the scope of this study was limited, the tests did investigate specific bond conditions which exist at deviators typical of U.S. structures. The results have enhanced the understanding of the bond mechanism at the deviator, and it is believed that meaningful preliminary recommendations can be made.

4.1.2 Discussion and Comparison of Test Results

4.1.2.1 Specimens with Curved Ducts. As outlined in Chapter 3, the curved-deviator specimen bond results were based on a calculated net bond component. For each load level during a test, the net bond value was the total measured force difference across the deviator less the calculated friction component. The friction component was calculated using the coefficient of curvature friction obtained from the first phase of each test. Tendon slip values were corrected for elastic shortening in the tendon between the point where potentiometers were connected to the epoxy collar on the tendon and the face of the deviator specimen (the point of slip measurement).

Specimen Behavior and Failure. For all curved-duct specimens, bond failure and slip occurred at the interface between the tendon and grout. The grout block did not move relative to the deviator duct and no displacement occurred between the duct and deviator block. The bond stress-loaded end slip and pullout force-slip performance of the four specimens with curved ducts are shown in Figs. 4.1 and 4.2. The results are also shown in Figs. 4.3 and 4.4 with the slip scale increased to make the overall behavior more clear. Bond stresses in the figures are based on an equivalent tendon area and uniform stress distribution as outlined in Section 3.1.9.3. General observations from the test results are summarized and discussed below.

93

BOND STRESS VS. LOADED END TENDON SLIP
TESTS WITH DEVIATED TENDONS
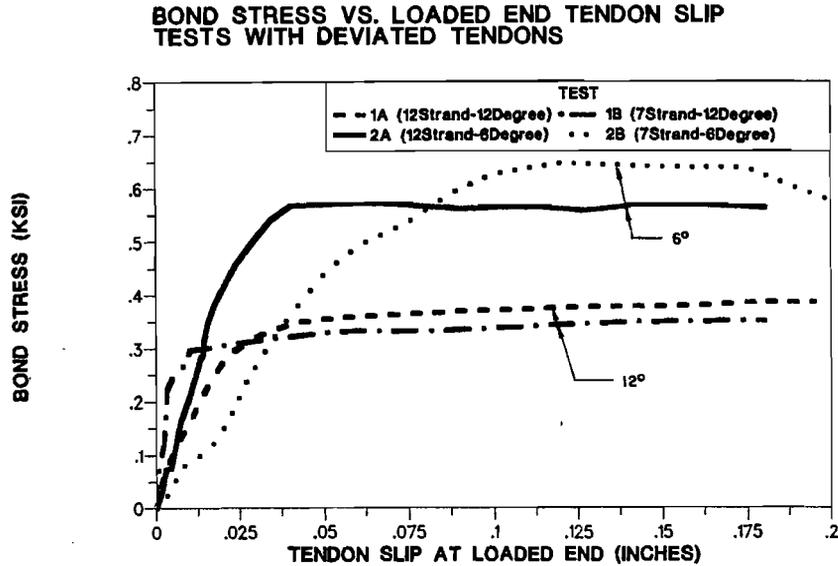
Figure 4.1   Bond Stress-Slip Performance of Specimens with Deviated Tendons.

FORCE DIFFERENCE ACROSS DEVIATOR VS.
LOADED END TENDON SLIP
TESTS WITH DEVIATED TENDONS
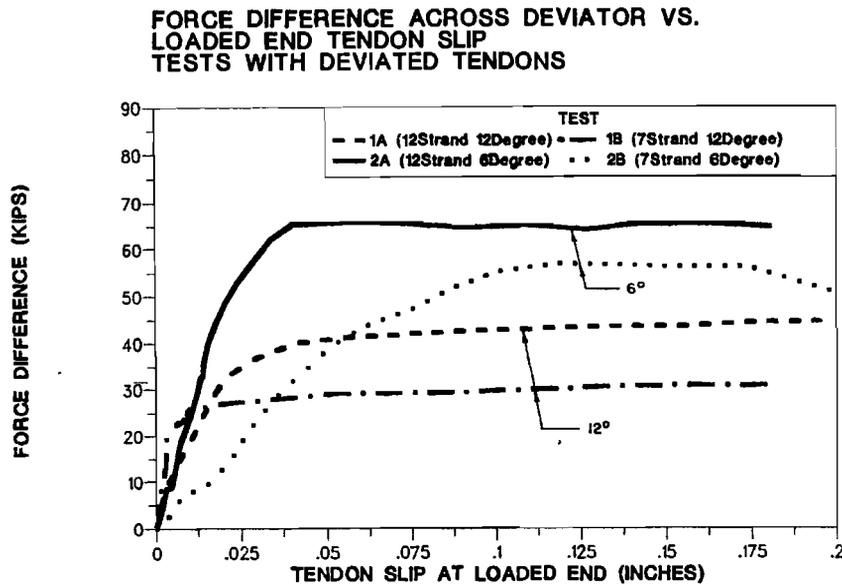
Figure 4.2   Pullout Force -Slip Performance of Specimens with Deviated Tendons.

(1)   Very stable pullout was obtained for all cases. For three of the four tests, maximum bond stresses started to deteriorate when loaded-end displacements were of the order of 0.35" (see Fig. 4.3). Pullout behavior of specimen 2B-7-6° was somewhat less stable than for the other three cases. The tests were stopped when tension in the tendon on the south side of the specimen was reduced to zero. At this point the bond stress and pullout force had just started to reduce from the maximum value (see Fig. 4.3). However, the loading technique did not permit application of additional load to fail the specimen. Consequently, it was not possible to obtain the descending portion of the bond stress-slip

BOND STRESS VS. LOADED END TENDON SLIP
TESTS WITH DEVIATED TENDONS
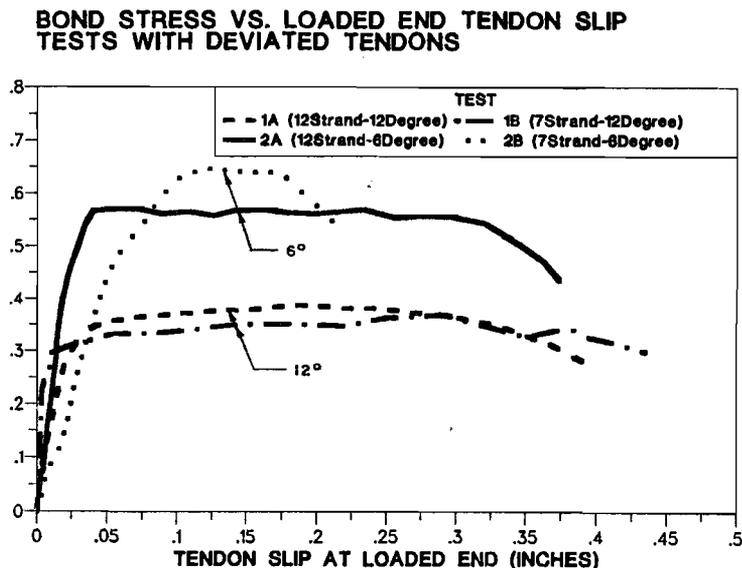
Figure 4.3   Bond Stress-Slip Performance of Specimens with Deviated Tendons.

FORCE DIFFERENCE ACROSS DEVIATOR VS.
LOADED END TENDON SLIP
TESTS WITH DEVIATED TENDONS
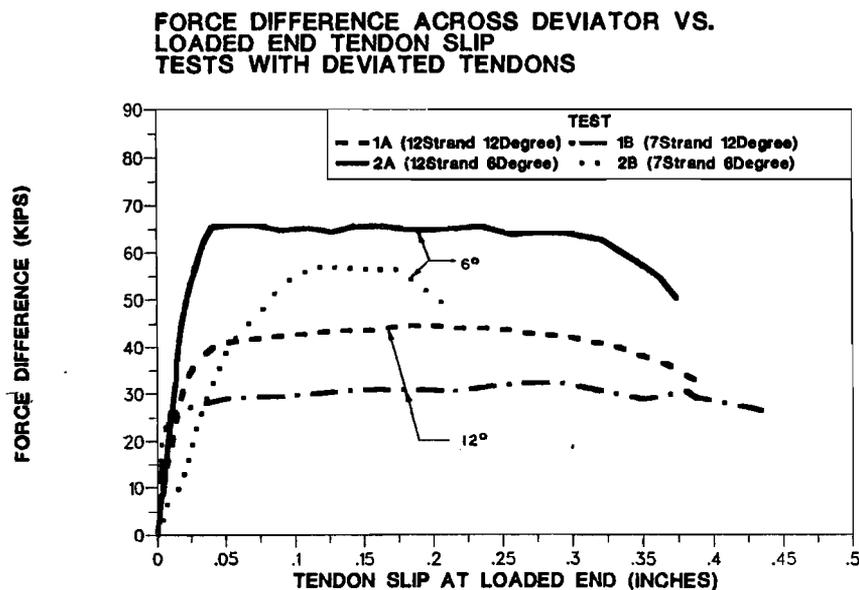
Figure 4.4   Pullout Force-Slip Performance of Specimens with Deviated Tendons.

curve.   Nevertheless, for the portion of the response obtained in the tests,   bond deteriorated slowly and progressively. Stable response beyond the point of general slip can be explained in terms of lack of fit and some degree of mechanical interlock between the strand and grout. For a long embedment length,   substantial differential slip develops between the loaded and unloaded end during pullout. Therefore, when slip initiates at the unloaded end (ie. adhesion eliminated),   slip developed at the loaded end will likely be large enough to cause the strand at that end to wedge because of lack of fit. Some degree of mechanical interlock will develop. As a result, it is unlikely that the entire bonded

length will slip suddenly after the initial bond strength is exceeded at the unloaded end.

It is also interesting to compare the stable pullout obtained in these tests with the sudden failure observed by Trost for large tendon tests (see Test Series C-4 in Section 2.4.2). For the tests by Trost, the ratio of tendon area to duct cross-sectional area was 41% (considerably higher than the maximum value of 25% for the tests presented here) and the tendon was positioned in the center of a straight ribbed duct. Trost observed sudden failure when bursting cracks developed in the grout between the tendon and ribs of the duct. The cracks were inclined against the direction of loading indicating interaction between the tendon and ribs of the duct wall. For a smooth wall deviator pipe with the tendon placed adjacent to the pipe wall, much more stable pullout can be expected if bond failure occurs between the tendon and grout. However, the ultimate bond strength may be limited by the bond developed at the duct-grout interface (depending on the ratio of tendon area to duct cross-sectional area).

(2) The general shape of the bond stress-slip curves for specimens 1A-12-12°, 1B-7-12°, and 2A-12-6° were very consistent (see Fig. 4.1). The bonded tendon was pulled out with approximately constant resistance after slip had extended over the entire length (see unloaded end slip values in Chapter 3). This response is similar to frictional sliding. Minimal reserve bond strength was observed beyond the point of general slip. However, since failure is very stable as outlined above, the general slip condition should provide a conservative estimate of the ultimate bond capacity.

As shown in Fig. 4.1, loaded and unloaded end slip at transition points in the bi-linear bond-stress curves were also relatively uniform for the three tests noted above. Loaded end slip was of the order of 0.04-0.05" at the point where maximum bond stress was initially attained. A very small amount of slip was required to achieve the maximum stress.

In the model bridge tests conducted by Hindi [6], bond performance at the deviators was similar to that of the tendon-grout behavior outlined above. Bond stresses at the deviators increased at a high rate until "full slip" (ie. general slip) occurred. Beyond this point, Hindi observed that the bond stresses increased at a slower rate or stabilized. Bond did not deteriorate as load was increased up to the ultimate load level. Although tendon slip values were not measured in these tests, the general behavior appears to be similar to that observed in the tendon-deviator tests.

(3) For the tendon and deviator duct sizes used in the tests, pullout capacity was not limited by the bond developed between the grout and curved deviator pipe. Failure was observed between the tendon and grout for a ratio of tendon area to duct cross-sectional area of 0.25. This value can be compared to the results obtained by Osborne [29] and Braverman [30] for tests of multi-strand tendons grouted in smooth straight ducts (see Sections 2.4.3. and 2.4.4). For Osborne's tests, bond failure occurred between the duct and grout when the tendon area exceeded 18% of the duct cross-sectional area. Braverman observed a similar failure mode for tendon areas which exceeded 14% of the duct area.

These results are also discussed in Section 4.1.2.2.

(4) Bond developed between the deviator pipe and deviator block concrete was not critical and was apparently not affected by shrinkage stresses in the deviator block concrete.

(5) Considerable scatter existed in the bond stress results. As discussed in Chapter 3, an apparently contradicting trend was also observed. As shown in Fig. 4.1, specimens with a 6 degree deviation angle exhibited significantly higher bond strengths than the 12 degree specimens. The difference between the two cases is most evident when the results are interpreted in terms of bond stresses. Possible reasons for this trend have been discussed in Chapter 3. As shown in Fig. 4.2, pullout forces tend to be somewhat more uniform than the bond stress results for different deviation angles, although the specimens with a 6 degree deviation angle again had consistently higher maximum values. This narrowing of the difference is due to the relative ratio of equivalent bond areas used for calculating bond stresses for the two tendon sizes. For the 24 inch bonded length, equivalent bond areas for the 7 and 12 strand tendons are 88.0 in^2 and 115.3 in^2 respectively (not in proportion to the tendon areas). If Test 1B-7-12° is excluded (poor grout strength), maximum pullout force values ranged from 44 to 66 kips (a variation of 50%). It may be possible that these results simply reflect the high degree of scatter for these tests, which depend to a great extent on the quality of grout. However, pullout force results indicate less of a trend and are therefore less meaningful than bond stress results. The effect of tendon deviation is also discussed in Section 4.1.3.1.

(6) Maximum bond stresses developed at a curved deviator appear to be independent of the tendon-duct area ratio (for ratios ranging from 0.145-0.25). For a given tendon deviation angle, maximum bond stresses vary by at most 16% for the two tendon sizes used in the tests (see Fig. 4.1).

For the curved deviator specimens, bond stresses were apparently not influenced by lateral contact pressure between the tendon and grout. Stocker and Sozen studied the effect of lateral pressure on the bond of strand [12]. In general, it was found that bond stress increased in proportion to applied lateral pressure, although the effect was reduced for large slip levels. For the curved specimen tests described herein, the tendons were compressed against the top of the duct. However, the majority of grout and interfacial bond area was below the tendon. Consequently, lateral pressure (from the duct curvature) was not applied against the grout, and apparently did not have a significant effect on the results.

4.1.2.2 Specimens with Straight Ducts. For the specimens with straight ducts, net bond stress values were obtained directly since no friction existed. Tendon slip values were corrected for elastic shortening of the tendon as outlined above.

Specimen Behavior and Failure. For both specimens with straight ducts, bond failure and slip occurred at the duct-grout interface. The duct did not displace in the

concrete deviator block and the tendon did not slip relative to the grout at the loaded end of the specimen. The grout core and tendon displaced through the duct at the loaded end. Although grout displacement was not measured at the unloaded end, it appeared that the tendon slipped through the grout at the unloaded end of the specimen. Differential strain was developed along the bonded length as a result of this slip.

For the curved deviator specimens, the strands were compressed against the top edge of the duct after stressing. For the straight deviator specimens, the tendon was also purposefully located adjacent to the top of the duct. In this case, however, the strand bundle was not compressed since minimal contact pressure existed between the tendon and the duct surface. Consequently, clear spaces of approximately 1/4" existed between the individual strands (see Fig. 4.5). As a result, grout was able to fully penetrate between strands. This meant that the interfacial bonded area between the tendon and grout was much more than for a tight strand grouping. For the straight-duct case the bond area can be estimated as the equivalent bond area per strand multiplied by the number of strands or:
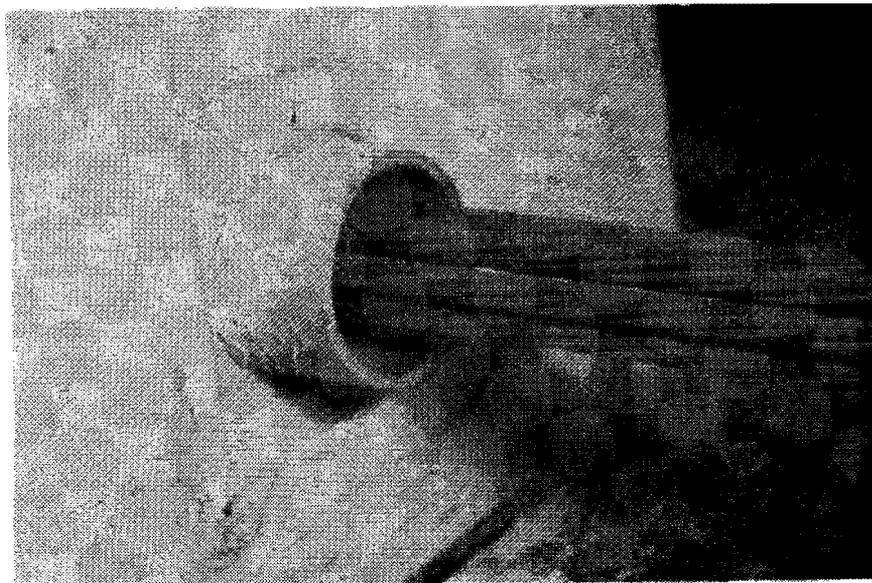
Figure 4.5   Spaces Between Strands in Specimens with Straight Ducts.

$$U = (\pi d_e) \, nL$$

where d_e = the equivalent strand diameter (Section 2.3.2)

U   =   bond area

L   =   bonded length

n   =   number of strands in tendon

One would expect bond failure to occur at the duct-grout interface when the tendon bond area approaches the bond area at the duct perimeter. This does not consider the mechanical interlock developed by the strands. Using the formula outlined above, the calculated bond area for the seven- strand tendon in a 24 inch long deviator is 232.9 in^2. The bond area for the inside perimeter of the duct is 231.3 in^2. If the mechanical interlock of the strands is considered, bond failure at the duct-grout interface can be expected. The test results confirm this. The failure mode changed as a result of increased bond area between the tendon and grout.

In an actual structure, the tendon would likely be compressed as it passed through a straight deviator (depending upon the deviator location along the span length). For a deviator with a straight duct located between deviators with tendon deviations, strands of the tendon would be compressed against one another as a result of lateral pressure due to curvature at the points of tendon deviation. For deviators located near the tendon anchorage points, however, the strands would spread apart to match the anchor spacing, and the tendon would not be as tightly bundled. It is reasonable to assume that the strand bundle is highly compressed throughout the middle region of a span where the greatest bond stresses are developed during ultimate loading. For the case where the strand bundle is compressed, grout cannot easily penetrate between the strands, and the bond area is reduced. The test results may not represent bond conditions of an actual structure for this case.

If the tendons were tightly bundled in the straight duct tests, bond failure may not have occurred between the grout and inside surface of the duct. Osborne and Braverman concluded that bond failure would occur at the duct-grout interface when the tendon area exceeded 18 and 14% of the duct cross-sectional area, respectively (see Sections 2.4.3 and 2.44). However, in Braverman's test with a tendon-duct ratio of 14%, the strands were not tightly bundled in the tendon, and grout was injected between strands. This may have caused bond failure to occur between the duct and grout. Considering these results, bond failure for the seven-strand tendon test (Specimen 3B-7-0°) could be expected to occur between the tendon and grout for a tendon-duct area ratio of 0.145 (assuming the strands were placed in contact prior to grouting).

It appears that the degree of compactness of the strand bundle is important for determining the effective bond area of a multi-strand tendon grouted in a straight duct (It also influences the bond performance of curved deviators as outlined in Section 4.1.4). The mode of bond failure at the deviator may change depending upon this effect as outlined above. It is suggested that tightness of the strand bundle has a much greater effect on the interpretation of test results than that of any of the alternate methods for calculating "actual" bond areas. This effect becomes increasingly important as the number of strands in the tendon increases. Previous studies have not considered this effect.

The bond stress-loaded end slip and pullout force-loaded end slip performance of the two specimens with straight ducts are shown in Figs. 4.6 and 4.7. Examination of the test data leads to the following observations:

BOND STRESS VS. TENDON SLIP
TESTS WITH STRAIGHT TENDONS
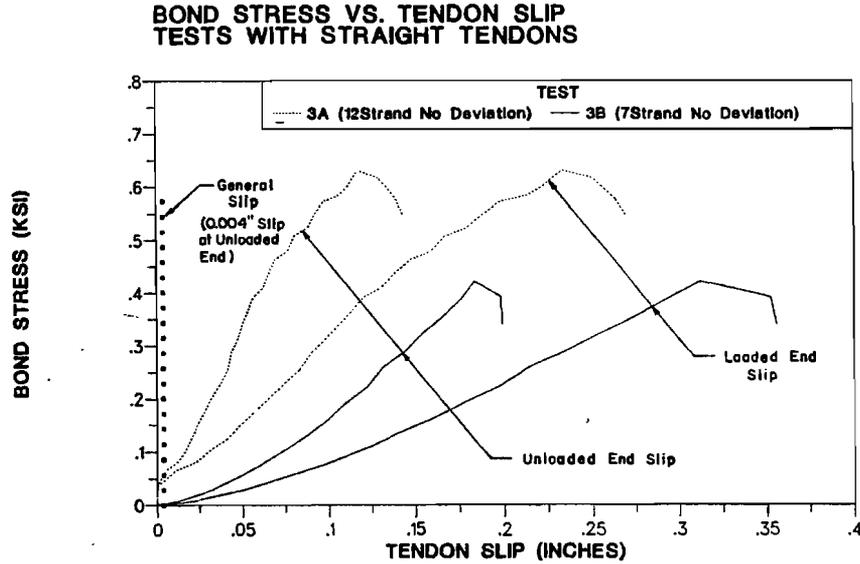
Figure 4.6   Bond Stress-Slip Performance of Specimens with Straight Tendons.

FORCE DIFFERENCE ACROSS DEVIATOR VS.
TENDON SLIP
SPECIMENS WITH STRAIGHT DUCTS
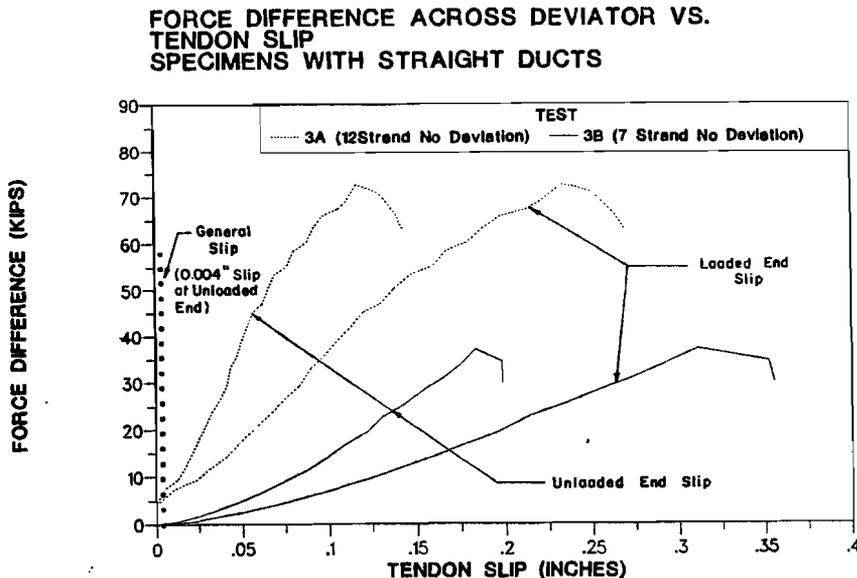
Figure 4.7   Pullout Force-Slip Performance of Specimens with Straight Tendons.

(1) Bond failure occurred suddenly when the grout core displaced out of the deviator pipe. After the maximum bond stresses were achieved, failure occurred suddenly without

warning. The maximum bond stress could not be maintained over any significant change in tendon slip. Since the failure occurred at the inside perimeter of the smooth steel pipe, there was no resistance to slip after the initial bond strength was exceeded over the full length of the specimen.

(2) As shown in Fig. 4.6, negligible bond stresses were developed at the point of general slip (ie. at 0.004" unloaded end slip).

(3) Ultimate bond stresses were comparable to values obtained for the curved duct cases. However, as shown in Figs. 4.8 and 4.9 (Section 4.1.2.3), these bond stresses were reached at much greater tendon slip (ie. the "stiffness" of the pullout force-slip response was considerably lower).
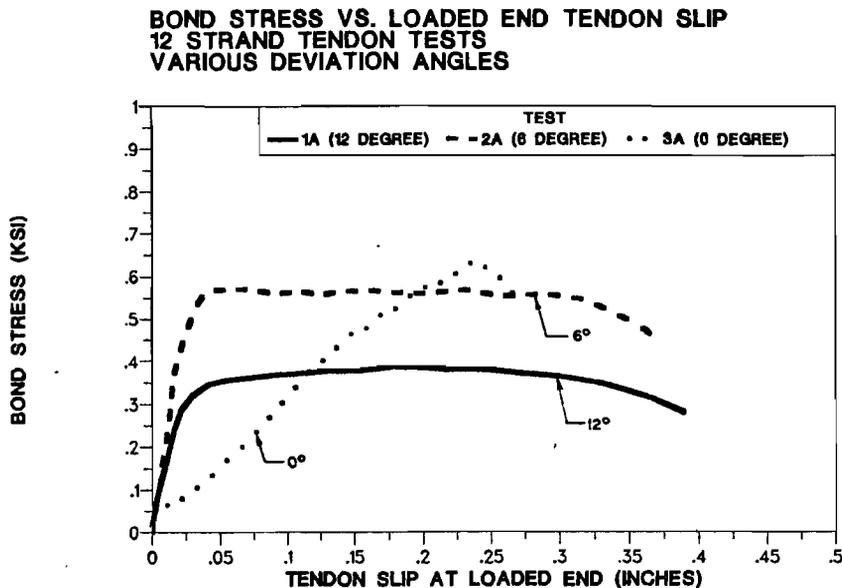
Figure 4.8   Bond Stress-Slip Performance of 12-Strand Tendon Specimens with 0, 6, and 12 Degree Deviations.

In order to reduce construction costs, current segmental bridge designs have emphasized the use of a minimum number of intermediate diaphragms in box girder sections. In general, diaphragms are only placed at sections where tendons are deviated (This is especially the case for short-span structures erected using the span-by-span method). Consequently, concerns regarding the bond performance of tendons through straight ducts may not be significant since the straight duct detail is not particularly common. However, the straight duct detail is still important for remedial bonding at diaphragm pass-through locations.

BOND STRESS VS. LOADED END TENDON SLIP
7 STRAND TENDON TESTS
VARIOUS DEVIATION ANGLES
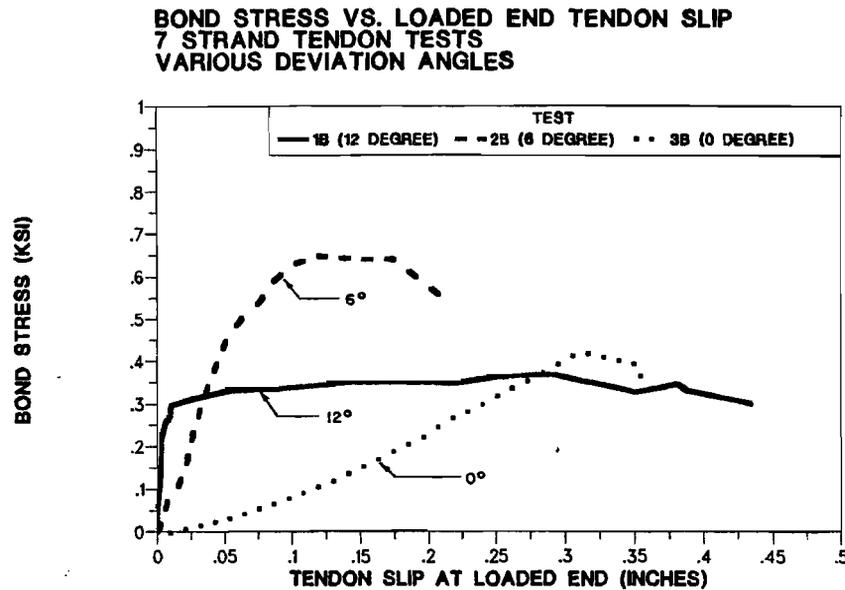
Figure 4.9   Bond Stress-Slip Performance of 7-Strand Tendon Specimens with 0, 6, and 12 Degree Deviations.

4.1.2.3 Comparison of Deviated and Straight Specimens.   The results of the tendon-deviator tests are summarized in Figs. 4.8 through 4.11. The first two figures show bond stress-slip performance of the 12 and 7-strand tendon tests for the three deviation angles (0, 6, and 12 degrees). Corresponding pullout force-slip behavior is shown in the latter two figures. Comparison of all of these test results indicated that the general behavior of specimens with curved ducts was significantly different from that of straight duct cases. The following is a brief summary of these differences.

The pullout response of the specimens with curved ducts was much more stable than for the straight duct cases. This difference was largely due to the mode of failure for each type of specimen. Progressive failure occurred between the tendon and grout in the curved duct tests. In the tests with straight ducts, bond between the grout and deviator pipe failed suddenly. For the tendon sizes used in these tests, it appears that the latter undesirable mode of failure can be avoided if some slight magnitude of tendon and duct deviation is used. However, it is believed that if the tendons were tightly bundled in the straight duct tests, bond failure may not have occurred between the grout and inside surface of the duct pipe (see Section 4.1.2.2). The failure mode for the straight duct case is difficult to predict since it is dependent upon an important additional variable, that is, the degree to which the strands are compressed in the tendon. For the specimens with curved ducts, the degree of tendon compactness was considered to be essentially equal for the 6 and 12 degree specimens. A small degree of tendon deviation seems to produce a sufficiently tight strand bundle.

Specimens with curved ducts developed maximum bond stresses at very small tendon slip values (ie. loaded end slip of the order of 0.04"). Approximately the same maximum bond stresses were developed by the straight tendon specimens. However, the magnitude of slip at the maximum stress was substantially greater. Bond stresses at low levels of tendon slip were negligible compared to bond stresses for the deviated specimens.

4.1.3 Evaluation of Primary Test Variables. The principal variables investigated in the tendon-deviator tests were the deviation angle of the tendon (or duct) and the ratio of prestressing tendon area to duct cross-sectional area. As discussed previously, the limited number of tests did not permit a complete evaluation of these variables. The tests focused on evaluating bond performance of tendon-deviator details typical of existing U.S structures. Specimens were tested with tendon deviation angles of 0, 6, and 12 degrees and ratios of tendon area to duct area of 0.145 and 0.25.

4.1.3.1 Tendon Deviation Angle. As shown previously, the 6 degree specimens exhibited significantly higher bond strengths than the 12 degree cases. Considering the limited number of tests, however, it is difficult to make conclusive statements regarding this trend. On the other hand, by comparing the results of the straight and curved duct tests, it can be seen that the absence of any tendon deviation angle will have a significant effect on the bond performance at the deviator (see Sections 4.1.2.2 and 4.1.2.3). Specimens with deviated tendons exhibited much more stable bond pullout behavior and developed notably higher bond stresses at low levels of tendon slip. The curved duct will also permit the use of a higher ratio of tendon-duct area while maintaining a progressive bond failure between the tendon and grout.

4.1.3.2 Ratio of Tendon Area to Duct Cross-Sectional Area. For the specimens with curved ducts, the maximum bond stresses developed through the deviator appear to be independent of the tendon-duct area ratio (for the two tendon sizes used in these tests). Bond failure was observed between the tendon and grout for a ratio of tendon area to duct cross-sectional area of 0.25. By comparison, Osborne [29] observed a similar failure mode (for straight duct specimens) for tendon sizes which were less than 18% of the duct area. Additional tests would be necessary to determine the maximum tendon-duct area ratio that could be used in curved ducts while maintaining this desirable mode of failure.

For the straight duct specimens, bond failure occurred at the duct-grout interface for both tendon sizes (ie. tendon-duct area ratios of 0.145 and 0.25). Although these results coincide with the observations of Braverman [30], it is believed that the tests were influenced by the grout which was injected between the strands (see Section 4.1.2.2).

4.1.4 Comparisons with Related Studies

4.1.4.1 General. The tendon-deviator tests in this report investigated the specific bond conditions which exist at deviators typical of U.S. structures. Pullout tests of multi-strand tendons grouted in curved smooth steel ducts were conducted. Tendons were

positioned against the duct wall and were stressed prior to grouting. As outlined in Chapter 2, there are no previous studies which have investigated these unique bond conditions at deviators. Nevertheless, the test results can be compared to a number of recent investigations with similar bond conditions. Clearly, the pullout tests of grouted multi-strand tendons conducted by Trost, Braverman, Osborne, and Rostasy are most pertinent. These studies have been outlined in detail in Section 2.4. The single strand test results of other investigators can be used to compare general pullout behavior and possibly to determine an upper bound for bond stresses. As is outlined below, test results are compared in terms of calculated bond stress and tendon displacements. General pullout behavior is also discussed.

4.1.4.2 Comparison and Evaluation of Results.

A) Bond Stresses. Two possible bond failure mechanisms must be considered for a tendon grouted through a cast-in-place deviator pipe. The first concerns the bond developed between the tendon and grout (when the grout does not slip relative to the deviator pipe). The second is the bond developed between the grout and inside perimeter of the duct. Since bond performance is notably different for the two cases, the results are presented separately in the comparisons outlined below.

<u>Tendon-Grout Bond Stresses.</u> The bond stress results from this investigation and from the studies of Trost, Braverman, Rostasy , and Osborne are shown in Table 4.1. Values shown in the table are based on an equivalent tendon diameter and an assumed uniform distribution of stress along the bonded length (Section 2.3.2). Bond areas used in the previous studies have been adjusted to an equivalent area for comparison. As outlined above, the results are for bond failures between the tendon and grout only. Stable pullout was observed for all of these cases. For test series C-4 reported by Trost (Section 2.4.2.), bond failure was the result of bursting stresses in the grout. Although these results are reported in this section, the mode of failure was not the same as that of the other tests. As outlined in Section 3.1.9.3, bond stress values at general slip were taken as the stresses at 0.004" (0.1mm) unloaded end slip.

The results shown in the table clearly indicate that both the bond stress at general slip (where available) and the maximum bond stresses observed in previous studies are significantly higher than the results of the tests in this report. Although the discrepancies in the test results appear to be unreasonably large, the following factors may account for these differences.

A tendon placed adjacent to the duct wall has a reduced effective (ie. "actual") bond area when compared to a tendon in the center of the duct. For the specimens with curved ducts in this study, the effective bond areas between the tendon and grout were approximately equal to the area based on an equivalent tendon diameter (Section 2.3.2). Using a method similar to the one outlined in Appendix A, the "actual" bond area for the 7-strand tendon was calculated to be approximately 93 in², as compared to the equivalent

Table 4.1 Comparison of Tendon-Grout Bond Stresses

Source	Tendon Size	Grout Strength (psi)	Bonded Length (in)	Bond Stress at General Slip (ksi)	Maximum Bond Stress (ksi)
Trost(1)					
Test A-9	4-0.6"	8090	5.25	1.23	1.54
Test A-10	4-0.6"	8225	5.25	0.93	1.32
Test C-4	19-0.6"	5180	11.6	1.03	NA
Test B	3-0.6"	7370	4.5	1.15	1.60
Osborne(2)					
3-Strand	3-3/8"	5830	24	NA	1.16
5-Strand	5-3/8"	2420	24	NA	1.58
Braverman(3)					
3-Strand	3-3/8"	NA	12	NA	2.17
Rostasy-VSL(4)	16-1/2"	NA	102	NA	0.87
This Program					
1A-12-12^P	12-1/2"	2710	24	0.33	0.39
1B-7-12^P	7-1/2"	1550	24	0.31	0.35
2A-12-6°	12-1/2"	2590	24	0.56	0.57
2B-7-6°	7-1/2"	2530	24	0.16	0.64

(1) See Section 2.4.3 for test details.

(2) See Section 2.4.4

(3) See Section 2.4.4

(4) See Section 2.4.5.

bond area of 88.0 in^2 (a difference of only 6%). For the 12 strand tendon, the actual and equivalent areas were 133 and 115.3 in^2 respectively (a 15% difference). By comparison, effective bond areas for the tests with tendons placed in the center of the duct (ie. previous studies) were considerably greater than those based on the equivalent tendon diameter. For example, Trost calculated actual bond areas which were of the order of two times the equivalent bond areas for tests with tendons in the center of the duct. Consequently, when

test results are interpreted in terms of equivalent bond areas, bond stresses from the previous studies are proportionately higher than for the tests covered in this report.

In one previous investigation (Trost's test A-10), the tendon was placed adjacent to the duct wall. For this case, the tendon consisted of only four strands, and the tendon layout in the duct was such that grout was able to form around the strands. As a result, the actual bond area for this case was approximately equal to the case with the tendon in the center of the duct (Test A-9). For the tests described herein, tendons consisted of more strands, and grout could not be easily injected between the strands. The actual bond area was based on the interfacial area between the grout and exposed bottom surface of the tendon. The portion of the tendon in contact with the duct was not included in the calculation of the actual bond area.

For the curved duct tests of this report which are shown in the table, the tendons were stressed through curved ducts prior to grouting. The lateral pressure due to the duct curvature compressed the tendon against the top surface of the duct and resulted in a very tight strand grouping. These bond conditions are much more adverse than those of the previous studies. Trost compared the bond performance of grouted tendons placed against the duct wall with tendons centered in the duct. As shown in Table 4.1, the specimen with the tendon in the center of the duct (Test A-9) developed notably higher bond stresses than that of the eccentric tendon (Test A-10). However, these tests used strands which were untensioned prior to grouting. Stressing the strands prior to grouting will amplify this effect. It appears that for tendons which are stressed prior to grouting, the ability of the grout to penetrate the tight strand grouping is severely impaired.

The effective bond areas used in the previous studies may be conservative. In all cases the bond area was based on the outer perimeter of the tendon. It was assumed that the strands in the tendon were placed close enough to prevent a significant thickness of grout from penetrating the voids (with the exception of Trost's test A-10). This may have been difficult to achieve for the case where the strands were unstressed over a long bonded length. The strands may have sagged along the bonded length since they were only held in position at the ends of the specimen. Consequently, grout may have formed between strands, and the bond failure surface may not have been uniform along the bonded length of the tendon.

The grout strengths for bond specimens in this study are of the order of 2 to 3 times lower than in the previous investigations (with the exception of the 5-strand test by Osborne). This difference may account for some of the variation in the values. In addition, different bonded lengths are used in the various tests. In general, specimens with long bonded lengths yield lower average bond strengths (see Section 2.3.2).

An interesting comparison can also be made between the results outlined in Table 4.1 for multi-strand tendons and those for the single-strand specimens in Table 2.1 (see Section 2.3 (bond stresses based on nominal strand diameter)). The bond stress values from

the previous studies in Table 4.1 are considerably greater than the single-strand test results. This observation is surprising since bond values for the multi-strand case would be expected to be less than the single-strand results. However, a possible explanation for this may be that larger tendons have a greater degree of confinement in the duct. On the other hand, Osborne concluded that expansion of grout within the duct (which should increase internal pressure and resistance to pullout) decreases as the size of the tendon increases [29]. By comparison, average bond stresses for the multi-strand tests in this report are just slightly lower than the single-strand results (the nominal bond stress values in Table 2.1 must be converted to equivalent bond stresses for comparison).

The reserve bond capacity beyond the point of general slip is also greater for the tests of Trost as compared to the present tests. The ratios of maximum and general slip bond stresses appear to be more in line with the single-strand tests outlined previously. This is expected, however, since the tendons in the previous studies (for which data is available) consisted of fewer strands. Larger tendons appear to have proportionately less reserve bond strength after slip has progressed over the entire bonded length.

Comparison with Bridge Model Test Results. This report is part of a larger study which investigated the effects of improved bonding of external tendons for externally post-tensioned bridges. Part of this study included bridge model tests conducted by Hindi [6] as outlined in Chapter 3 (Sections 3.2 and 3.3). External tendons in the bridge model were bonded by cement grout at diaphragm locations. Post-tensioning details used in the bridge model have been described previously. During testing, tendon forces were measured at six points along the span. By measuring the change in tendon stresses on both sides of the deviators it was possible to determine the bond developed between the grout and tendon through the diaphragm. At the ultimate load condition, Hindi [6] observed that the average stress differential achieved across each diaphragm was 10 ksi per strand. For the tendon consisting of 5-3/8 inch diameter strands, this stress differential corresponds to a force difference of 4.25 kips. Using an equivalent tendon diameter and assuming a uniform bond stress distribution along the 5 inch bonded length, a bond stress of 0.37 ksi is calculated at the diaphragms. This value compares reasonably well with the maximum bond stresses for the tendon-deviator tests described in this report shown in Table 4.1 (average of 0.49 ksi).

Duct-Grout Bond Stresses. For the tests of straight duct specimens described herein, bond failure occurred between the duct and grout. This type of failure also occurred in a number of previous studies which used tendons bonded through straight smooth steel pipe sections. The test results for these cases are summarized in Table 4.2. Also included are two tests by Leonhardt for tendons grouted within smooth and ribbed steel box-sections [51]. The bond stresses noted in the table are based on a uniform stress distribution along the bonded length.

Bond stresses outlined in the table vary over a considerable range. However, if the results of Braverman and the ribbed duct test by Leonhardt are excluded, the variation is considerably less. A comparison can be made between the duct-grout bond stresses and the

Table 4.2 Comparison of Duct-Grout Bond Stresses

Source	Duct Diameter (in)	Grout Strength (psi)	Bonded Length (in)	Maximum Bond Stress at duct Surface (ksi)
Osborne	2	2420	24	0.22
Braverman	1.5	NA	12	0.48
Rostasy- Losinger	10.7	NA	394	0.15
Leonhardt 1(1) 2(2)	Box Section 2.44"x2.44"	 5970 5970	 23.6 23.6	 0.20(1) 0.44(2)
This Program 3A-12-0⁰ 3B-7-0⁰	 3 3	 2555 2760	 24 24	 0.32 0.16

(1) Test for steel box with smooth walls.

(2) Test for steel box with ribbed walls.

Rib depth-2mm, Rib width-10mm, Spacing of Ribs-25mm.

tendon-grout stresses shown previously in Table 4.1. Maximum bond stress between the tendon and grout is consistently higher than the bond stress at the duct perimeter (even considering corrections for the effective (actual) bond areas). This reflects the mechanical interlock developed by the strands. This also suggests that bond failure will occur between the duct and grout when the effective bond area of the tendon approaches the bond area at the duct perimeter.

B) Tendon Slip Values. Tendon slip values obtained for the curved duct specimens in this study are compared to the results of Trost [17] for tendons grouted through straight ducts (see Section 2.4.2). Osborne and Braverman observed large variations in tendon slip. Furthermore, the slip of the loaded and unloaded ends of the specimens were inconsistent. Consequently, these tests are not included for comparison. Other multi-strand tendon tests did not provide sufficient documentation of tendon slip values for comparison.

As discussed in Chapter 2, loaded end slip in a pullout test is the integration of the differential strain between the tendon and grout over the bonded length. Consequently,

care must be taken when comparing loaded end slip values for tests with different bonded lengths. The effect of the bonded length on the loaded and unloaded end slip is clearly illustrated in Fig. 4.12. The difference in slip between the loaded and unloaded end increases for longer bonded lengths and increasing loads. By comparing the transition points in the load-slip curves for different bonded lengths, it can also be seen that unloaded end slip varies much less than loaded end slip. For tests with different bonded lengths, this means that unloaded end slip values should compare much better than the values of loaded end slip. Since Trost used bonded lengths which ranged from 4.5-11.6 inches (compared to the 24 inch bonded length for the tests of this study), a comparison of unloaded end slip values was considered to be most meaningful.

The unloaded end slip values from three of the curved duct tests in this study and Trost's tests A-10 (4 strands) and C-4 (19 strands) are shown in Fig. 4.13. Test A-10 used a 5.25 inch bonded length with the tendon placed against the duct wall. Trost observed that this eccentric tendon test exhibited greater slip than the case where the tendon was placed in the middle of the duct. The bonded length for test C-4 was 11.6 inches. Figure 4.13 indicates that specimens with shorter bonded lengths exhibit somewhat greater unloaded end slip for a given load (similar to the results shown in Figure 4.12). For curved duct specimens shown in the table, unloaded end slip values are very consistent at the point where maximum bond stresses are achieved (ie. at a slip value of approximately 0.0030 inches). Since the rate of slip increases suddenly beyond this point, it can be considered to be the point of general slip. By comparison, Trost [17] recommended that the point of general slip be taken at 0.004" unloaded end slip. At the transition point in the bi-linear bond stress curves, specimens with curved ducts also exhibit less slip than the straight duct cases. However, this difference may also be due to the longer bonded length for the curved duct specimens. In any case, the differences in slip are relatively insignificant when the overall behavior is considered. The unloaded end tendon slip response for the curved duct specimens reported here appear to compare very well with the results of Trost's tests for tendons grouted in straight ducts.

4.1.5 Bond Stress-Slip Model For Grouted Multi-Strand Tendons

4.1.5.1 Background. As discussed in Chapter 1, this report is part of the overall project 1209 which included an investigation of the effects of improved bonding of external tendons for externally post-tensioned bridges. The scope of this investigation included the development of a non-linear finite element program for analysis of the ultimate flexural behavior of segmental, externally post-tensioned bridges [6]. The program, BRIDGE, was written by Hindi [6] for use on a personal computer. It consisted of a beam element with external tendon forces applied as external forces at the point where the tendon was bonded to the element (ie. at the diaphragm).

Slip of the external tendons has been shown to have a substantial effect on the overall behavior of an externally post-tensioned bridge, especially at large deformations [6]. Consequently, the effects of slipping of the external tendons were modelled by the program.

Furthermore, since slipping of the tendons is not reversible, the program solution used a step-by-step time history loading process [6]. Tension variations in the external tendons were first calculated assuming that no slip occurred at the deviators (these forces develop from the variation in the segment length as a result of the nodal displacements). Then a slip check at each deviator was carried out using an iterative process to determine if slip was possible (for the magnitude of bond stress developed at the deviator). The magnitude of the bond stress developed for a given tendon slip was determined using a bond stress-slip relationship. The total force developed across the deviator was then taken to be the sum of the friction and bond component. This section covers the development of a bond stress-slip model for use in program BRIDGE. Specific bond stress and tendon slip values used in the model were based primarily upon the results of the tendon-deviator tests outlined previously. Results of the bridge model tests [6] and dismantled span tests, outlined in Chapter 3, are also used for comparison. The bond stress-slip relationship proposed by Martins [38] is reviewed and discussed in Section 4.1.5.4.

4.1.5.2 Development of Bond Stress-Slip Model. As discussed in detail in Section 2.2.3, tendon stress increases and alternating tension in the external tendons are negligible for loads less than the joint or crack opening loads. Since joint opening and cracking occur at loads substantially higher than service load levels, high tension variations in the external tendons are limited to special and extreme overload cases. For these cases, a single load cycle is appropriate. Therefore, a bond-slip model for monotonic loading was assumed in this study.

Results of the tendon-deviator tests (Section 4.1.2) have shown that the bond-slip mechanism between the tendon and grout was significantly different from that of the duct-grout bond performance. In general, bond between the tendon and grout developed rapidly for small levels of tendon slip. After the maximum bond was achieved (and slip had extended over the entire bonded length), bond stresses increased at a slower rate or remained roughly constant. Very stable pull-out was observed as the bonded tendon was pulled out with approximately constant load. Maximum bond stresses were maintained up to high levels of tendon slip. By comparison, bond between the duct and grout was negligible at the general slip condition, and significant bond stresses only developed at high levels of tendon slip. For this case, pullout performance was also very unstable. For the bond stress-slip model in this study, bond failure was assumed to occur between the tendon and grout (ie. the results for the curved duct specimens were used). As discussed in detail in Section 4.1.2.1, it appears that this type of failure can be expected for smooth curved ducts with tendon-duct area ratios up to 0.25 (and possibly higher). For straight ducts, Osborne [29] concluded that bond failure at the duct interface could be avoided if the tendon area was limited to 18% of the duct cross-sectional area. However, it may be possible to use a higher ratio of tendon-duct area if the strands of the tendon are tightly bundled (see Section 4.1.2.2).

In the bridge model tests conducted by Hindi [6], observed bond performance at the deviators was similar to that of the tendon-grout behavior outlined above. Bond stresses at

the deviator increased at a high rate until "full slip" (ie. general slip) had occurred. Beyond this point, Hindi observed that bond stresses increased at a slower rate or stabilized. In no case did the bond stresses deteriorate as loading was increased up to the ultimate load condition. These results appear to confirm the bond performance observed in the tendon-deviator tests. It also suggests that bond failure occurred between the tendon and grout in the bridge model tests.

For modelling of the overall structure it was assumed that no relative movement occurs between the deviator block and concrete box section. This is a reasonable assumption for deviator blocks which are cast monolithically with the concrete sections. For typical U.S. practice, the steel deviator pipe is also cast and held rigidly within the deviator block. With this arrangement, relative movements between the duct and saddle block are also considered to be negligible. If movements of the deviator block were to occur, they would affect the overall modelling of the structure (although the influence is likely insignificant). On the other hand, bond stresses which develop at the deviator are the result of relative slip between the tendon and grout only. Movements of the deviator block do not affect the bond and slip between the tendon and grout (or the bond stress-slip model at the deviator).

4.1.5.3 Proposed Bond Stress-Slip Model for Grouted Multi-Strand Tendons. The bond stress-slip relationship developed in this study is shown in Fig. 4.14. The basis for the values used to define this relationship are discussed below.

The tendon slip values used to define the bond slip relation were essentially taken from results of the tendon-deviator tests with curved ducts. The test results indicated that bond stresses developed rapidly up to the point of general slip. Beyond this point, bond stresses remained roughly constant. Thus, the point of general slip coincides with an important transition point in the bond-slip relation. Unloaded end slip values were used to define this point accurately. Unloaded end slip values for the curved deviator tests are shown in Fig. 4.13. The value of S_o was taken to be 0.004 inches. This value was only slightly greater than the average value observed for the curved duct specimens (approximately 0.003 inches) and was equal to the value proposed by Martins [38]. For specimens with different bonded lengths, loaded end slip varies over a greater range than that of unloaded end slip. Consequently, unloaded end slip tends to define the point of general slip more accurately than the slip at the loaded end. In this sense, a model based on unloaded end slip tends to be more applicable to different deviator lengths. However, the actual tendon slip is more accurately defined as the average of the loaded and unloaded end slip values. For example, for the curved deviator tests outlined herein, average slip at the loaded end was observed to be approximately 0.04 inches at the point where maximum bond stress was achieved (see Section 3.1.9.3). The corresponding slip at the unloaded end was on average 0.003 inches. The difference is due to the differential slip over the 24 inch bonded length. Thus it can be seen that average tendon slip $((0.003+0.04)/2)$ is considerably greater than the slip at the unloaded end of the specimen (especially for specimens with long bonded lengths). Fortunately, the overall behavior of

the structure does not appear to be particularly sensitive to these small changes in tendon slip values. Based on a number of analytical analyses, Hindi [6] observed that the overall behavior of the structure was not significantly affected by small changes in S_0 (especially at ultimate load). The bond stress-slip model proposed by Martins [38] was also based on values of unloaded end slip (see Section 2.6.3). This model is discussed in Section 4.1.5.4.

The maximum bond stress, τ_0, was based on the average bond stress developed at general slip for specimens 1A-12-12° and 2A-12-6°. Bond stress values for these specimens are shown in Table 4.1. Results from specimens 1B-7-12° (poor grout strength) and 2B-7-6° (early unloaded end slip) were not used. Limited reserve bond strength was observed beyond the point of general slip in the tendon-deviator tests. However, since maximum bond stresses could be maintained up to high levels of tendon slip, the general slip condition was considered to be a safe estimate of the ultimate bond strength. The bond stress in the model is intended to be used with an equivalent tendon bond area (Section 2.3.2) and a uniform bond distribution along the bonded length at the deviator. The model is generally applicable to deviators with either straight or deviated tendons. The bond stress value is conservative for the straight tendon case with the tendon placed in the center of the duct. The maximum bond capacity also compares reasonably well with the value calculated from results observed by Hindi in the bridge model tests [6] (ie. 0.37 ksi) (see Section 4.1.4.2)).

The bi-linear shape of the proposed bond-slip model reflects the results of the tendon deviator tests. In these tests, maximum bond stresses remained roughly constant up to loaded end slip values approaching 0.35 inches (see Fig. 4.3). Consequently, the value of S_y was taken as 0.35 inches. As discussed previously, it was not possible to obtain the descending portion of the bond stress-slip curve during the tests. However, from analytical studies of the bridge model test results, Hindi [6] calculated tendon slips of at most 0.3 inches (ie. less than S_y). Consequently, the descending portion of the bond slip curve was unnecessary for the model.

4.1.5.4 Comparison with Model Proposed by Martins. The bond stress-slip model proposed by Martins [38] was discussed in detail in Section 2.6.3. This model is shown in Fig. 2.28, and values used to define the model have been outlined previously in Table 2.4. For ease of comparison, the bond-slip model of Martins is repeated in Fig. 4.15. This section presents a comparison between the bond stress-slip relationship outlined in this study and the model proposed by Martins.

In order to compare the two models it is necessary to convert the bond stresses presented in Table 2.4 to equivalent bond stresses. The model of Martins was based on Trost's [17] alternating tension pullout tests of tendons containing 4-0.6" diameter strands (see Section 2.6.3). The tendon-duct arrangements for these tests are the same as test series A-9 and A-10 which are shown in Table 2.2. Bond stress results taken from these tests were based on "actual" bond areas as calculated by Trost [17] (see Table 2.2 and Appendix A). However, the report of Martins does not indicate how the bond stresses in the model were

to be applied. It is assumed that the values were intended to be used with the "actual" bond areas on which they were based. Since tthe"actual" bond area is greater than the equivalent area, bond stresses based on equivalent area are higher. Table 4.3 shows a comparison between bond stress values for the two models (based on equivalent bond areas). The tendon slip values are also included in the table.

Table 4.3 Comparison of Bond Stress-Slip Parameters for Grouted Multi-Strand Tendons.

Parameter	Martins Normal Conditions of Injection (1)	This Program
S_o	0.0008-0.0014 in.	-(2)
τ_o	0.21-0.50 ksi	-(2)
S_1	0.0028-0.004 in.	$=S_o$ 0.004 in.
τ_y	0.89-0.94 ksi	$=\tau_o$ 0.5 ksi
S_2	0.0035-0.006 in.	$=S_y$ 0.35 in.
τ_2	1.28-1.53 ksi	$=\tau_y$ 0.5 ksi
S_3	0.008-0.012 in.	-(2)
τ_u	0.34 ksi	-(2)

(1) Tendon adjacent to the duct wall.

(2) No corresponding value in model.

The tendon slip values correspond closely at the point where maximum bond stresses are initially achieved (see Figs. 4.10 and 4.11). However, the bond stress values of Martins are notably higher than the values proposed in this study. In Martins' model, bond stresses reduce at S_2. As discussed in Chapter 2, this degrading response was based on the cyclic load behavior observed by Trost. By comparison, a bond-slip model for monotonic loading was assumed in this study. For this case, the maximum bond stress is constant for values of slip ranging from 0.004" (S_o) to 0.35" (S_y).

FORCE DIFFERENCE ACROSS DEVIATOR VS.
LOADED END TENDON SLIP
12 STRAND TENDONS-VARIOUS DEVIATION ANGLES

TEST
—— 1A (12 DEGREE) — —2A (6 DEGREE) · · 3A (0 DEGREE)

FORCE DIFFERENCE (KIPS)

TENDON SLIP AT LOADED END (INCHES)
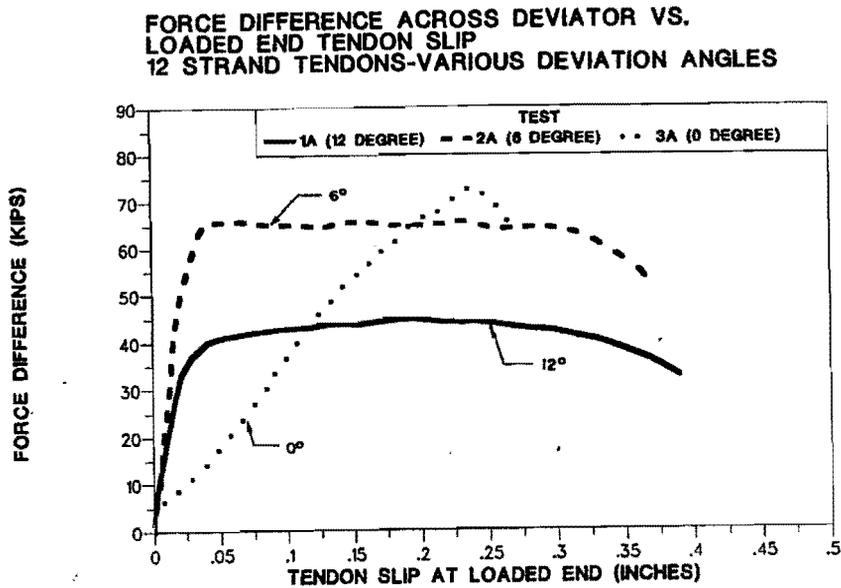
Figure 4.10   Pullout Force-Slip Performance of 12-Strand Tendon Specimens with 0, 6, and 12 Degree Deviations.

FORCE DIFFERENCE ACROSS DEVIATOR VS.
LOADED END TENDON SLIP
7 STRAND TENDONS-VARIOUS DEVIATION ANGLES

TEST
—— 1B (12 DEGREE) — —2B (6 DEGREE) · · 3B (0 DEGREE)

FORCE DIFFERENCE (KIPS)

TENDON SLIP AT LOADED END (INCHES)
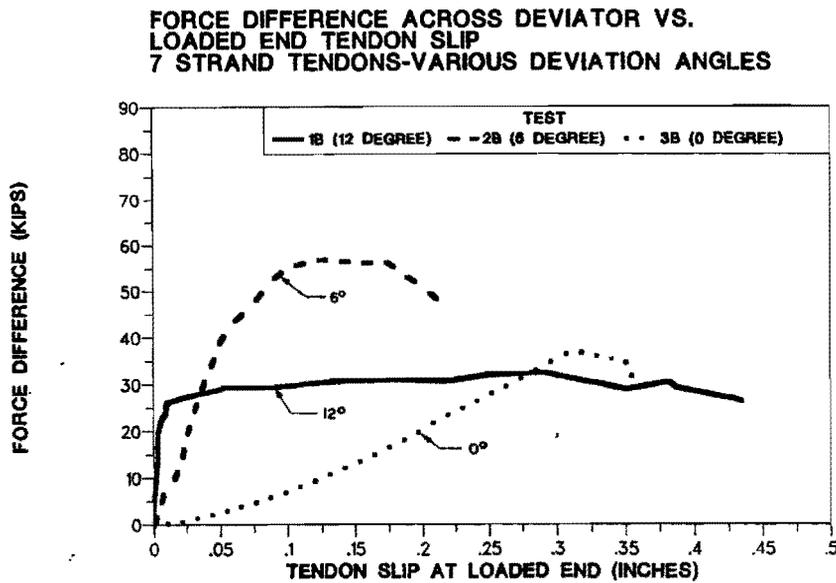
Figure 4.11   Pullout Force-Slip Performance of 7-Strand Tendon Specimens with 0, 6, and 12 Degree Deviations.

The two bond-slip models outlined above are notably different. In the author's relationship, high levels of tendon slip do not limit the bond stresses that are developed. However, stresses at slip values less than 0.006" are significantly lower than the values
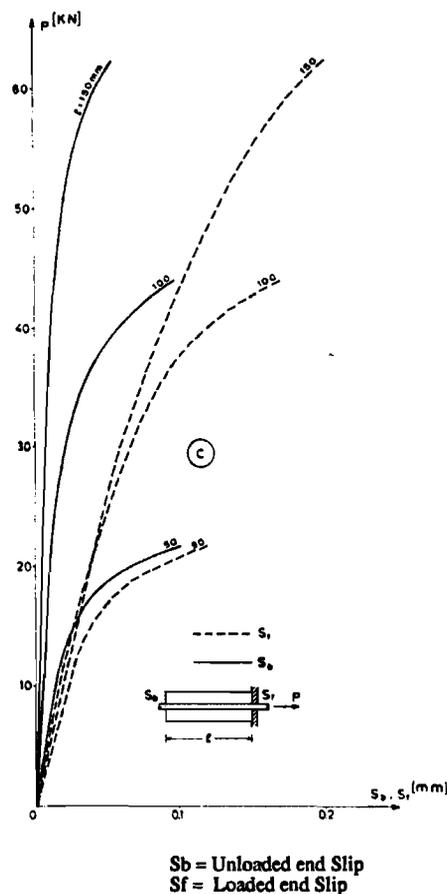
Figure 4.12   Effect of Bonded Length on Loaded and Unloaded End Slip (from Ref. 20)

Sb = Unloaded end Slip
Sf = Loaded end Slip

proposed by Martins. By comparison, Martin's model is very sensitive to the amount of tendon slip. Bond stresses change over a wide range as the slip increases from 0.004-0.012". For the ultimate load condition, tendon slip will easily exceed 0.012". For this ultimate case, Martin's relationship predicts a residual bond stress of 0.34 ksi. This value is somewhat lower than the corresponding bond stress of 0.5 ksi proposed in this study.

4.2 Dismantled Bridge Span Tests

4.2.1 Discussion of Test Results.   The dismantled span test results are outlined in Table 3.8. Bond developed at a deviator was calculated from the observed changes in tendon stress after the tendon was cut on both sides of the diaphragm. No consideration was given to the friction component of the bond force (for deviated tendons) since it was considered to be a small portion of the total force developed across the deviator.

The scatter in the test results shown in Table 3.8 is considerable. These results may reflect the variability of the grout quality in the bridge model. In addition, no trend exists between the results of the straight and deviated tendon cases.

As discussed in chapter 3, the loading condition at the deviators was extremely severe. After the tendons were cut, a stress differential of up to 170 ksi per strand was transferred to the deviator adjacent to the cut. Although the tendons slipped through the deviators at these locations, it is important to note that the bond between the tendon and the grout did not fail completely. Considerable bond capacity was maintained through the deviator after the tendon had slipped. This indicates that significant bond can be developed at the deviators even after severe ultimate loads have been applied.

4.2.2 Comparison with Tendon-Deviator Results.   The test conditions for the dismantled span and tendon-deviator tests were notably dissimilar. The bonded length used in the dismantled span tests was much shorter than in the tendon-deviator tests (ie. 5" vs. 24"). The loading for the dismantled span tests was also much more severe. Despite these and other differences, the maximum bond stresses observed in the two cases compare

APPLIED LOAD VS. UNLOADED END TENDON SLIP
COMPARISON WITH TESTS OF TROST

Figure 4.13   Comparison of Tendon Slip Values at Unloaded End.

reasonably well.   As shown in Table 3.8, the maximum bond stress was 0.57 ksi (based on the average of 8 tests) for the dismantled span tests. For the four tendon-deviator tests outlined in Table 4.1, the corresponding value was 0.49 ksi. In both cases the stresses were obtained at high levels of tendon slip.

4.2.3 Comparison with Bridge Model Tests.   The bridge model tests conducted by Hindi [6] have been outlined previously in Chapter 3 and Section 4.1.4.2. In these tests, Hindi observed that the stress differential achieved across each diaphragm was on average 10 ksi per strand (equivalent to a bond stress of 0.37 ksi) at ultimate load on the structure. After the flexural strength tests were completed by Hindi, the dismantled spans from the bridge model were tested outside the laboratory. For the dismantled span test results shown in Table 3.8, the average stress differential achieved across the diaphragm was calculated to be 15.5 ksi per strand (corresponding to a bond stress of 0.57 ksi). Although the same spans were tested, the results were obtained for different diaphragms along the span length. In the dismantled span tests, the results were obtained for deviators located adjacent to mid-span while Hindi's results were based on an average obtained from six deviators along the span. The disparity in the results may be due to the variation in grout quality along the span length. Furthermore, the rate of loading in the dismantled span tests was higher than in the tests by Hindi. In the bridge model tests, tendon tension was also increasing during testing, while in the dismantled span tests the tension was reduced. The difference in tendon slip in the two cases should not result in any appreciable differences since bond is expected to be essentially constant up to high levels of slip.

4.3 Remedial Bonding Tests.

4.3.1 Discussion of Test Results.
As outlined in Chapter 3, 18 bond specimens were tested with different adhesive injection and sealing materials. The tests were used to model the remedial bonding of external tendons at diaphragm pass-through locations. The bond specimen test results are shown in Fig. 3.39.

The epoxy adhesive specimens developed significantly greater bond strength than the grouted specimens. Of the three epoxy materials tested, A-103 Epoxy with 50% sand filler resulted in the best bond performance. These results indicate that epoxy bond materials are most suitable for achieving a rigid linkage between the pass-through duct and diaphragm. Based on the results of the bond tests, Hindi used the A-103 epoxy-sand mix for remedial bonding of the external tendons at diaphragms in the bridge model [6] (see Section 3.3).

τ - Bond Stress

So = 0.004 in.
Sy = 0.35 in.

$\tau_o = \tau_y = 0.5$ ksi

Figure 4.14 Proposed Bond-Slip Relationship for Grouted Multi-Strand Tendons in Smooth Steel Ducts.

The long term bond performance of the epoxy bond materials was not investigated in this study. However, as discussed in Chapter 2, significant bond stresses would only be developed at the diaphragms for infrequent overloads. This means that the epoxy would not be subjected to a constant sustained loading, and effects of creep in the bond material are probably not significant.

4.3.2 Comparison with Bridge Model and Dismantled Span Test Results.
The bridge model tests of Hindi [6] were discussed previously in Section 4.1.4.2. As noted in that section, Hindi observed that the stress differential achieved across each diaphragm was on average 10 ksi per strand at the ultimate load condition [6] (equivalent to a bond force of 4.25 kips across one diaphragm). This bond was developed between tendon and grout. An interesting comparison can be made between these results and those of the epoxy bond adhesives shown in Fig. 3.39. For an equivalent bonded length, bond strengths developed by the epoxy materials (between the duct and concrete diaphragm) are of the order of two to three times as great as the bond developed between the tendon and grout. A similar comparison can be made with bond stresses obtained from the dismantled span tests. As shown in Table 3.8, the tendon-grout bond force developed across the diaphragm ranged from 3.0-10.5 kips. Bond developed by the A-103 epoxy and sand mixture is approximately

118

one and one-half times the maximum tendon-grout bond observed in the dismantled span tests (ie. 14.7 kips vs. 10.5 kips). These comparisons indicate that bond developed by the epoxy materials (between the duct and diaphragm) is easily sufficient to ensure bond failure at the tendon-grout (or grout-duct) interface for ultimate load conditions. The bond failure between the tendon and grout is desirable since it is relatively stable and predictable.
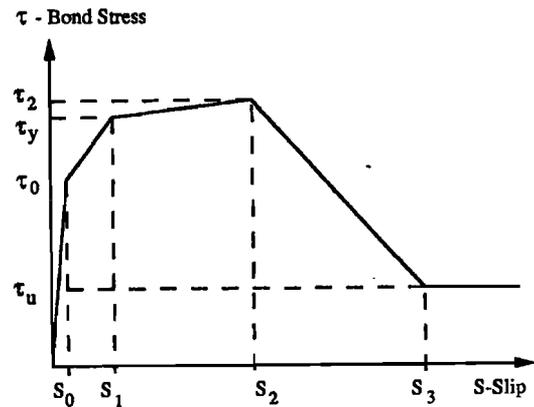
4.4 Design Implications and Recommendations

4.4.1 Background.
As discussed in Chapter 2, tendon stress increases in typical external tendons in post-tensioned segmental box girder bridges are negligible for loads less

Figure 4.15 Bond-Slip Relationship for Grouted Multi-Strand Tendons in Steel Ducts Proposed by Martins (from Ref. 38).

than the dry joint or crack opening loads. Since joint opening (decompression) or cracking should occur at loads substantially higher than service load levels, significant tendon stress increases in the external tendons are limited to extreme overload cases. This also means that bond stresses between the tendon and deviator will not be of consequence for normal service loads.

While the bond developed at deviators is not of consequence for the serviceability case, it is important for the ultimate load condition. In general, a structure with unbonded external tendons will have less reserve strength beyond the point of cracking (or joint opening) than a structure with bonded internal tendons. Furthermore, for the unbonded case, flexural rotations tend to concentrate at initial crack (or joint opening) locations resulting in premature crushing of the concrete and reduced ductility. Bonding external tendons at deviator locations will reduce the unbonded length of the tendon and develop higher tendon stresses at critical sections, thereby increasing the flexural strength of the structure. Bonding tendons at discrete points along the span will also distribute flexural deformations and improve ductility. Increasing the ratio of ultimate flexural resistance to cracking or joint opening load will result in a more forgiving behavior for the structure.

In the design of externally post-tensioned structures, tendon sizes are usually governed by the service level stress condition, rather than ultimate load conditions. Consequently, recent designs of externally post-tensioned bridges have neglected the beneficial effects of partial bond at deviators due to friction or cement grout. Since there is no fundamental difference between girders with bonded and unbonded tendons for load levels below cracking or decompression, this approach is acceptable for design. However, the approach outlined above will result in a conservative estimate of the ultimate capacity.

More refined methods of analysis are currently being used to predict the ultimate capacity of these structures. One example of this is the non-linear finite element program developed by Hindi [6]. The bond-slip model outlined in Section 4.1.5 is recommended for use in this analysis program.

4.4.2 Recommended Bond Stress at Deviators.   A maximum (ultimate) bond stress is recommended based on the results of the tendon-deviator and dismantled span tests. As discussed in Section 4.2.2, the calculated bond stresses from these two series of tests compare very well. The maximum bond stress was 0.57 ksi (average of eight tests) for the dismantled span tests, and the corresponding value for the tendon-deviator tests was 0.49 ksi (average of four tests with curved ducts). For the tendon-deviator tests the ultimate bond stress at general slip was also approximately 0.5 ksi (see Section 4.1.5.3). Since the maximum bond capacity can be maintained well beyond the point of general slip, the bond stress at the general slip condition was considered to be a safe estimate of ultimate bond capacity. Considering the results outlined above, a maximum bond stress of 0.5 ksi is recommended for calculating the pullout capacity of tendons grouted through smooth steel deviator pipes. The bond stress is intended to be used with an equivalent bond area (Section 2.3.2) and a uniform bond distribution along the bonded length at the deviator. Since the recommended value was obtained from full-scale tests with tendons positioned against the duct wall, the bond force can be determined without a time consuming calculation of the "actual" bond area. The bond stress value is generally applicable to curved and straight deviator specimens. For tendons placed in the center of straight ducts, the bond stress value will be conservative (assuming that the bond capacity is not limited by the bond between the duct and grout). The results are based on tests with tendon areas ranging from 14-25 % of the duct cross-sectional area and bonded lengths of 5 and 24 inches.

4.4.3 Remedial Bonding Methods.   The results of the bond specimen tests indicate that epoxy adhesives are most suitable for remedial bonding of tendons at diaphragm pass-through locations. Based on this preliminary study, a mixture of Type A-103 Epoxy and 50% sand filler is recommended as outlined above. The remedial bonding detail developed by Macgregor [3] (see Fig. 3.37) may also be used to effectively bond the metal duct (and tendon) to the concrete diaphragm.

4.4.4 Friction Losses Through Deviators During Stressing.   By measuring the tendon forces on either side of the deviators during stressing, friction losses through the curved ducts were determined (see Section 3.1.9). From these results, the coefficient of curvature friction for the smooth galvanized duct was calculated. The recommended value for the coefficient of curvature friction is 0.2 (based on the average of four tests with tendon deviation angles of 6 and 12 degrees).

CHAPTER 5

Summary and Conclusions

5.1 Summary

This research study was initiated to investigate the bond stress-slip performance of multi-strand tendons which are discretely bonded by grouting through short lengths of curved and straight smooth steel ducts as used in deviators of externally post-tensioned bridges. A preliminary study was also conducted to examine the remedial bonding of external tendons at diaphragm pass-through locations. The following series of tests are reported herein: (1) direct tension bond stress-slip tests of full scale tendon-deviator specimens, (2) dismantled span residual tension load tests (after partial release of tendon stresses in an externally post-tensioned box-girder bridge model), and (3) tests for remedial bonding of tendons at pass-through locations. A literature review of related investigations is also included.

The tendon-deviator tests investigated the bond performance of tendons cement grouted through short deviators typical of existing U.S. structures. Six specimens were tested with varying tendon deviation angles and ratios of prestressing tendon area to duct cross-sectional area. The primary objectives of these tests were: (1) to determine the level of effective bond stress developed through curved and straight deviator ducts and (2) to establish a bond stress-slip model for grouted multi-strand tendons in short lengths of rigid steel ducts. A secondary objective was to determine friction losses through curved deviator ducts during stressing of the external tendons. The dismantled spans of a comprehensive external tendon bridge model were also tested to determine the bond performance of tendons which were discretely bonded by grouting through the diaphragms along the span length. Insight into the ultimate bond mechanism at deviators was obtained by a qualitative evaluation of the data and a comparison of the results with related studies. A method for remedial bonding of external tendons at diaphragm pass-throughs was also recommended based on the results of 18 tests with various cement grout and epoxy adhesive materials.

5.2 Conclusions

The conclusions for the three series of tests are presented separately in the following sections.

5.2.1 Tendon-Deviator Tests. The following conclusions are drawn from tests with tendon deviation angles of 0, 6, and 12 degrees, and ratios of tendon area to duct cross-sectional area of 0.145 and 0.25.

121

122

<u>General Behavior:</u>

(1)   The bond stress-slip performance of the specimens with deviated tendons, and consequent angle changes, was notably superior to that of the straight duct cases.

        a)   Very stable pullout bond failure was observed between the tendon and grout for all tests with deviated tendons. There were no failures at the duct-grout interface for curved duct specimens. For the specimens with straight ducts, bond failure occurred relatively suddenly and all failures were at the duct-grout interface.

        b)   Specimens with deviated tendons developed a maximum bond stress of approximately 0.5 ksi at very small levels of tendon slip (ie. loaded end slip of the order of 0.04"). These maximum bond stresses were sustained for a large range of loaded end slip, often up to 0.35". Straight tendon specimens developed approximately the same maximum bond stress. However, the magnitude of slip at maximum stress was substantially greater (Loaded end slip in the range of 0.3"). Bond stress at low levels of tendon slip (loaded end slip of 0.04") was negligible compared to bond stress for deviated specimens.

        c)   For deviated tendons, the maximum bond stress was maintained well beyond the point of general slip (ie. after slip progressed over the entire bonded length and unloaded end slip reached 0.004"). Bond capacity started to deteriorate at loaded end slip of the order of 0.35". For the straight duct tests, failure occurred soon after the maximum bond stress was achieved at a loaded end slip of the order of 0.3".

        d)   Bond failure between the duct and grout can probably be avoided if some reasonable magnitude (say 3°) of tendon deviation exists at the deviator .

(2)   Negligible reserve bond strength was observed beyond the point of general slip for all specimens with curved ducts. The tendons were pulled out with approximately constant load after slip had progressed over the entire bonded length. Bond capacity was found to be independent of the level of tendon slip after the point of general slip was reached.

(3)   For the curved duct tests, tendon slip and maximum bond stresses were essentially independent of the ratio of tendon area to duct cross-sectional area. The magnitude of tendon slip was also approximately equal for the 6 and 12 degree specimens.

(4)   Tendon slip of 0.004" at the unloaded end was a very good indicator of the point of general slip for the curved duct specimens. The rate of slip increased significantly after slip at the unloaded end exceeded this value.

(5)   Bond stresses could not be developed between the tendon and the grout until minimal tendon slip occurred.

(6)   Bond developed between the duct and deviator-block concrete was not critical in any of the tests.

(7)   The effective interfacial bond area between the tendon and grout is significantly influenced by the degree of compactness of the strands in the tendon bundle (ie. by stressing of the strands prior to grouting).

Comparison with Previous Studies:

(1)   Tendons stressed prior to grouting through curved ducts, and hence, both placed in firm contact with the inner side of the duct and located eccentrically in the duct, exhibited substantially lower bond stresses (of the order of one-half) as compared to tests of tendons which were untensioned and located in the center of straight ducts when grouted. This difference seemed to due primarily to the difference in effective bond area between the two cases and the inability of the grout to penetrate the tight tendon bundle of stressed strands. The effective bond area for a tendon stressed against the curved duct wall was significantly less than the bond area for a tendon placed in the center of the duct.

5.2.2 Dismantled Span Tests.

(1)   Considerable bond was maintained between the tendon and grout after severe pullout loads were applied across the deviator and the tendon had slipped.

(2)   Maximum bond stresses from the dismantled span tests were approximately equal to those obtained in the tendon-deviator tests.

5.2.3 Remedial Bonding Tests.

(1)   Epoxy adhesive materials developed notably higher bond stresses than cement grouted specimens. It appears that epoxy adhesives are most suitable for remedial bonding of tendons at diaphragm pass-through locations.

(2)   Bond developed by the epoxy adhesives (between the pass-through duct and concrete diaphragm) was significantly greater than the observed bond between the tendon and cement grout within the duct. Therefore, the use of epoxy adhesives for remedial bonding will ensure bond failure between the tendon and grout for ultimate load conditions.

5.3 General Recommendations

5.3.1 Bond Stresses. A maximum bond stress of 0.50 ksi is recommended for calculating the potential tendon stress differential (pullout capacity) for tendons grouted through smooth steel deviator ducts typical of U.S. construction. This proposed bond stress is intended to be used with an equivalent bond area (Section 2.3.2) and a uniform bond stress distribution along the bonded length at the deviator. The recommended value is generally applicable to straight or curved deviator ducts. It is conservative for tendons grouted in the center of straight ducts (assuming that bond failure occurs at the tendon-grout interface).

5.3.2 Bond Stress-Slip Model. The bond stress-slip model shown in Figure 5.1 is recommended for analysis of the bond mechanism for tendons grouted through steel deviator ducts. The suggested relationship is based on a monotonically applied load (appropriate for the overload condition) and assumes bond-slip between the tendon and grout.

5.3.3 Friction Losses Through Deviators During Stressing. For the rigid galvanized steel ducts used in this study, the Post-Tensioning Institute [44] recommends a value of 0.20 for the coefficient of curvature friction. An average value of 0.21 was obtained from the tendon-deviator tests with curved ducts. By comparison, VSL International recommends a coefficient of curvature friction of 0.25 for bare dry strands stressed over a rigid steel saddle [52].

τ - Bond Stress

So = 0.004 in.
Sy = 0.35 in.

$\tau_o = \tau_y = 0.5$ ksi

Figure 5.1 Proposed Bond-Slip Relationship for Grouted Multi-Strand Tendons in Smooth Steel Ducts.

5.3.4 Remedial Bonding Methods. Epoxy adhesive materials are recommended for remedial bonding of external tendons at diaphragm pass-through locations. The results of this preliminary study indicate that a mixture of Texas State Department of Highways and Public Transportation Type A-103 epoxy and 50% sand filler yields excellent bond performance. The remedial bonding detail developed by MacGregor [2] (Section 3.3) is also recommended.

5.3.5 Recommendations for Further Research. In order to improve bond

performance at the deviators it appears that further research is required. Future experimental investigations could profitably address the following research topics which were not covered in this study:

(1) Tests of this study were restricted to tendon area to duct area ratios ranging from 0.14-0.25. In actual bridges, values may range up to 0.4. Additional tests would be useful to establish the bond stress-slip performance of curved duct specimens with ratios of tendon area to duct cross-sectional area between 0.25 and 0.40. These tests could indicate the ratio where the observed failure between the strand and grout transitions into a different mechanism (possibly a bond failure at the duct-grout interface).

(2) The use of epoxy adhesives for improving the tendon bond capacity through short lengths of steel duct at the deviator would be interesting. The remedial bonding tests indicated superior performance of epoxy based systems with lessened corrosion potential. However, detailing for this system may be somewhat complex. It would be necessary to use intermediate seals at the deviator ends. Since the tendon duct would then have to be grouted in sections from the ends of the span and between successive deviators, it might be desirable to replace the grouting between deviators with an alternate corrosion protection system. Silica-fume or other improved grouts could also be studied to improve the bond performance at the deviator.

(3) In some cases, graphite grease or wax has been injected through the deviator ducts to reduce friction losses and facilitate tendon stressing operations. After stressing, the post-tensioning ducts are cleaned out by flushing with a mixture of water and solvent. The effectiveness of this operation may affect the subsequent bond developed at the deviators after grouting. Tests are necessary to determine if residual grease exists and, if so, whether it effects the bond capacity at the deviator.

(4) Steel ducts with intermittent ribs may also improve the duct-grout bond developed through the deviator, especially for straight duct cases. However, these ribs may result in more adverse fretting fatigue conditions, and bond at the tendon-grout interface may still be critical.

(5) Further tests would be desirable to study the bond performance of large tendons grouted through curved ducts (say for tendons consisting of more than 27 strands).

(6) Unbonded mono-strands in individual plastic sheaths separated by cast iron or plastic strand spacers have been used through curved ducts. The interstices between sheaths are then grouted prior to stressing (Section 1.4). The grout between strands ensures proper spacing and prevents contact between individual strands. Since the grout is placed prior to stressing, the tendon follows a relatively smooth path and is supported along the full length of the curved duct. This system is then an unbonded tendon and cannot develop high strand forces at ultimate. It would be interesting to

explore the use of intermediate spacers for tendons grouted after stressing. Such spacers could improve the effective bond area of tendons through curved ducts. However, tendon forces and angle changes would be concentrated at strand spacer locations. This might result in very adverse fretting fatigue conditions and might cause cracking of the deviator block.

Appendix A

Sample Calculation of "Actual" Bond Area as used by Trost
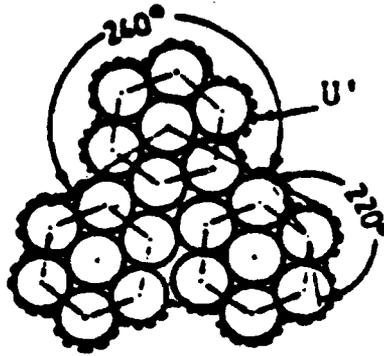
For example, for test Series B (3-0.6" diameter strands):

$$U' = \pi \times 0.5 \times 6 \times 220/360 \times 3 \times 240/360 = 11.52 \text{ cm}^2 \text{ per linear cm.}$$

U'	=	"actual" bond area
0.5	=	individual wire diameter in cm.
6	=	number of exterior wires in one strand
220/360	=	portion of each wire exposed
3	=	number of strands
240/360	=	portion of each strand exposed

127

REFERENCES

1.   Podolny, W and Muller, J., *Construction and Design of Prestressed Concrete Segmental Bridges*, John Wiley and Sons., 1982.

2.   Powell, L.C., Breen J.E., and Kreger M.E., "State of the Art for Externally Post-tensioned Bridges with Deviators", The University of Texas at Austin, Center for Transportation Research, Research Report 365-1, June 1988.

3.   MacGregor, R.J.G., "Evaluation of Strength and Ductility of a Three-Span Externally Post-tensioned Box Girder Bridge Model", Unpublished PhD. Dissertation, The University of Texas at Austin, August 1989.

4.   Virlogeux M., "Non-Linear Analysis of Externally Prestressed Structures", Proceedings of XI FIP (Federation Internationale De La Precontrainte) Congress, June 1990, Hamburg, pp.165-193.

5.   Hoang, L.H., and Pasquignon, M., "Essais de Flexion sur des Poutres en Beton Precontraintes par des Cables Exterieurs", Volume 1 and 2, Contrat SERTA-CEBTP 1985, Dossier de Recherche 91017, November 1985.

6.   Hindi, A., "Enhancing the Strength and Ductility of Post-Tensioned Segmental Box-Girder Bridges", Unpublished PhD. Dissertation, The University of Texas at Austin, December 1990.

7.   Sowlat, K., and Rabbat B.G., "Testing of Segmental Concrete Girders with External Tendons", PCI Journal, March-April 1987, pp.86.

8.   Jartoux, P., and Lacroix, R., "Development of External Prestressing: Evolution of the Technique", Proceedings of XI FIP (Federation Internationale De La Precontrainte) Congress, June 1990, Hamburg, pp 91-98.

9.   Janney, J.R., "Nature of Bond in Pre-Tensioned Prestressed Concrete", ACI Journal, Proceedings Vol. 50, No. 9, May 1954, pp.717-736.

10.   Hanson, N.W., and Karr, P.H., "Flexural Bond Tests of Pretensioned Prestressed Beams", ACI Journal Proceedings Vol. 55, No. 7, Jan. 1959, pp.783-803.

11.   Salmons, J., and McCrate, T., "Bond Characteristics of Untensioned Prestressing Strand", PCI Journal, Vol. 22, No. 1, Jan-Feb. 1977, pp.52-65.

130

12.	Stocker, M.F., and Sozen, M.A., "Investigation of Prestressed Reinforced Highway Bridges, Part V: Bond Characteristics of Prestressing Strand", Engineering Experiment Station, Bulletin 503, University of Illinois, College of Engineering, 1970.

13.	Anderson, A.R., and Anderson, R.G., "An Assurance Criteria for Flexural Bond in Pretensioned Hollow Core Units", ACI Journal, Proceedings Vol. 73, No. 8, August 1976, pp.457-464.

14.	Karr, P.H., Lafraugh, R.W., and Mass, M.A., "Influence of Concrete Strength on Strand Transfer Length", PCI Journal, Vol. 8, No. 5, October 1963, pp.47-67.

15.	Vos, E., and Rienhardt, H.W., "Bond Stress-Slip Behavior of Deformed Bars, Plain Bars, and Strands under Impact Loading", Bond In Concrete, P. Bartos (ed.), Applied Science Publishers, London, 1982.

16.	Trost, H., Cordes, H., and Hagen, H., "Auswirkungen des Verbundverhaltens Zwischen Spannglied und Einpressmortel Bei Verwendung Von Spanngliedern Mit Uber 1500 Kn Zulassiger Spannkraft", Technischen Hochschule Aachen, July 1978.

17.	Trost, H., Cordes, H., Thormahlen, U., and Hagen, H., "Verbundfestigkeit von Spanngliedern und ihre Bedeutung fur Ribbilung und Ribbreietenbeschrankung", Deutscher Ausschuss Fur Stahlbeton, Heft 310, W. Ernst and Sohn, Berlin, West Germany, 1980.

18.	Popov, E.P., "Bond and Anchorage of Reinforcing Bars Under Cyclic Loading", ACI Journal, Vol. 81, No. 4, July-August 1984, pp.340-349.

19.	Ferguson, P.M., "Bond Stress-The State of the Art", ACI Journal, Vol. 63, No. 11, Nov. 1966, pp.1161-1188.

20.	Tassios, T.P., and Yannopoulos, P.J., "Analytical Studies of Reinforced Concrete Members Under Cyclic Loading Based on Bond Stress-Slip Relationships", ACI Journal, Vol. 78, No. 3, May-June 1981, pp.206-216.

21.	Lutz, L.A., and Gergely, P., "Mechanics of Bond and Slip of Deformed Bars is Concrete", ACI Journal, Vol. 64, No. 11, Nov. 1967, pp.711-721.

22.	Giuriani, E., "Experimental Investigation on the Bond-Slip Law of Deformed Bars in Concrete", I.A.B.S.E. Colloquium: Advanced Mechanics of Reinforced Concrete, Reports of the Working Commissions Vol. 34, Delft 1981.

23.	Rehm, G., "Uber die Grundlagen des Verbundes zwischen Stahl und Beton", Deutscher Ausschuss Fur Stahlbeton, Heft 138, W. Ernst and Sohn, Berlin, West Germany, 1961.

24. Ferguson, P.M., Breen, J.E., and Thompson, J.N., "Pullout Tests on High Strength Reinforcing Bars", ACI Journal, Proceedings Vol. 62, No. 55, Aug. 1965, pp.933-950.

25. Burnett, E.F.P., and Anis, A.H., "Bond Characteristics of Initially Untensioned Strand", Journal of the Structural Division, ASCE, Vol. 107, No. ST5, Proc. Paper 16273, May 1981, pp.953-964.

26. Naus, D., "Structural Model Testing for Prestressed Concrete Pressure Vessels: A Study of Grouted vs. Nongrouted Post-tensioned Prestressing Tendon Systems", Oak Ridge National Lab., Tenn., April 1979.

27. Schupack, M, and Mizuma, K., "Bond Strength of High Strength Low Carbon Bars with Drawn-in Helical Deformation for Use in Pretensioning and as Special Normal Reinforcement", ACI Journal, Feb. 1979, pp. 249-270.

28. VSL International, "Considerations Concernant le Dimensionnement et L'arrangement de la Zone de Scellement du Tirant".

29. Osborne, W.R., "Bond Performance of Grouted Untensioned Multi-Strand Bundles during Pull-Out Tests", Masters Report. The University of Texas at Austin, December 1986.

30. Braverman, F., "Pull-Out Tests of Prestressing Strands Grouted inside Smooth-wall Steel Ducts", Master's Report, The University of Texas at Austin, December 1985.

31. Schupack, M. and Johnston, D.W., "Bond Development Length Tests of a Grouted 54 Strand Post-Tensioning Tendon", ACI Journal, Proceedings Vol. 71, No. 10, October 1974, pp.522-525.

32. Losinger AG.(VSL International), "Zugversuche an Felsanker E 6-52.", Berne, Switzerland, December 1977.

33. VSL Corporation (USA), "Duct Pullout Test - Sunshine Skyway Bridge", March 1984. Private Correspondence.

34. C.E.B. Bulletin d'Information No. 151, "Bond Action and Bond Behavior of Reinforcement. State of the Art Report", Contribution a la 22eme. Session Pleniere du C.E.B., Munich, Avril 1982.

35. Hawkins, M.N, Lin, I.J, and Jeang, F.L., "Local Bond Strength of Concrete for Cyclic Reversed Loading", Bond In Concrete, P. Bartos (ed.), Applied Science Publishers, London, 1982.

132

36.   Jiang, D.H., Shah, S.P., and Andonian, A.T., "Study of the Transfer of Tensile Forces by Bond", ACI Journal, Vol. 81, No. 3, May-June 1984, pp.251-259.

37.   Evans, R.H., and Robinson, G.W., "Bond Stresses in Prestressed Concrete from X-Ray Photographs", Proceedings of the Institute of Civil Engineers, Part I, Vol. 4, No.2, 1955, pp.212-235.

38.   Martins, P.C. de R., "Modelisation du Comportement Jusqu'a la Rupture en Flexion de Poutres en Beton a Precontrainte Exterieure ou Mixte", PhD Thesis, Ecole Centrale des Arts et Manufactures, Paris, France, Sept. 1989.

39.   Tassios, T.P., and Koroneos, E.G., "Preliminary results of Local Bond-Slip Relationships by Means of Moire Method", AICAP CEB Symposium on Structural Concrete Under Seismic Action(Rome, 1979), C.E.B. Bulletin d'Information No.132, Paris 1979, pp.85-94.

40.   Yankelevsky, D.Z., "New Finite Element for Bond-Slip Analysis", A.S.C.E. Journal of Structural Engineering, Vol. 111, No. 7, July 1985, pp.1533-1542.

41.   C.E.B. Bulletin d'Information No. 190a, C.E.B.- F.I.P. Model Code 1990 -First Predraft 1988, Contribution a la 26eme. Session Pleniere du C.E.B., Dubrovnik, Sept. 1988.

42.   Foure, B., and Martins, P.C. de R., "Flexural Behavior up to Failure of Externally Prestressed Concrete Beams", Volume 2, Proceedings of XI FIP (Federation Internationale De La Precontrainte) Congress, June 1990, Hamburg, pp.195-215.

43.   Standard Specification for Highway Bridges, Thirteenth edition, American Association of State Highway and Transportation Officials (AASHTO), 1983.

44.   Post-Tensioning Manual, Fourth edition, Post-Tensioning Institute, Pheonix, Arizona, 1985.

45.   Post-Tensioning Institute, "Design and Construction Specifications for Segmental Concrete Bridges", Final Report on NCHRP Project 20-7/32, Feb. 1988.

46.   Hoang, L.H., and Foure, B., "Essais de Traction sur des Cables Appuyes sur un Deviateur", Tranche Conditionnelle 1986 (Phase D), Contrat SERTA-CEBTP 1985, Dossier de Recherche 91.024, Juin 1987.

47.   Arrellaga, J., "State of the Art Instrumentation System for Post-Tensioned Segmental Box-Girder Bridges", Masters Thesis in Preparation, The University of Texas at Austin, December 1990.

48. Schupack, M., "Grouting of Post-Tensioning Tendons", Civil Engineering-ASCE, Vol. 48, No. 3, Mar. 1978, pp.72-73.

49. Schupack, M., "Water-retentive Admixtures for grouts serve Post-Tensioning needs", Concrete Construction, Vol. 29, No. 1, Jan. 1984, pp.47-51.

50. Virlogeux M., "La Precontrainte Exterieure", Annales de l"Institut Technique du Baitment et des Travaux Publics, Decembre 1983.

51. Leonhardt, F. Prestressed Concrete: Design and Construction, 2nd Edition, W. Ernst and Sohn, Berlin, West Germany, 1964.

52. VSL International Ltd., "External Post-Tensioning", Berne, Switzerland, April 1988.

53. Radloff, B.J., "Bonding of External Tendons at Deviators," M.S. Thesis, The University of Texas at Austin, December 1990.